

The University of San Francisco

## USF Scholarship: a digital repository @ Gleeson Library | Geschke Center

---

Master's Theses

Theses, Dissertations, Capstones and Projects

---

Summer 8-13-2021

### Examination of Methylation Status and Occupancy of DNA Methylation Modifying Proteins on Regulatory Regions of the DAX-1 Gene

Caroline P. Riedstra

University of San Francisco, cprcaroline@gmail.com

Follow this and additional works at: <https://repository.usfca.edu/thes>



Part of the [Biology Commons](#), and the [Molecular Biology Commons](#)

---

#### Recommended Citation

Riedstra, Caroline P., "Examination of Methylation Status and Occupancy of DNA Methylation Modifying Proteins on Regulatory Regions of the DAX-1 Gene" (2021). *Master's Theses*. 1393.

<https://repository.usfca.edu/thes/1393>

This Thesis is brought to you for free and open access by the Theses, Dissertations, Capstones and Projects at USF Scholarship: a digital repository @ Gleeson Library | Geschke Center. It has been accepted for inclusion in Master's Theses by an authorized administrator of USF Scholarship: a digital repository @ Gleeson Library | Geschke Center. For more information, please contact [repository@usfca.edu](mailto:repository@usfca.edu).

Examination of Methylation Status and Occupancy of  
DNA Methylation Modifying Proteins on Regulatory  
Regions of the *DAX-1* Gene

Thesis title

by

Caroline Petronyi Riedstra

Student name


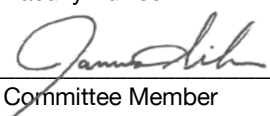
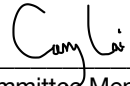
Thesis

Submitted in partial Satisfaction of the Requirements  
For the degree of

**Master of Science  
In Biology**

In the  
College of Arts and Sciences  
University of San Francisco  
San Francisco, California

Committee in Charge

Approved 	<u>8/13/2021</u>
Faculty Advisor	Date
Approved 	<u>08/13/2021</u>
Committee Member	Date
Approved 	<u>08/13/2021</u>
Committee Member	Date
Approved _____	_____
Dean, College of Arts and Sciences	Date

## **Acknowledgments**

### *The Tzagarakis-Foster Lab:*

My incredible PI and mentor Dr. Christina Tzagarakis-Foster, who has supported and encouraged all my research endeavors. Meghana Vijayraghavan and other graduate students before me. As well the undergraduate students, Fiona Ticho and Victoria Sclar who helped my first semester. To the current graduate student in the TRoEL, Nicholas Monares, and undergraduate Dishaa Ramesh.

### *My Thesis Committee:*

Many thanks to Dr. Cary Lai and Dr. James Sikes, for support and guidance during stressful times and their patience when my project had to adapt with changing times. Also the Sikes Lab, for listening to me practice my talks and for providing feedback at joint lab meetings.

### *Biology and Biotech Master's Candidates:*

Getting through this work together has been challenging, without the community we have at USF, some days would have seemed impossible.

### *Biology Staff and Faculty:*

Special thanks to Jeff Oda, Craig Conforti, and Matt Helm. For fixing things when they broke, always having spare materials, and endless support during long days in the lab.

And to my grandfather, Jozsef Petrányi, who was my biggest supporter and strongest advocate of research and academia.

## Abstract

Epigenetic modifications influence gene expression and thereby play a pivotal role in development and disease. Misregulation and mutations in the *DAX-1* gene, or Dosage-Sensitive Sex Reversal, Adrenal Hypoplasia Congenita, Critical Region on the X chromosome, gene 1, have been implicated in Adrenal Hypoplasia Congenita (AHC) and Dosage Sensitive Sex Reversal (DSS). The orphan nuclear hormone receptor *DAX-1* is expressed predominantly in tissues such as the testes, ovaries, breast, adrenal cortex, and lung. Critically, *DAX-1* may serve as an indicator of aberrant growth in these tissues. Here we hypothesize that *DAX-1* is epigenetically regulated, specifically in cancer cells, thereby reducing its expression. In a survey of several human cancer cell lines, the methylation status of the promoter region of *DAX-1* was investigated in order to determine whether epigenetic control played a role in repressing *DAX-1* gene expression. Through molecular techniques such as qPCR and western blots, differential expression of *DAX-1* in human cell lines was confirmed. Additionally, methylation specific restriction enzyme analysis and bisulfite sequencing identified the location of methylation in breast, adrenal, lung, liver, and kidney cancer cell lines. Following these experiments, a correlation of the methylation status of the *DAX-1* promoter and *DAX-1* expression is evident. In tandem with bisulfite sequence analysis, chromatin immunoprecipitation experiments elucidated a primary region of interest in which methylation may be critical to the silencing of *DAX-1* gene expression. Centered around the transcriptional start site, a stark difference in methyl binding protein occupancy between cancerous and noncancerous breast tissue was identified and likely plays a critical role in gene repression via methylation. Ultimately, this research aims to elucidate the role of epigenetic regulation in gene expression as well as further our understanding of the role of *DAX-1* in human cancers.

# Table of Contents

<i>Cover page</i> .....	<b>1</b>
<i>Acknowledgments</i> .....	<b>2</b>
<i>Abstract</i> .....	<b>3</b>
<i>List of Figures</i> .....	<b>6</b>
<i>List of Tables</i> .....	<b>8</b>
<i>List of Abbreviations</i> .....	<b>9</b>
<b>Chapter 1: Introduction</b> .....	<b>11</b>
<i>Background</i> .....	<b>12</b>
<i>DNA Methylation</i> .....	<b>17</b>
<i>Cancer Epigenetics</i> .....	<b>21</b>
<i>Nuclear Hormone Receptors</i> .....	<b>24</b>
<i>DAX 1/NR0B1</i> .....	<b>31</b>
<b>Chapter 2: Determination of the level of DAX-1 expression across different human cell lines</b> .....	<b>44</b>
<i>Introduction</i> .....	<b>44</b>
<i>Materials and Methods</i> .....	<b>46</b>
<i>Tissue Culture</i> .....	46
<i>PCR</i> .....	48
<i>qPCR</i> .....	49
<i>Protein Isolation and Western Blot Analysis</i> .....	51
<i>Methylation Specific Restriction Enzyme Analysis and PCR</i> .....	54
<b>Results</b> .....	<b>61</b>
<i>gDNA DAX-1 Detection</i> .....	61
<i>DAX-1 RNA Level Expression</i> .....	63
<i>DAX-1 Protein Level Expression</i> .....	67
<i>MSRE</i> .....	69

<i>Conclusion</i> .....	<b>82</b>
<b>Chapter 3: Identification of methylated CpG islands in the DAX-1 promoter</b> .....	<b>85</b>
<i>Introduction</i> .....	<b>85</b>
<i>Materials and Methods</i> .....	<b>90</b>
<i>Bisulfite treatment</i> .....	90
<i>ChIP assays</i> .....	97
<i>Bisulfite Sequencing</i> .....	100
<i>ChIP</i> .....	108
<i>Conclusion</i> .....	<b>114</b>
<b>Chapter 4: Discussion</b> .....	<b>115</b>
<b>Appendix A: Supplementary Figures and Tables</b> .....	<b>117</b>
<b>References</b> .....	<b>123</b>

## List of Figures

<b>Figure 1.1</b> The interconnection of genetic, epigenetic, the environment and phenotypic results.	Page 16
<b>Figure 1.2</b> The biochemical reaction of cytosine methylation in DNA results in the silencing of gene expression.	Page 18
<b>Figure 1.3</b> Locations of hyper and hypomethylation in colorectal cancer.	Page 23
<b>Figure 1.4</b> Activation of the nuclear hormone receptor (NHR) pathway.	Page 25
<b>Figure 1.5</b> Multi-dimensional representation of a standard NHR.	Page 27
<b>Figure 1.6</b> Structure of the DAX-1 NHR compared to a typical NHR.	Page 33
<b>Figure 1.7</b> Ligand independent binding nuclear hormone receptor pathway.	Page 35
<b>Figure 1.8</b> Mechanism of a Type 2 NHR binding with coactivator.	Page 37
<b>Figure 1.9</b> The three ways in which DAX-1 can repress transcription.	Page 39
<b>Figure 1.10</b> Promoter region of Exon 1 of the <i>DAX-1</i> gene.	Page 42
<b>Figure 2.1</b> Optimization of primary antibody selection for assessing DAX-1 protein expression.	Page 53
<b>Figure 2.2</b> Methylation status sensitivity to enzymes <i>HpaII</i> and <i>MspI</i> .	Page 55
<b>Figure 2.3</b> CpG rich regions of the <i>DAX-1</i> promoter.	Page 57
<b>Figure 2.4</b> The DNA sequence of <i>DAX-1</i> promoter region with MSRE primers.	Page 59
<b>Figure 2.5</b> Detection of DAX-1 in the genome.	Page 62
<b>Figure 2.6</b> Quantitative assessment of the <i>DAX-1</i> RNA level expression compared to a standard curve developed from the <i>DAX-1</i> plasmid at varying concentrations.	Page 64
<b>Figure 2.7</b> Fold 'Relative' Expression of <i>DAX-1</i> .	Page 66
<b>Figure 2.8</b> DAX-1 protein expression assessed via western blot.	Page 68
<b>Figure 2.9</b> Methylation status of DAX-1 Region A as assayed by MSRE.	Page 71
<b>Figure 2.10</b> Methylation status of DAX-1 Region B as assayed by MSRE.	Page 73
<b>Figure 2.11</b> Methylation status of DAX-1 Region C as assayed by MSRE.	Page 75
<b>Figure 2.12</b> Methylation status of DAX-1 Region D as assayed by MSRE.	Page 77
<b>Figure 2.13</b> Methylation status of DAX-1 Region E as assayed by MSRE.	Page 79

<b>Figure 3.1</b> Methodology of bisulfite conversion.	Page 86
<b>Figure 3.2</b> Summary of MBD proteins mechanism for repressing transcription.	Page 89
<b>Figure 3.3</b> The DNA sequence of <i>DAX-1</i> promoter region with bisulfite primers.	Page 91
<b>Figure 3.4</b> Comparison of source of gDNA used for bisulfite modification.	Page 92
<b>Figure 3.5</b> pGEM®-T Easy Vector map.	Page 95
<b>Figure 3.6</b> Comparison of different chromatin sonication times in the cancerous MCF7 and control MCF10A cell lines.	Page 98
<b>Figure 3.7</b> Sequence alignment of <i>DAX-1</i> promoter region.	Page 101
<b>Figure 3.8</b> Sequence alignment of deaminated cytosines in <i>DAX-1</i> promoter region of bisulfite modified DNA.	Page 103
<b>Figure 3.9</b> Sequence alignment of protected cytosines in <i>DAX-1</i> promoter region of bisulfite modified DNA.	Page 105
<b>Figure 3.10</b> Sequence alignment of CpG island in the <i>DAX-1</i> promoter region of bisulfite modified DNA.	Page 107
<b>Figure 3.11</b> PCR amplification product following ChIP in MCF10A non-cancerous mammary gland control cells.	Page 109
<b>Figure 3.12</b> PCR amplification product following ChIP in MCF7 breast cancer cells.	Page 111
<b>Figure 3.13</b> Model of methyl-CpG binding protein occupancy on the <i>DAX-1</i> gene in MCF10A control and MCF7 breast cancer cell lines.	Page 113
<b>Figure A.1</b> Restriction digest analysis of pGEM-T Easy and converted or control DNA constructs.	Page 117
<b>Figure A.2</b> Sequence alignment of A549 bisulfite modified gDNA.	Page 118
<b>Figure A.3</b> Sequence alignment of MCF7 bisulfite modified gDNA.	Page 119
<b>Figure A.4</b> Sequence alignment of MCF10A bisulfite modified gDNA.	Page 120



## List of Tables

<b>Table 1.1</b> The four subclasses of nuclear hormone receptors.	Page 29
<b>Table 2.1</b> Cell lines used to investigate <i>DAX-1</i> expression.	Page 47
<b>Table 2.2</b> Summary of MSRE results grouped by cell line and amplified region of the promoter.	Page 81
<b>Table A.1</b> Summary table of PCR running protocol parameters	Page 121
<b>Table A.2</b> Summary table of the primers used in PCR and qPCR	Page 122

## List of Abbreviations<sup>1</sup>

AF-1: Activation Factor 2

BSA: Bovine Albumin Serum

AHC: Adrenal Hypoplasia Congenita

AML: Acute Myeloid Leukemia

ChIP: Chromatin Immunoprecipitation

CpG: 5'-C-phosphate-G-3'

CVD: Cardiovascular Disease

DAX-1: Dosage-Sensitive Sex Reversal, Adrenal Hypoplasia Congenita, Critical Region on the X Chromosome, gene 1

DBD: DNA Binding Domain

DNMT: DNA Methyltransferase

DSS: Dosage Sensitive Sex Reversal

ECM: Extracellular Matrix

ER $\beta$ : Estrogen Receptor beta

ER $\alpha$ : Estrogen Receptor alpha

GAPDH: Glyceraldehyde 3-phosphate Dehydrogenase

gDNA: genomic DNA

HDAC: Histone Deacetylase

HHG: Hypogonadotropic Hypogonadism

HPAG: Hypothalamic-Pituitary-Adrenal-Gonadal

HRE: Hormone Response Element

---

<sup>1</sup> In alphabetical order

hMLH1: human mutL homolog1

hMSH2: human mutS homolog 2

ICF: Facial Anomalies Syndrome

LBD: Ligand Binding Domain

LMX1A: LIM homeobox transcription factor 1 alpha

LXR: Liver X Receptor - symmetrical repeat binding receptors

MBD: Methyl-CpG Binding Domain

MBP: Methyl-CpG Binding Protein

NHR: Nuclear Hormone Receptor

PAX1: Paired box gene 1

PCR: Polymerase Chain Reaction

qPCR: quantitative PCR

RXR: Retinoid X Receptor - repeat binding receptors

SFRP: Secreted Frizzled Receptor Proteins

SHP: Small Heterodimer Partner

SRA: Set and Ring Associated domain proteins

SOX1: SRY-box 1

TF: Transcription Factor

TR: Thyroid Hormone Nuclear Receptor

## Chapter 1: Introduction

The epigenome is a collection of heritable modifications to DNA that results in genotypic and phenotypic variability. Physiologically, these modifications are common occurrences observed between different types of cells within the body. However, aberrant epigenetic mutations can lead to disease and in some cases, be used as an identifier of cancer. Studies of epigenetics have elucidated a great deal of information about both the genesis of disease as well as its heritability. Specifically, cancer epigenetics is a popular new topic on the forefront of scientific research. However, before understanding the mutations and possible misregulation brought forth through epigenetic modifications, it is critical to understand the basic process. My thesis focuses on the epigenetic regulation of the *DAX-1* (Dosage-Sensitive Sex Reversal, Adrenal Hypoplasia Congenita, Critical Region on the X chromosome, gene 1) gene and the fundamental role of epigenetics in gene expression. Central to this thesis research is understanding the gene, its current implications on growth and development, and how epigenetics may be playing a significant role. I have investigated key commonalities found in breast, prostate, lung, adrenal, and liver cancer (Conde et al., 2004; He et al., 2008; Heskett, 2014; Jiang et al., 2014; Kudryavtseva et al., 2018; Kumata et al., 2018). All of these forms of cancer express, to varying degrees, the *DAX-1* gene. Nevertheless, the exact role *DAX-1* plays in each of these cancers is not yet fully understood. **The goal of this thesis project is to investigate the epigenetic mechanisms that control *DAX-1* gene expression in normal as well as cancer cells lines.**

## ***Background***

Epigenetic modifications are an important mechanism that regulate gene expression during development, but these modifications also play a key role in diseases such as diabetes, cardiovascular disease, and cancer. Before delving into how epigenetics plays a role in development and disease, it is important to first define epigenetics, epigenetic modifications, and the epigenome. Epigenetics has been of prominent interest for the past few decades, however, an agreed upon definition has yet to emerge. Starting in the late 1950s, epigenetics was defined as the study of genotypes that lead to specific phenotypes in development (Bird, 2002, 2007). However, more recently in the 1990s, a new interpretation arose when Arthur Riggs and colleagues defined epigenetics as the heritable modifications to genes that are beyond what the DNA encrypts (Bird, 2007; Russo et al., 1996; Waddington, 2014). Further debates came in the early 2000s, as epigenetics took on a new form as a biomarker and possible means of diagnosis. Alternatively, epigenetics was also defined as “all the heritable changes in gene regulation other than nucleotide sequence and chromatin organization that depend on the DNA sequences itself” (Abi Khalil, 2014; Egger et al., 2004; Rodenhiser & Mann, 2006). The increasing diversity in defining epigenetics has led some scientists to call for a new ‘standard’ that all epigeneticists can utilize. In 2007, a modified statement was suggested, one that encompassed many schools of thought: “the structural adaptation of chromosomal regions so as to register, signal or perpetuate altered activity state” (Bird, 2007). Although discrepancies continue, the field of epigenomics has begun to answer questions regarding heritable traits. Newer interpretations have evolved and epigenetics is quickly becoming the science that can explain how cells adapt to and are altered by their environment through modifications of the gene that lead to phenotypic differences not expressed in the genotype (Ordovás & Smith, 2010; Turan et al., 2010). For the purpose of the research outlined in this thesis,

I will focus on the resulting epigenetic modification, rather than the origin of that change. Epigenetic modifications are post-translational changes in the DNA sequence that control gene expression. There are three primary classes of epigenetic modification mechanisms in human cells: DNA methylation, histone modification, and micro-RNA based mechanisms. All three mechanisms are often interrelated and pivotal to cell differentiation, gene activity, and aging (Abi Khalil, 2014; Jintaridth & Mutirangura, 2010; Kwabi-Addo et al., 2007; Murgatroyd & Spengler, 2011).

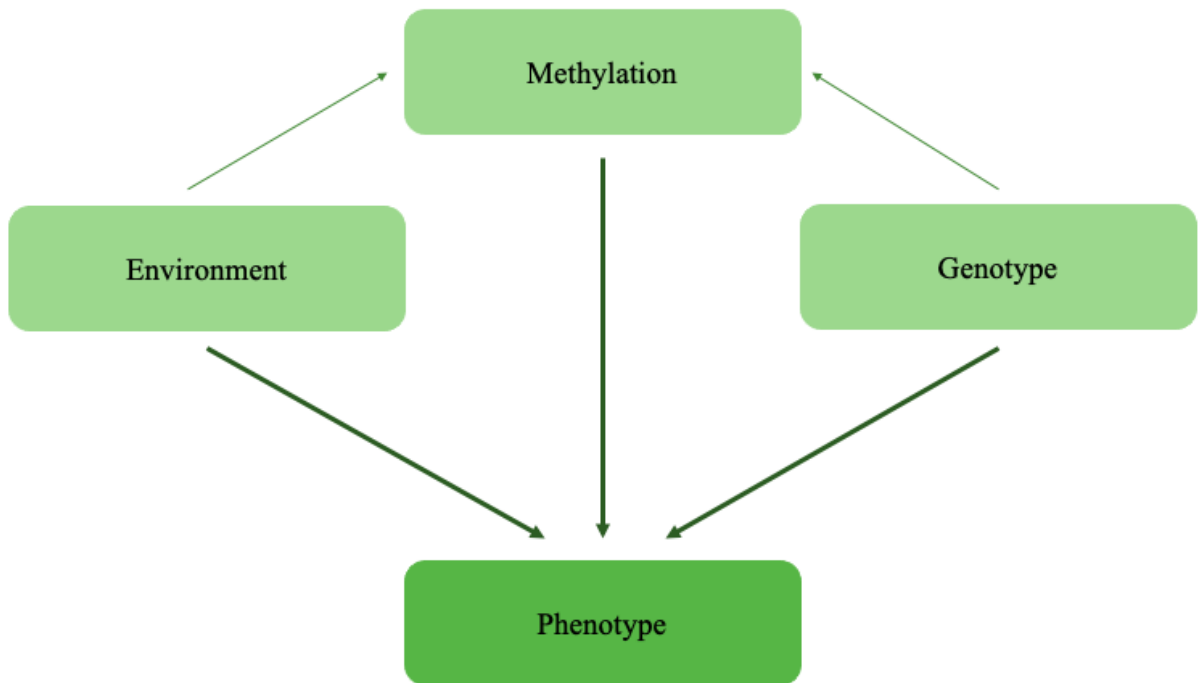
As fundamental mechanisms to gene expression, epigenetic modifications are heritable, occasionally reversible, and have been tied to disease. Among some of the more studied cases, epigenetics has been associated with developmental diseases, mental illness, cardiovascular disease (CVD), and cancer (Ball et al., 2009; Bird, 2002; Brown et al., 2008; Eckhardt et al., 2006; Halušková, 2009; Hansen et al., 2011; He et al., 2008; Jintaridth & Mutirangura, 2010; Kerachian et al., 2020; Kudryavtseva et al., 2018; Kwabi-Addo et al., 2007; Manel, 2008; Manoochehri et al., 2016; Martin et al., 2011; Murgatroyd & Spengler, 2011; Rakyan et al., 2004; Robertson, 2005; Suzuki & Bird, 2008; van IJzendoorn et al., 2011; E. M. Wong et al., 2020; Zhu & Yao, 2007). Early development is heavily impacted by epigenetic marks that influence gene expression and cell differentiation (Cedar & Bergman, 2011). Critical cellular processes, such as hematopoietic cell development, are mediated by epigenetic changes that include histone deacetylation and demethylation. These modification patterns determine a cell's fate to either remain in a pluripotent state or commit to a specific cell type. For example, the decision required for a cell to progress towards myeloid versus lymphoid differentiation depends on the expression of the V(D)J gene segments and the 'assembly' of antibodies through V(D)J recombination in both B and T cells. Notably, this process is regulated by histone activation (Cedar & Bergman, 2011). In neurological

development, epigenetic alteration of gene expression in early years has been shown to impact brain function and mental illness later in life (Murgatroyd & Spengler, 2011). Similar to the differentiation produced by V(D)J recombination, neurons contain the same DNA but carry out diverse functions due to differential gene expression. Pre- and postnatal development is influenced by environmental conditions. Therefore, gene expression can be mediated by epigenetic modifications brought about not only through natural mechanisms, but also external influences such as maternal care or early life adversity and stress. Such variations to the epigenome caused by gene silencing or inappropriate expression have been identified in neurodegenerative diseases, mental retardation, and schizophrenia. Still, the impacts of epigenetic modification and dysregulation are not limited to developmental diseases. As the global leading cause of death, cardiovascular disease is a prominent target for therapeutic research (*Cardiovascular Diseases*, n.d.). Previous studies have linked all three forms of epigenetic modifications (methylation, histone modification, and micro-RNA based mechanisms) to various cardiovascular diseases including heart hypertrophy, heart failure, arrhythmias, and vascular diseases (Abi Khalil, 2014). In some instances, the epigenetic involvement is more direct, impacting inflammation and vascular function. In other cases, the role of epigenetics is more pertinent through the lens of increased risk factors (Abi Khalil, 2014; Ordovás & Smith, 2010). Environmental and behavioral factors such as pollution, smoking, stress, nutrition and circadian rhythm have been shown to influence the risk and progression of CVDs.

Although the correlation between epigenetics and disease has been established, uncertainty remains around whether epigenetics is a precursor to disease or the result of a disease (Bell & Spector, 2011; Martin et al., 2011). It is evident that aberrant epigenetic modifications overlap with disease; therefore an addendum to the definition of epigenetics is inevitably required: “one

caused by a stable alteration in the epigenetic state of a gene (epimutation) without any contributory genetic mutation” (Martin et al., 2011). Although this may seem to lead towards a causal relationship between epigenetics and disease, this is not the case. Environment plays a fundamental role in development, and epigenetics is the mechanism for rapid cellular adaptation (Bell & Spector, 2011; Murgatroyd & Spengler, 2011; van IJzendoorn et al., 2011). Therefore, it may be the environment or the disease that leads to the aberrant modifications, and not the other way around. This line of behavioral epigenetic research can often unravel into a question of nature versus nurture, and which came first. Regardless, the theme remains that epigenetics is prevalent in disease, particularly those that correlate with gene silencing via DNA methylation (**Figure 1.1**).

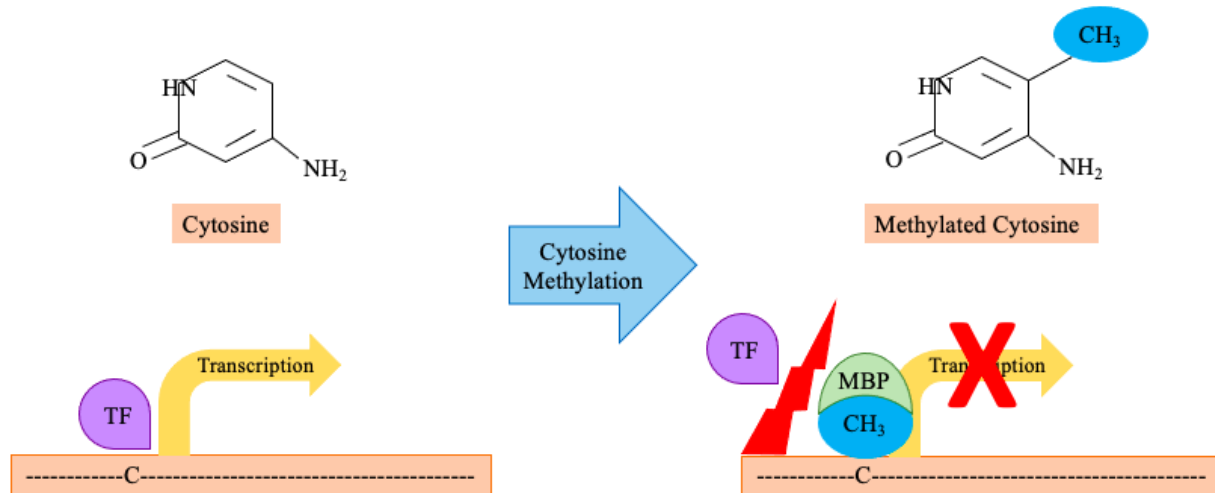




**Figure 1.1** The interconnection of genetic, epigenetic, the environment and phenotypic results. Figure adapted from van IJzendoorn et al., 2011 depicting the theory of behavioral epigenetics, where the outcome of modification by any of these three factors is a phenotypical alteration.

## ***DNA Methylation***

The focus of this thesis research is on one particular type of epigenetic modification: DNA methylation. DNA methylation is the process by which a methyl group is transferred onto the C5 position of a cytosine (Moore et al., 2013; Zeisel, 2009). The transfer can be done by DNA Methyltransferases (DNMTs), methyl-CpG binding domain proteins, and the Kaiso family of proteins (Fournier et al., 2012). The Kaiso family of proteins are unique in their ability to bind both methylated CpG-containing DNA sequences, as well as non-methylatable regions without CpG islands. Kaiso family proteins can bind to sequence-specific methylated regions of promoters and thereby repress transcription (Fournier et al., 2012; Sasai et al., 2010). Cytosine DNA methylation is crucial to our understanding of human development as it is the only known DNA modification fundamental to mammalian growth (Jones & Takai, 2001; Robertson, 2005). Following the completion of the Human Genome Project in 2003, new attention was granted to the Human Epigenome Project because it became clear that epigenetic marks are heritable and contribute significantly to embryonic development and phenotype expression (Rakyan et al., 2004; Robertson, 2005). Functionally, DNA methylation often results in the silencing of gene expression and promoter activity (**Figure 1.2**) (Bird, 2002; Moore et al., 2013; Suzuki & Bird, 2008; van IJzendoorn et al., 2011).



**Figure 1.2** The biochemical reaction of cytosine methylation in DNA results in the silencing of gene expression. Figure adapted from van IJzendoorn et al., 2011 and Zeisel, 2007; the addition of  $\text{CH}_3$  to a cytosine molecule via a methyl binding protein (MBP) prevents the transcription factor (TF) from initiating transcription and gene expression.

This epigenetic mark caused by DNA methylation goes beyond differential expression of genes necessary during development and underlies human disease, X-chromosome inactivation, and genomic imprinting disorders (Egger et al., 2004; Halušková, 2009; Heard et al., 1997; E. Li et al., 1992, 1993; Robertson, 2005; Weber et al., 2007). Looking more closely at some of the conditions mentioned above, methylation has a prominent place in disease. Specifically in CVD, hypermethylation associated with the epidermal growth factor receptor (*EGFR*) gene in animal models correlates with aortic valve calcification that leads to cardiac hypertrophy (Abi Khalil, 2014). Furthermore, DNA hypomethylation in mice with atherosclerosis contrasts the hypermethylation of estrogen receptor alpha (*ERα*) and estrogen receptor beta (*ERβ*) genes found in human patients with atherosclerosis (Abi Khalil, 2014). Although not fully understood, differential methylation status appears to be an underlying mechanism of various examples of CVD, yet this genetic contribution to CVD remains elusive. A better understanding of the epigenetic regulation of genes associated with CVD may lead to a new path of prevention and therapy (Ordovás & Smith, 2010). Heritable epigenetic modifications due to behavior such as smoking may also increase CVD risk. In children exposed to tobacco smoke while still in the womb, CpG islands (5'-C-phosphate-G-3' regions in DNA) typically hypermethylated are observed at a significantly reduced level of methylation (Breton et al., 2009; Ordovás & Smith, 2010). The possible connection of reduced methylation as an epigenetic adaptation to increase predisposition to disease later in life may provide further understanding of CVD and risk associated factors. Beyond CVD, DNA methylation patterns established during development, particularly in the hippocampus, extend well into adulthood (Brown et al., 2008). The spatial organization of and degrees of methylation impact physiological function and determination of

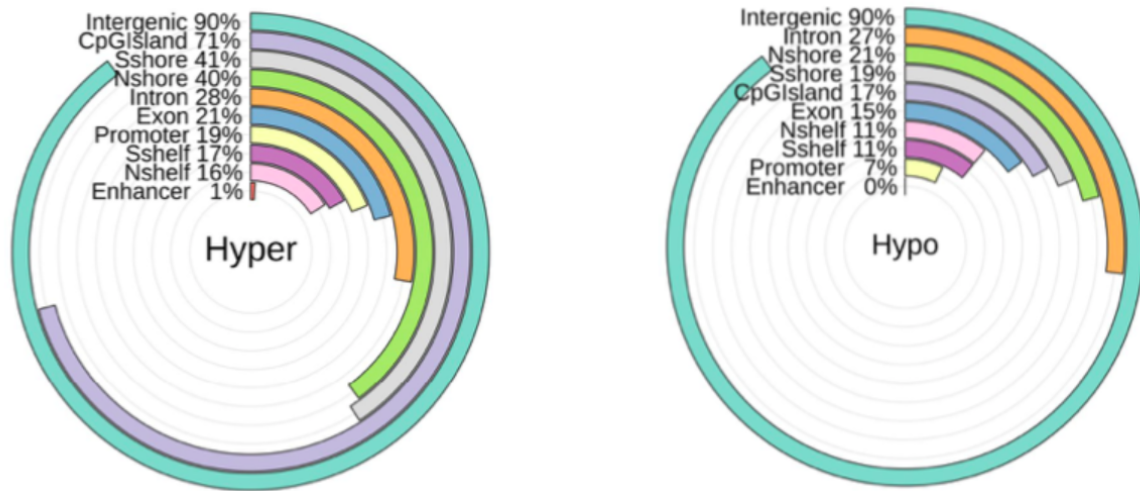
cell type. In this way, the prenatal methylation by DNA methyltransferases influences the hippocampus and development of the adult brain (van IJzendoorn et al., 2011).

Changes in methylation and methylation machinery leading to abnormal methylation status of promoters and regulatory regions of gene expression underlie rare diseases of immunodeficiency, centromeric instability, facial anomalies syndrome (ICF), and Rhatt syndrome (Jones & Takai, 2001). Aberrant epigenetic changes lead to other cognitive dysfunctions as well. Synaptic plasticity from epigenetic regulation is misregulated in cases such as Alzheimer's disease, Huntington's disease, and psychiatric disorders including schizophrenia and addiction (Halušková, 2009). Ultimately, while more thoroughly researched in some diseases compared to others, epigenetics - specifically methylation - may serve as possible biomarkers in development and disease.

## ***Cancer Epigenetics***

A disease that has plagued the world since Egyptian times and a medical undertaking since the early 1900s, cancer has captivated the research world for many years. The National Cancer Institute predicts that in 2020, approximately 1.8 million people will be diagnosed with cancer in the US alone, and roughly 606,520 people will die of cancer (*Cancer Statistics - National Cancer Institute*, 2015). As both a genetic and epigenetic disease, cancer studies attract a variety of attention, with fields of research focusing on prevention, detection, and treatment. Previous research in cancer epigenetics has demonstrated the power of tracing methylation status of candidate genes (Halušková, 2009). For example, in the bladder, methylation of the *Rbl* gene has been investigated as a potential indicator for cancer progression and development (Halušková, 2009; Malekzadeh et al., 2009). Additionally, in the study of biomarkers for cancer screening and prognostic markers, eight genes of interest have been identified in ovarian cancer (Halušková, 2009; Su et al., 2009; Zhang et al., 2008). Hypermethylation of DNA mismatch repair genes such as human mutL homolog1 (hMLH1) and human mutS homolog 2 (hMSH2) in ovarian cancer were identified as potential prognostic markers (Zhang et al., 2008). Furthermore, methylation status of three genes from the secreted frizzled receptor proteins (*SFRP1*, *SFRP 2*, and *SFRP 5*) family, SRY-box 1 (*SOX1*), paired box gene 1 (*PAX1*), and LIM homeobox transcription factor 1 alpha (*LMX1A*) were investigated as markers for ovarian cancer screening and potential prognostic indicators (Su et al., 2009). Downregulation of the SFRP family has also been linked to aberrant activation of the Wnt signaling pathway which promotes tumor progression (Kawano & Kypta, 2003). Hypermethylation of genes in the SFRP family has also been implicated in multiple cancers, specifically the hypermethylation of *SFRP1* in hepatomas, of *SFRP2* in gastric cancers, and of *SFRP4* in colorectal cancers (Cheng et al., 2007; Feng Han et al., 2006; Shih et al., 2007).

With an abundance of research that continues to grow, cancer epigenetics has become a very specific scientific niche that has been defined as “the study of somatically heritable changes in molecular processes that influence the flow of information between the DNA of cancer cells and their gene expression patterns” (*Cancer Epigenetics - Latest Research and News | Nature*, n.d.). While this definition encompasses many fields of interest, including histone modifications and nuclear organization in tumor cells, this thesis focuses specifically on DNA methylation. As previously stated, DNA methylation is required for normal mammalian development, gene regulation, genomic imprinting, and chromatin structure (Bird, 2002). Using DNA methylation and subsequent alterations in gene expression is increasingly popular as a potential biomarker and risk assessor for cancer (Kerachian et al., 2020; Verma & Manne, 2006; E. M. Wong et al., 2020). Particular attention has been directed at analyzing the varying degrees of DNA methylations and identifying patterns common amongst cancer forms. DNA methylation predominantly occurs in three degrees of severity: hyper, hypo, and simple methylation. However, hundreds of methylations can occur at a time at many locations on a strand of DNA. Identifying specific methylation sites in cancer tissue versus normal tissues continues to be a source of screening and prognostic evaluators. In squamous cell lung carcinoma, significant hypermethylation in tissue derived from tumors versus non-tumor derived lung tissue has led to the identification of twenty-two methylation markers, across eight different genes (Anglim et al., 2008; Halušková, 2009). **Figure 1.3** compares the distribution and frequency of hypermethylation and hypomethylation in colorectal cancer cells to that found in healthy tissue (Kerachian et al., 2020).

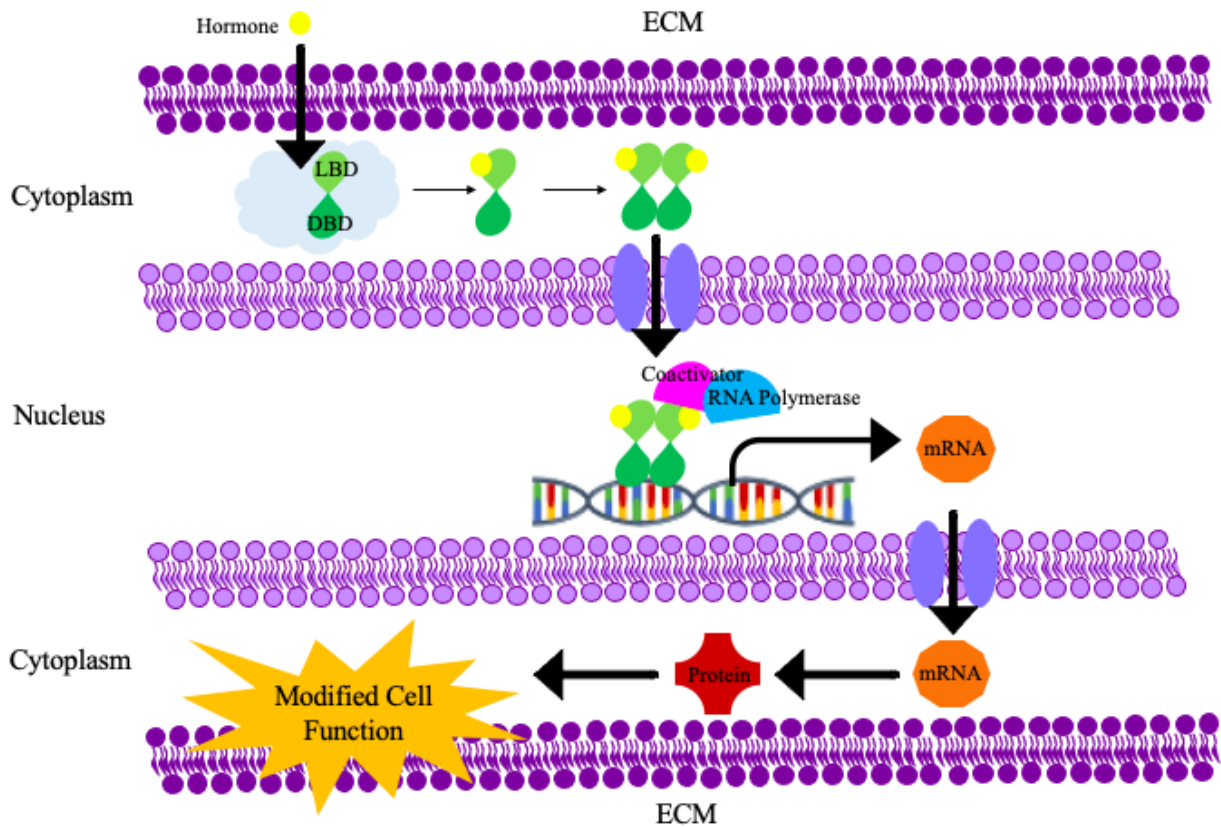


**Figure 1.3 Locations of hyper and hypomethylation in colorectal cancer.** Figure from Kerachian et al., 2020 showing a data summary schematic of the location and frequency of hypermethylation and hypomethylation uncovered in colorectal cancer tissue as opposed to healthy tissue. 71% of CpG islands have been hypermethylated in the cancerous tissue sampled.



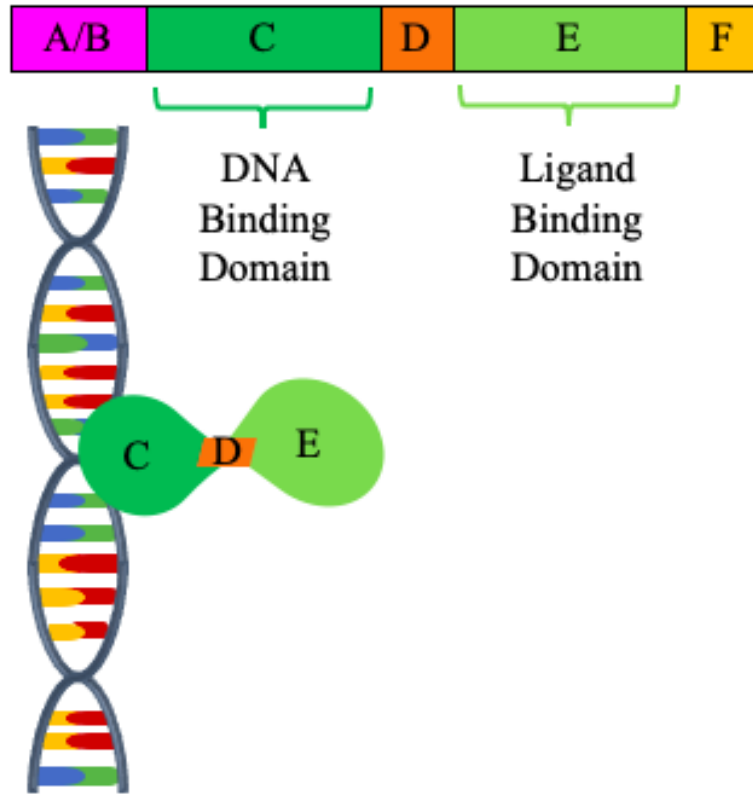
## *Nuclear Hormone Receptors*

Nuclear hormone receptors (NHRs) are a group of ligand activated transcription factors that can bind to both steroid hormones and lipophilic, non-steroid hormones and serve as signal transducing molecules in multicellular organisms (Lalli, 2014; McCabe, 2007; Vanden Heuvel, 2015). An overview of the ligand binding NHR pathway is shown in **Figure 1.4**, where an extracellular hormone signal initiates a cascade reaction that travels through the cytoplasm and into the nucleus where the NHR binds to DNA promoter regions and induces a change in gene expression. NHRs control a broad range of processes, including the regulation of cell growth and proliferation, cardiovascular function, reproduction and sexual determination in development, just to name a few.



**Figure 1.4 Activation of the nuclear hormone receptor (NHR) pathway.** Figure adapted from Heskett, 2014 demonstrating the nuclear hormone pathway at a cellular level. The process begins inside the cytoplasm where a hormone binds to the nuclear hormone receptor complex and dimerizes. The dimer is actively transported into the nucleus where a coactivator attaches to the dimer to assist in the binding of RNA polymerase. This complex attaches to the hormone response element (HRE) region on the target gene and modifies gene expression.

The functionality of NHRs follows their unique structure consisting primarily of two major regions: the DNA Binding Domain (DBD) and the Ligand Binding Domain (LBD) (**Figure 1.5**). The DBD, located near the N-terminus of most NHRs, is composed of two highly conserved zinc-finger regions that mediate binding to specific DNA sequences typically located in the promoter region of target genes. The DNA regions that are bound by a NHR are called hormone response elements, or HREs, and consist of two repeats of a hexanucleotide sequence. The LBD is located at the C-terminal region of NHRs and is responsible for hormone binding which, in turn, results in a conformational change in the NHR structure. This conformational change affects the interaction of various NHR cofactors, which can be classified as either coactivators or corepressors, and functions together with the NHR to mediate changes in gene expression.



**Figure 1.5 Multi-dimensional representation of a standard NHR.** Figure adapted from Fruchart et al., 2019 providing the general structure of NHRs. The A/B, D, and F regions are variable while the C and E regions are conserved through all classes of NHRs. Region A/B is the variable N-Terminal, Region C is the DNA binding domain or DBD, Region D denotes the hinge region, E is the ligand binding domain or LBD, and F is the variable C-terminal domain.

Based on dimerization and DNA-binding properties, NHRs fit into one of four different groups: steroid hormone receptors, repeat (RXR) and symmetrical repeat (LXR) binding receptors, ligand-dependent receptors, and monomeric receptors that bind to core sites (**Table 1.1**) (Mangelsdorf et al., 1995). All of these NHRs share certain common structures and functional domains, but they differ in how and where they bind to target HRE sequences based on variations occurring in the N-terminal region, C-terminal region, and hinge region. For instance, steroid receptors (Type 1) typically bind ligands in the cytoplasm before being actively transported into the nucleus, while RXR heterodimers (Type 2) remain in the nucleus at all times. Both steroid receptors (Type 1) and dimeric orphan receptors (Type 3) bind HREs with sequence specific binding recognition half-sites, but Type 1 binds to inverted HREs that are separated by a variable region, and Type 3 binds to HREs that are direct repeats. Unlike Types 1, 2, and 3, Type 4 NHRs bind to only a single half-site HRE on the target gene (Klinge, 1997). Most orphan nuclear hormone receptors fall into either the dimeric or monomeric categories.

**Table 1.1 The four subclasses of nuclear hormone receptors.** Adapted from Mangelsdorf et al., 1995, each class of NHR is identified by the variable region based on dimerization and DNA-binding properties. The regions labeled with question marks represent orphan segments where the ligands remain unknown.

	<b>Dimerization</b>	<b>HRE Binding</b>	<b>Examples</b>
<b>Type 1:</b> Steroid Receptors	Homodimer	Inverted specific half-sites	Glucocorticoid Receptor, Progesterone Receptor, Androgen Receptor, Estrogen Receptor
<b>Type 2:</b> Heterodimers with RXR	Heterodimer	Repeat, half-sites separated by a variable region	Thyroid Hormone Receptor, Eicosanoid Receptor
<b>Type 3:</b> Dimeric Orphan Receptors	Homodimer	Direct repeat half-sites	Retinoid X Receptor
<b>Type 4:</b> Monomeric Orphan Receptors	Monomer	Single, half sites	DAX-1 Receptor

Critically, nuclear hormone receptors play complex roles in cancer progression and tumorigenesis. One such example of the complexity of NHRs in cancer is the repression of thyroid hormone nuclear receptors (TRs) that mediate the growth, differentiation, and metabolic functions that are promoted by thyroid hormone. Studied in breast and colon cancer, TR is expressed in low quantities and due to crosstalk with the tumor suppressor protein p53, TR cannot function as a gene activator and regulator of cancer cell growth (Bhat et al., 1997). Other studies have highlighted the importance of NHRs as drug targets for cancer treatment. Specifically, the expression of orphan nuclear hormone receptors in the subfamily NR4A1/NUr77/NGFIB have been implicated in the progression of cervical cancer. Research suggests that these NHRs are affiliated with the survival of cervical cancer cells and that the downregulation of gene expression of NR4A2 may suppress cancer progression (Ke et al., 2004). Alternatively, the NR4A nuclear receptor family serves as tumor suppressors in Acute Myeloid Leukemia (AML) where oncogenic promoting pathways are aberrantly activated and overexpressed (Call et al., 2020). Other tumor suppressors such as the Nuclear Receptor Subfamily 0, Group B Member 2 (NR0B2), also referred to as the small heterodimer partner, SHP, are epigenetically silenced via hypermethylation in the promoter region in hepatocellular carcinoma (He et al., 2008). Thus, expression of nuclear receptors have increasingly become possible therapeutic targets for cancer treatment (Call et al., 2020). This further gives rise to the possibility that expression of the gene of interest for this thesis, *DAX-1*, may have oncogenic correlations.

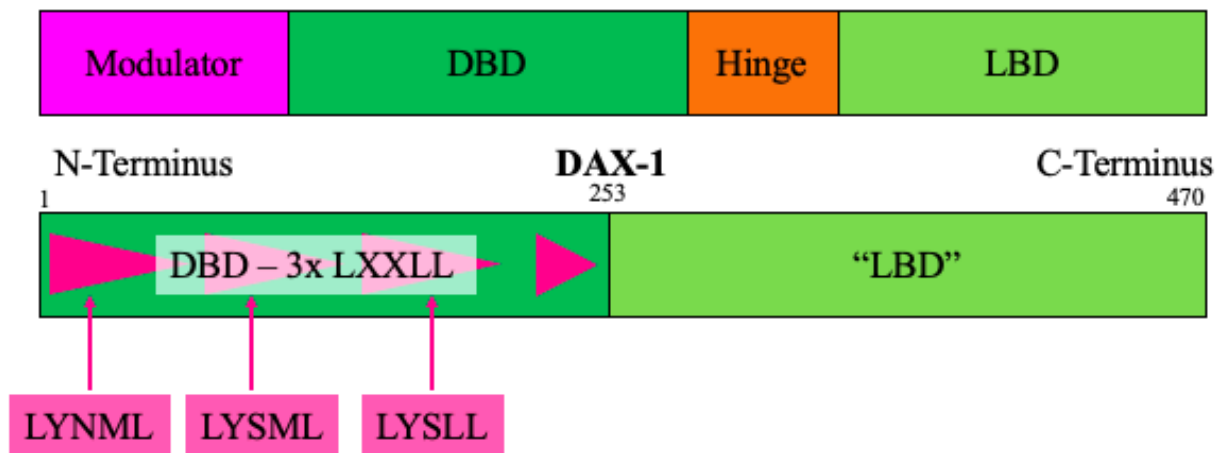
## ***DAX 1/NR0B1***

The gene and nuclear hormone receptor DAX-1, is the focus of the experiments outlined in this thesis. As previously described, most nuclear receptors bind directly to HRE sequences in the promoter regions of target genes. However, orphan nuclear receptors, including DAX-1, lack a ligand binding domain (LBD) yet can still mediate functions such as dimerization and coactivator interactions. DAX-1 specifically belongs to the subfamily of orphan hormone nuclear receptors. It is identified as an orphan because, unlike the steroid and non-steroid hormone receptors, DAX-1 has not been shown to bind to a specific ligand. As its name implies, multiple copies of the *DAX-1* gene region on the X chromosome are associated with male to female sex reversal in human development (Dosage Sensitive Sex Reversal, or DSS). The role of DAX-1 in this context is as a negative regulator of estrogen, progesterone, and androgen receptors and therefore, antagonizes testicular development through inhibition of gene expression (Iyer & McCabe, 2004). More generally, DAX-1 is characterized as a repressor of gene expression activated by ligand-induced transcriptional activation (Lalli, 2014; Lalli et al., 1997). DAX-1 suppresses steroidogenesis in adrenal cells by binding to hairpin DNA structures. However, the function of DAX-1 goes beyond suppression; the unique structure of this NHR allows for transcriptional silencing. DAX-1 serves as a form of tumor assessor in prostate cancer and pituitary adenomas as well as an indirect tool for measuring androgen receptor expression in breast cancer and estrogen receptor expression in endometrial carcinoma (Lalli, 2014).



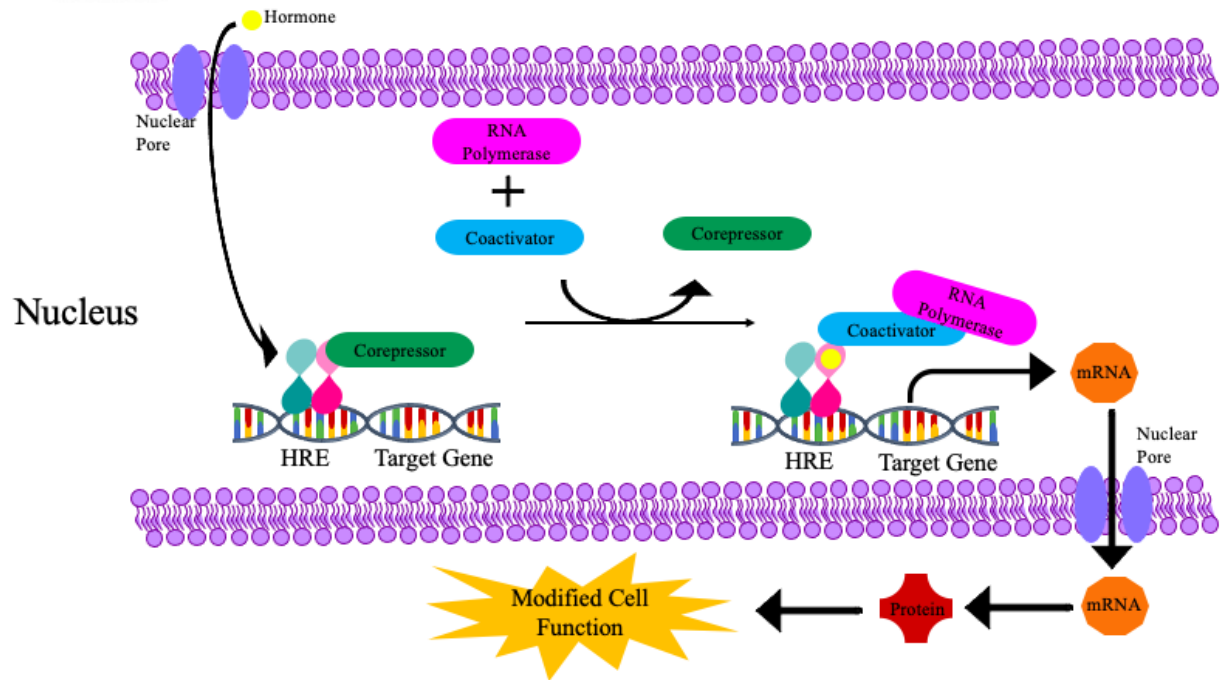
As an orphan receptor, DAX-1 does not follow the typical NHR structure. Instead, DAX-1 lacks the modulator and hinge regions as well as the conserved zinc finger DNA binding domain (**Figure 1.6**). Intriguingly, DAX-1 has three times as many leucine rich LXXLL repeats than are commonly found in coactivator proteins that are important in mediating binding to ligand induced, AF-2 (Activating Function 2) domains on other NHRs (Lalli, 2014; Zanaria et al., 1994). The complex formed by the LXXLL motif and the LBD can then recruit the silencing domain in the DAX-1 C-terminus leading to transcriptional silencing (Lalli, 2014).

## Nuclear Receptor



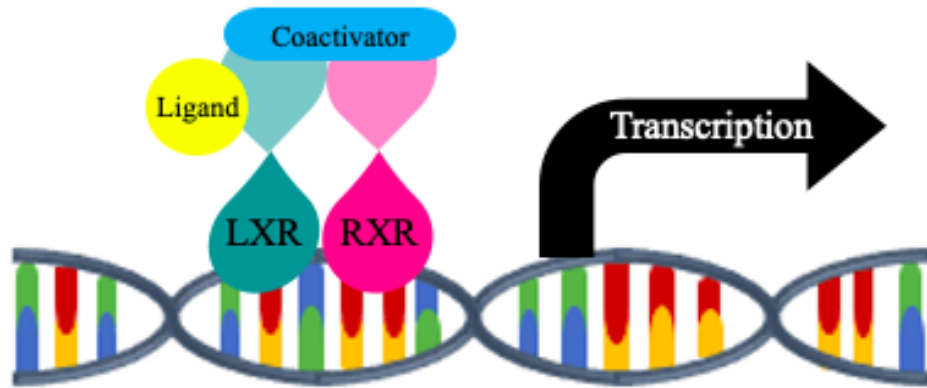
**Figure 1.6 Structure of the DAX-1 NHR compared to a typical NHR.** Unlike other nuclear receptors, DAX-1 does not have a modulator (A/B) or hinge region (D) and what would be the DNA binding domain (DBD, region C) is missing the zinc finger region that is typical in other nuclear hormone receptors. Instead, the DAX-1 DBD contains three leucine rich LXXLL repeats that have been shown to mediate cofactor binding in other nuclear hormone receptors. The DAX-1 protein consists of 470 total amino acids, with the N-terminal region spanning the first 253 amino acids. The DBD is located in this region and includes 3 complete and one incomplete Alanine/Glycine (A/G) rich repeats. Each of these A/G rich repeat regions contains 3 LXXLL-like motifs.

Orphan NHR's can regulate gene expression and endocrine responses without binding to a ligand. This process is referred to as the ligand independent pathway (**Figure 1.7**). In the absence of a ligand, nuclear receptors work in conjunction with coregulators through protein-protein interactions to recruit proteins such as RNA polymerase.



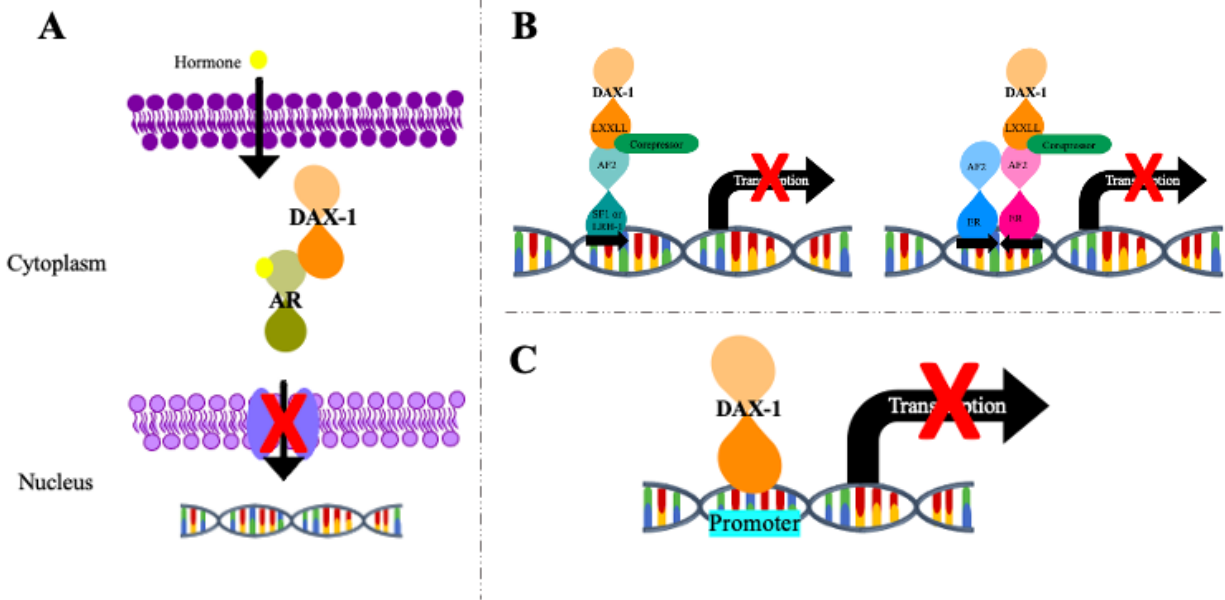
**Figure 1.7 Ligand independent binding nuclear hormone receptor pathway.** Figure adapted from Guo & Ren, 2013, highlights the mechanism of NHRs within the nucleus. In the absence of a ligand, the NHR binds a corepressor that leads to transcriptional repression. Upon ligand binding, the NHR releases the corepressor and binds a coactivator that allows for the recruitment of RNA polymerase.

Coregulators are classified as either coactivators or corepressors. Coactivators bind to the ligand-dependent (or ligand activated) NHRs to increase target gene expression. **Figure 1.8** shows the activated Liver X Receptor (LXR) bound by a ligand which will form a heterodimer with Retinoid X Receptor (RXR). Together, they are bound by a coactivator that recognizes target genes (Zanaria et al., 1994). Conversely, corepressors bind to unliganded NHRs, resulting in a decrease in gene expression.



**Figure 1.8 Mechanism of a Type 2 NHR binding with coactivator.** Figure adapted from Heskett, 2014; only one nuclear receptor of this heterodimer can bind a ligand, in the example shown it is LXR. However, RXR recruits a coactivator to allow for dimerization and to induce transcription.

Thus, while the ligand binding domain (LBD) of an orphan NHR such as DAX-1 does not bind to any specific ligand, it does have other functions. Namely, the LBD is important for receptor dimerization and coactivator interactions. There are three pathways (**Figure 1.9**) that describe the mechanisms by which DAX-1 can repress transcription during gene regulation: by binding the AF-2 site of another NHR, by hijacking the coactivator binding domain in other NHRs, or by binding directly to the promoter of single stranded DNA (Iyer & McCabe, 2004).



**Figure 1.9 The three ways in which DAX-1 can repress transcription.** Adapted from Iyer & McCabe, 2004, DAX-1 can silence gene expression via three pathways. A) DAX-1 hijacks an activator (AR) and prevents it from entering into the nucleus. B) DAX-1 inhibits gene expression by binding the AF-2 site of another NHR and works in conjunction with corepressors. C) DAX-1 can also bind directly to the promoter region of single stranded DNA of target genes and inhibit transcription.



Previous research has shown that NHRs regulate a wide-range of normal biological processes, including embryonic development and sex determination (Lalli, 2014). In embryonic stem cells, orphan NHRs, specifically LRH-1, DAX-1, and SF-1, work together with a complex of proteins to maintain pluripotency. DAX-1, in particular, functions to maintain totipotency in embryonic stem cells and was first associated with X-linked adrenal hypoplasia congenita (AHC) and dosage sensitive sex reversal (DSS) in these cells (Lalli et al., 1997; McCabe, 2007). In DSS, mutations on the X chromosome result in sex reversal due to a duplication in the region containing the *DAX-1* gene (Lalli, 2014). When expressed in the hypothalamus and pituitary, mutations in DAX-1 are responsible for most cases of cytomegalic AHC and may also cause hypogonadotropic hypogonadism (HHG) (McCabe, 2007). AHC specifically is the result of mutations in the *DAX-1* gene that cause diminished development of adrenal tissue, leading to a reduction in adrenal hormone production (Lalli et al., 1997). Since this initial discovery of DAX-1 function, DAX-1 has quickly become a topic of scientific interest because of its presence in all regions of the hypothalamic-pituitary-adrenal-gonadal (HPAG) axis during development and in adult tissues.

NHRs have been shown to play important roles in abnormal physiological processes, including tumor cell initiation and cancer progression. Previous studies by our lab and others have shown DAX-1 is expressed in different breast and prostate cancer cell lines, however, expression levels vary widely (Boitano, 2009; Heskett, 2014). Our lab has found that DAX-1 functions, in general, as a repressor of cancer cell growth. While the potential correlative effects of DAX-1 and cancer have been studied in breast, prostate, lung, adrenal, and liver cancer, the precise mechanism of this action is not well understood. In order to better understand the role of DAX-1 not only in regulating cancer cell growth, but also in normal physiological functions, it is essential to determine what factors are directly responsible for controlling its expression (Conde et al., 2004;

He et al., 2008; Heskett, 2014; Jiang et al., 2014; Kudryavtseva et al., 2018; Kumata et al., 2018).

**We hypothesize that the *DAX-1* gene is epigenetically regulated, specifically via methylation, in cancer cells, thereby reducing its expression. Differences in the methylation of CpG islands located near the *DAX-1* promoter result in the variation of DAX-1 expression in different human cell lines.** To investigate this hypothesis, a broad assessment of the promoter region of the *DAX-1* gene was initially performed. Initial experiments explored *DAX-1* expression at the RNA and protein levels. These results were then followed by assays broadly identifying degrees of methylation of CpG islands. Most DNA methylation occurs at CpG islands where there is a high concentration of CpG dinucleotides and can suppress the expression of nearby genes (Manoochehri et al., 2016). Within the promoter region of the human *DAX-1* gene, there are nine CpG islands of CCGG sequence (**Figure 1.10**).

## Human orphan nuclear receptor (DAX1) gene

1306 - 3106 shown

**TATA Box:** 1521-1525

Exon 1: 1580-2747

Intron: 2748-6132

Exon 2: 6133-6377

```
CAGGGAAAGGGGTAATGAGAGGAAGGAGGAAAGTGTCCAGGAGCTCCCACGCTGCTGTTCTTCC
ATTTCCAGCTTTTAAAGAGCACCCGCCCTTCGAACCACCGAGGTCATGGGCGAACACA CCGGA
GCGCAGCACCGCGCCCCCGCACACACCGCCCGCTCCGCGCCCTTGCCCAGACCGAGGCGGC
CGACGCGCCTGCGTGCGCGCTAGG TATAAATAGGTCCAGGAGGCAGCCACTGGGCAGAACTGG
GCTACGGGCGCCGCGGGCCATGGCGGGCGAGAACCACAGTGGCAGGGCAGCATCCTCTACAAC
ATGCTTATGAGCGGAAGCAAACGCGCGCGGCTCCTGAGGCTCCAGAGACGCGGCTGGTGGATC
AGTGCTGGGGCTGTTTCGTGCGGCGATGAGC CCGGGGTGGGCAGAGAGGGGCTGCTGGGCGGGCG
GAACGTGGCGCTCCTGTACCGCTGCTGCTTTTTCGGTAAAGACCACCCACGGCAGGGCAGCATC
CTCTACAGCATGCTGACGAGCGCAAAGCAAACGTACGCGGCACCGAAGGCGCCGAGGCGACGC
TGGGTCCGTGCTGGGGCTGTTTCGTGCGGCTCTGATC CCGGGGTGGGCAGAGCGGGGCTT CCGGG
TGGGCGGCCCGTGGCACTCCTGTACCGCTGCTGCTTTTGTGGTGAAGACCACCCGCGGCAGGGC
AGCATCCTCTACAGCTTGCTCACTAGCTCAAAGCAAACGCACGTGGCT CCGGCAGCGCCCGAGG
CACGGCCAGGGGGCGCGTGGTGGGACCGCTCCTACTTCGCGCAGAGGCCAGGGGGTAAAGAGGC
GCTACCAGGCGGGCGGGCCACGGCGCTTCTGTACCGCTGCTGCTTTTTCGGTGAAGACCACCCG
CAGCAGGGCAGCACCCCTCTACTGCGTGCCCACGAGCACAAATCAAGCGCAGGCGGCT CCGGAGG
AGCGGCCGAGGGCCCCCTGGTGGGACACCTCCTCTGGTGCCTGCGG CCGGTGGCGCTCAAGAG
TCCACAGGTGGTCTGCGAGGCAGCCTCAGCGGGCCTGTTGAAGACGCTGCGCTTCGTCAAGTAC
TTGCCCTGCTTCCAGGTGCTGCCCTGGACCAGCAGCTGGTGGTGGTGCGCAACTGCTGGGCGT
CCCTGCTCATGCTTGAGCTGGCCAGGACCGCTTGCAGTTCGAGACTGTGGAAGTCTCGGAGCC
CAGCATGCTGCAGAAGATCCTCACCACCAGGCGGCGGGAGACCAGGGGGCAACGAGCCACTGCC
GTGCCACGCTGCAGCACCATTGGCACCG CCGGCGGAGGCCAGGAAGGTGCCCTCCGCCTCCC
AGGTCCAAGCCATCAAGTGCTTTCTTTCCAAATGCTGGAGTCTGAACATCAGTACCAAGGAGTA
CGCCTACCTCAAGGGGACCGTGCTCTTTAACC GGTAAGGGTACTGGCCTTAGGCG CCGGCTT
TTCCAGCTCACAAAAGCATCGGGCAGTGCCTATCTAGGGGCGCGGGCAGTAACGAGTTTTTCAG
TGATCAGGAGAGTGTGGGGCAAAGGTGAAGAAATCGTGAATAACTCAGCAGAGTTGGGGTGGG
GAGCTCCAGGAACCACTTCTGCTGGGTGGGCTGCTATCAGAACTCAGCCAAGAGGAGGGGAGT
TGTTTGTTTAGGTTTGTACTTGGCTCTCTACACATTTCTTACCATAGAAAAGTTTGTGCCTTCA
TGGGAAATGGTTATTCTTTCTTTAGCTTTCTTTAAGTCCAGAGCATATCTTTTTCTAAAA
AAAGTTTT
```

**Figure 1.10 Promoter region of Exon 1 of the *DAX-1* gene.** Highlighted in red is the transcriptional start site. Each region highlighted in yellow is a CCGG CpG island that may be a target of cytosine methylation.

Following this initial analysis, the focus of this project was refined to investigate three cell lines: one cancerous cell line with a high degree of methylation, one cancerous cell line with a low degree of methylation, and one non-cancerous control cell line. Within these three cell lines, sequence analysis of bisulfite modified gDNA was utilized to more accurately assess the degree of methylation in a region of interest. Finally, the mechanism of DNA methylation in these cell lines through the use of chromatin immunoprecipitation (ChIP) assays was investigated in order to hone in on the different methylating protein occupancy between cancerous and non-cancerous breast cells. Through the following experiments, a better understanding of the factors that control *DAX-1* expression in a variety of human cell lines was obtained. The contribution of these results will provide a deeper understanding as to how *DAX-1* expression may be controlled in human disease and may lead to the development of more efficacious and targeted therapies in the future.

## **Chapter 2: Determination of the level of *DAX-1* expression across different human cell lines**

### ***Introduction***

Previous research in the Tzagarakis-Foster lab has shown that the *DAX-1* promoter region and exon 1 contain CpG islands that can be methylated (Dishington, 2017; Heskett, 2014; Judge, 2011). These earlier experiments examined only a few cell lines for *DAX-1* expression and methylation status. Thus, the first specific aim of this thesis research was to determine the level of *DAX-1* expression across cancerous and noncancerous human cells using various molecular techniques including polymerase chain reaction (PCR), quantitative PCR (qPCR), western blot, and restriction digestion analysis.

Each of the cell lines examined were selected for their association with DAX-1 or other nuclear hormone receptors based on previous research in the Tzagarakis-Foster lab or literature reviews (Conde et al., 2004; He et al., 2008; Heskett, 2014; Jiang et al., 2014; Kudryavtseva et al., 2018; Kumata et al., 2018). Amongst the cell lines not previously investigated by the Tzagarakis-Foster lab but included in this research are those derived from cervical and hepatocellular cancer. In 2018, cervical cancer was the fourth most lethal form of cancer in women worldwide. Studies have found that the DAX-1 protein is upregulated in cervical cancer and when silenced, tumorigenicity is inhibited (Liu et al., 2018). Furthermore, DAX-1 has been shown to transcriptionally repress genes that regulate oncogenic gene expression downstream. Most of the cell lines included in this study (e.g. testes, ovaries and breast) are associated with sex steroid synthesis. The exception to this is the Hep-3B cell line, which is isolated from a hepatocellular carcinoma. Previous findings immunolocalized synthesized sex steroids and hormone receptors, including DAX-1, in the mucous epithelial cells of neoplasms on the liver (Kumata et al., 2018).

Examination of *DAX-1* expression in liver cells was included in this study to provide a comparison against the steroid hormone producing tissues previously investigated in the Tzagarakis-Foster lab.

Ultimately, experiments confirmed the detection of DAX-1 in the genome of the cancerous and control cell lines. Following successful detection of DAX-1 at the genome level, RNA and protein level analyses confirmed differential expression of DAX-1 within the cancer cell lines. General analysis of methylation status was assessed with methylation specific restriction enzyme assays. The restriction enzyme analysis highlighted the diverse levels of methylation across the promoter region, indicating a correlation between increased methylation and decreased DAX-1 expression.

## ***Materials and Methods***

### *Tissue Culture*

Cell lines, obtained from American Type Culture Collection, were cultured according to the recommended guidelines (*ATCC Cell Lines*, n.d.). Antimycotic and antibiotics were added to the media to prevent bacterial and fungal infection of the lines. Multiple cancer cell lines were analyzed for the differential expression and varying degrees of hypermethylation of the *DAX-1* gene. The MCF10A cell line is derived from an immortalized breast tissue and serves as a non-cancerous control. While MCF10A cells are non-cancerous and not derived from a tumor, they are not considered 'normal'. The MCF10A cells originate from a tissue sample of a patient with fibrocystic disease and were immortalized through consistent passaging of the cells in a low calcium media. In addition to this control cell line, five cancerous cell lines (**Table 2.1**) were analyzed for *DAX-1* expression. Each cell line was chosen based on prior investigation by the Tzagarakis-Foster lab or the association that each particular cancer has with nuclear hormone receptors such as DAX-1. Previous work in the Tzagarakis-Foster lab has shown that DAX-1 is expressed in varying degrees within breast, lung, and adrenal cancer cell lines. In addition to these cell lines, cervical adenocarcinoma cells and liver cells, shown to express *DAX-1*, were also assessed (Kumata et al., 2018; Liu et al., 2018). MCF7 cells are human epithelial cells from a female with breast cancer (adenocarcinoma) and express estrogen receptors alpha and beta and are responsive to estrogen hormones. Human lung cancer cells, A549 cells, were taken from an adult male with carcinoma. SW13 cells are derived from a female with grade IV carcinoma in the adrenal gland/cortex. Hep-3B cells are isolated from tissue samples of a child with hepatocellular carcinoma.

**Table 2.1 Cell lines used to investigate *DAX-1* expression.**

MCF7	Metastatic (pleural effusion) mammary gland, breast cancer
A549	Lung, Carcinoma
HeLa	Cervical adenocarcinoma
SW13	Carcinoma, adrenal gland/cortex
Hep-3B	Liver, hepatocellular carcinoma
MCF10A	Mammary gland/breast, fibrocystic disease (immortalized)



## PCR

Standard polymerase chain reaction (PCR) was performed to confirm the presence of *DAX-1* in each cell line. Genomic DNA (gDNA) was isolated from cultures grown in T75 tissue culture flasks using the PureLink® Genomic DNA Mini Kit (Invitrogen, Life Technologies, catalog # K1820-02). Following gDNA isolation, samples were quantified using a Nanodrop spectrophotometer and each sample was normalized to 150ng per  $\mu\text{L}$ . Genomic DNA samples were analyzed for *DAX-1* genomic detection using PCR. Samples were prepared using GoTaq 2x Master Mix (Promega), and primers were designed to two different regions of the X chromosome region containing the *DAX-1* gene region. The first primer set amplified a region spanning from Exon 1 into Intron 1, and the second targeted a region entirely within the first intron. Targeting these regions ensured that amplified products were generated from genomic DNA as opposed to mRNA. PCR conditions and primers (**Tables A.1 and A.2; Appendix A**) obtained from Integrated DNA Technologies were optimized over multiple trials.

## *qPCR*

In order to assess *DAX-1* mRNA expression in the cell lines, quantitative PCR, or qPCR, was utilized. qPCR, as opposed to “end-point” PCR, combines the amplification and detection steps and allows for quick and highly accurate data collection. Furthermore, the process is highly sensitive compared to alternative methods, and can detect differential gene expression more precisely between samples with lower degrees of variation (M. L. Wong & Medrano, 2005). Confluent cells were isolated from T75 tissue culture flasks and total RNA was isolated using the Monarch® Total RNA Miniprep Kit from New England Biolabs® Inc. (Product # T2010S). Following RNA isolation and quantification using a Nanodrop spectrophotometer, cDNA was synthesized using Maxima H Minus First Strand cDNA Synthesis Kit (Thermo Fisher, Product # K1651). qPCR reactions were prepared using PerfeCTa® SYBR® Green Fast Mix® from QuantaBio (Cat. # 95072-250, -012, -05K). SYBR green exhibits very little fluorescence when it is free in solution, but the fluorescent signal increases substantially when it binds non-specifically to double stranded DNA. cDNA samples were amplified using primers directed to the *DAX-1* gene. Primer and qPCR parameters (**Tables A.1 and A.2; Appendix A**) were used to isolate a region of the *DAX-1* gene that was not removed during RNA splicing.

The first means of assessing *DAX-1* RNA expression utilized the standard curve method (Qiagen, n.d.). In this approach, a set of serial dilutions was prepared from a DNA template of known concentration. These samples were used to obtain a standard curve that was used for the relative quantification of unknown samples. The DNA template used to prepare a standard curve was generated from the same *DAX-1* amplicon that was generated using a *DAX-1* plasmid. The amplified *DAX-1* plasmid DNA was prepared with the Wizard® SV Gel and PCR Clean-Up System (Product # A9281, Promega). Amplification and analysis was performed using the BioRad

CFX-96 system. Utilizing this plasmid as a control allowed for direct quantitative comparison of *DAX-1* expression in the experimental cell lines. Data was collected in sets of three technical replicates per biological sample and over a minimum of three biological replicates. The standard deviation corresponds with the triplicate samples analyzed on a single 96-well plate and was calculated in Microsoft Excel with the following equation (Microsoft, n.d.):

$$\text{Standard Deviation} = \text{STDEV} = \sqrt{\frac{\sum(x_i - x_{ave})^2}{(n-1)}}; \text{ Where } x_i \text{ is a single value, } x_{ave} \text{ is the mean of the sample set, and } n \text{ is the number of samples.}$$

In addition to utilizing a standard curve of DAX-1 plasmid for comparison described above, a second means of analysis was also implemented. In this approach, each of the cancerous cell lines was normalized against the control cell line to compare relative DAX-1 expression in cancerous versus noncancerous cells. The normalization was calculated based on the C<sub>q</sub> value (the number of amplification cycles) with the following equation:

$$2^{-\Delta C_q}, \text{ where } \Delta C_q = C_{q \text{ sample}} - C_{q \text{ control}}, \text{ or } \Delta C_q = C_{q \text{ cancerous}} - C_{q \text{ MCF10A}}$$

The following equation was used to calculate the standard error of the two means from the normalized cell lines against the noncancerous MCF10A cells (*Comparison of Means Calculator*, 2021):

$$\text{Standard Error} = \sqrt{\frac{(n_1-1)s_1^2 + (n_2-1)s_2^2}{(n_1 + n_2) - 2}}; \text{ where } n_1 \text{ is a single } C_{q \text{ sample}}, n_2 \text{ is a single } C_{q \text{ MCF10A}},$$

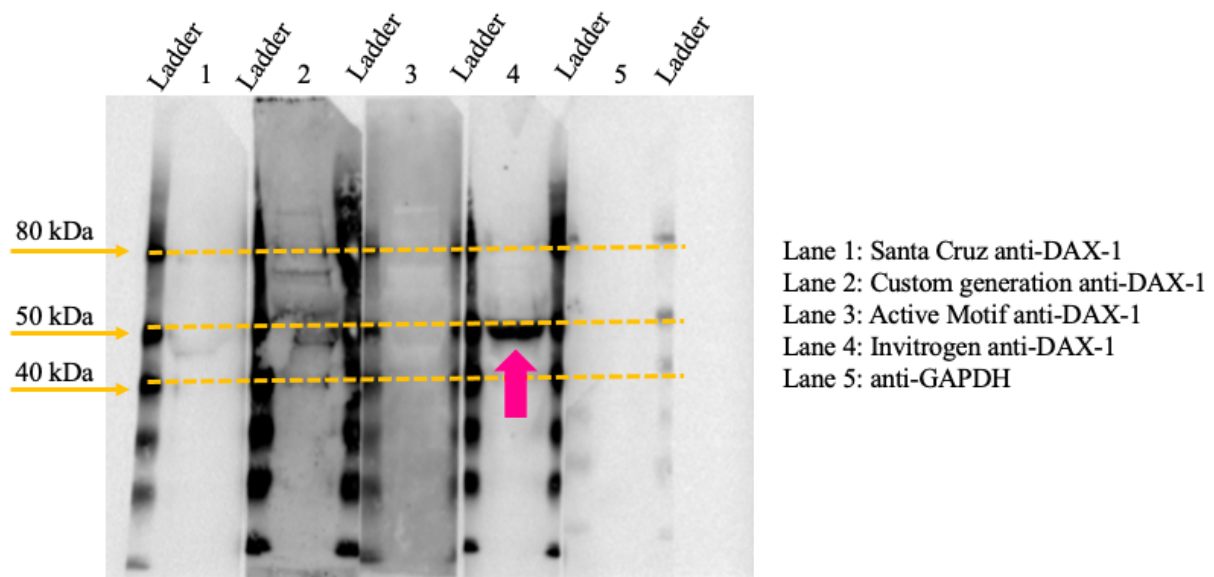
$s_1$  is the standard deviation between the sample replicates,  $s_2$  is the standard deviation between the MCF10A replicates, and  $n$  is the number of technical replicates of each sample respectively.

### *Protein Isolation and Western Blot Analysis*

Total protein lysate from confluent 10 cm tissue culture dishes was collected using the Cell Extraction Buffer kit (Invitrogen, Life Technologies, Ref# FNN0011) and Halt™ Protease Inhibitor Single-Use Cocktail (1000X) from Thermo Scientific (Ref #1860932). Protein lysates were quantified using a Bradford protein assay. Pre-Diluted Protein Assay Standards: Bovine Albumin (BSA) set from Thermo Scientific (Prod. #23208) were used to generate a standard curve, and samples and standards were prepared using the Bio-Rad Protein Assay Dye Reagent Concentrate (5x) from Bio Rad (Cat. #5000006). All samples were measured via spectroscopy.

Western blot analysis was carried out according to the NuPAGE Novex Bis-Tris protocol (Invitrogen, Carlsbad, CA). 10µg of each isolated protein sample was added to NuPAGE LDS sample loading buffer (1X final concentration), NuPAGE reducing agent (1X final concentration) and nuclease free water to a total volume of 20µl. 5µL of a 10-20% Tris-glycine Gel Ladder from Protein Tech was loaded into one lane for sample analysis after imaging. Samples were electrophoresed using the XCell II Blot Module (Invitrogen, Carlsbad, CA) at 200V for 60 minutes. Proteins were transferred to PVDF membranes using the XCell II Blot Module apparatus. Following transfer, PVDF membranes were washed three times in 1X TBST for 10 minutes per wash at room temperature. Membranes were blocked in 5% milk in 1X TBST for 1 hour at room temperature. Primary antibodies (DAX-1: Invitrogen anti-rabbit, GAPDH: GeneTex anti-mouse) were diluted 1:1000 in 5% milk in 1X TBST, and added to blots to incubate overnight on a rotator at 4°C. This antibody was selected following a survey of anti-DAX-1 antibodies (**Figure 2.1**). Following overnight incubation, blots were washed three times for ten minutes in 1X TBST and incubated for 60 minutes at room temperature in secondary antibody diluted 1:2000 (GeneTex anti-rabbit, BD Pharmingen anti-mouse) in 5% milk in 1X TBST. PVDF membranes were washed

three times for 10 minutes in 1X TBST. In order to detect protein-antibody complexes, chemiluminescent SuperSignal™ West Femto Maximum Sensitivity Substrate (Thermo Scientific REF 34095) was added to each membrane and incubated according to the manufacturer's recommendation. Membranes were exposed and images captured using the GelDoc Imager and camera system (BioRad, Hercules, CA).



**Figure 2.1 Optimization of primary antibody selection for assessing DAX-1 protein expression.** While faint ‘on-target’ bands are visible at 50kDa indicating antibody binding the DAX-1 in lanes 1-4, maximum signal was detected with the primary anti-DAX-1 antibody for Invitrogen (Lane 4). Protein size is denoted with YesBlot™ Western Marker 1 (SmoBio, Product #WM1000).

### *Methylation Specific Restriction Enzyme Analysis and PCR*

For each cell line, genomic DNA was isolated and used for methylation specific restriction enzyme digestion and analysis. Genomic DNA (gDNA) was isolated through the same technique described previously. The gDNA samples were digested using methylation-sensitive restriction enzyme *HpaII* and its isoschizomer *MspI*, which has the same recognition site but is methylation insensitive (New England BioLabs, Inc.). A fragment was designated ‘unmethylated’ if no PCR product was observed after digestion; alternatively, the fragment was designated ‘methylated’ if it was amplified after digestion (Melnikov, 2005; Salmon et al., 2008; Yang et al., 2011). Together, these enzymes can differentiate methylation status of CCGG dinucleotide sequences (**Figure 2.2**).

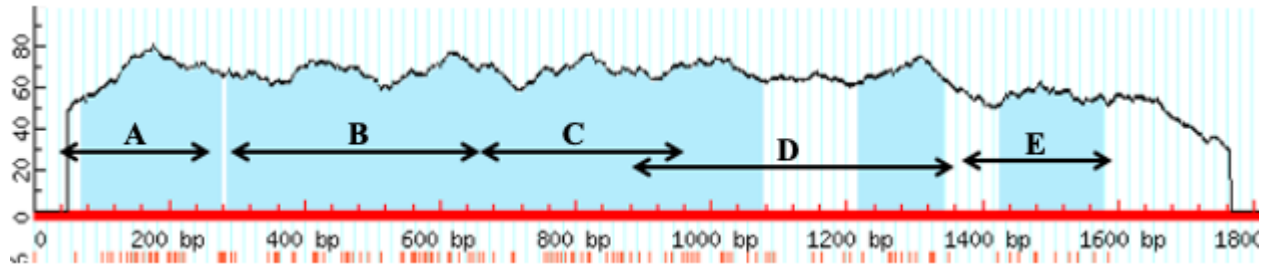
No Methylation	CpG Methylated	CpCpG Methylated	Hemi-Methylated	Hyper Methylated
<p><i>HPA II</i>: cut</p> <p><i>MSP I</i>: cut</p>	<p><i>HPA II</i>: cut</p> <p><i>MSP I</i>: cut</p>	<p><i>HPA II</i>: not cut</p> <p><i>MSP I</i>: cut</p>	<p><i>HPA II</i>: not cut</p> <p><i>MSP I</i>: cut</p>	<p><i>HPA II</i>: not cut</p> <p><i>MSP I</i>: cut</p>

**Figure 2.2 Methylation status sensitivity to enzymes *HpaII* and *MspI*.** Figure adapted from Fu et al., 2012, these enzymes target CCGG CpG islands and ‘cut’ depending on the location of the methyl group. These enzymes have a sensitivity to CCGG methylation status and can determine the location of methylation through a restriction digest of the gDNA when primed to target the promoter region of DAX-1. The addition of a methyl group (CH<sub>3</sub>) protects against enzyme digestion. Therefore, regions marked as ‘cut’ are unprotected and regions marked as ‘not cut’ are protected via methylation (Salmon et al., 2008; Yang et al., 2011).



Both of these enzymes target CpG islands, specifically those of CCGG sequence. Reactions containing enzyme, specific buffer, and gDNA were incubated at 37°C for 2 hours. This method, while limited in that it is only a very crude examination of methylation status, can be used to quickly assess the methylation status of the *DAX-1* genomic region in the cell lines described previously. When compared alongside control gDNA, the intensity of products was used to determine whether a CpG-rich region was either hemi-methylated or methylated, unmethylated, or fully methylated. Both the gel image product and the corresponding band intensity were used to categorize CpG islands into one of these three degrees of methylation. A region and its respective CpG island(s) were marked as hemi-methylated or methylated if the product in the *HpaII* lane was of similar intensity as the undigested control, or if the *HpaII* and *MspI* lanes both showed relatively similar products to each other and the control. Alternatively, a region of CpG island(s) was considered methylated following MSRE if the product of the *HpaII* digest was more intense than the control or if it was less than the control and there was negligible product following digestion by *MspI*. Finally, a region and the associated CpG island(s) was deemed unmethylated if there was little to no PCR amplified product following both *HpaII* and *MspI* digestion.

Following the restriction digest with *HpaII* or *MspI* enzymes, DNA was purified (Monarch PCR DNA cleanup kit, New England Biolabs, Inc.) and used as template for standard PCR reactions. CpG islands targeted by *HpaII/MspI* enzymes were located on the NR0B1/DAX-1 sequence using the Li Lab MethPrimer software (L. C. Li & Dahiya, 2002). This software identifies CpG-rich regions containing high densities of CG or CCGG sequences (**Figure 2.3**).



**Figure 2.3 CpG rich regions of the *DAX-1* promoter.** CpG rich regions were identified and compiled using the Meth Primer tool for the Li Lab (L. C. Li & Dahiya, 2002). The transcriptional start site and TATA box are located at the end of Region A, located at approximately 240 base pairs.

Having identified CpG-rich regions, primers for the PCR reactions were designed using Primer3 software v0.4.0 (Kõressaar et al., 2018; Koressaar & Remm, 2007; Untergasser et al., 2012), so that primers would flank the *HpaII/MspI* enzyme cutting site (5'-CCGG-3') in the sequences. Particular attention was given to designing these primers, breaking the CpG-rich region of the DAX-1 promoter into five sub-regions that each contained at least one CCGG sequence (**Figure 2.3**). Furthermore, the primers were developed such that melting temperatures were relatively similar with 5-10°C difference between primer sets (**Table A.2; Appendix A**). In an effort to use these primers in tandem with the digested gDNA, some of the amplified regions overlap and encompass the same CpG islands (**Figure 2.4**). Region A isolated one CpG island and Region B encompassed three unique CpG islands. Regions C and D overlapped, each including 1 unique CpG island, and Region E targeted one CpG island. While MSRE provided a crude assessment of methylation status, minimizing the number of CpG islands targeted within each PCR region allowed for increased specificity in the location of methylation.

## Human orphan nuclear receptor (DAX1) gene

1306 - 3106 shown

**TATA Box:** 1521-1525

Exon 1: 1580-2747

Intron: 2748-6132

Exon 2: 6133-6377

```
CAGGGAAAGGGGTAATGAGAGGAAGGAGGAAAGTGTCCAGGAGCTCCCACGCTGCTGTTCTTCC
ATTTCCAGCTTTTAAAGAGCACCCGCCCTTCGAACCACCGAGGTCATGGGCGAACACACCGGA
GCGCAGCACCGCGCCCCCGCACACACCGCCCGCCTCCGCGCCCTTGCCAGACCGAGGCGGC
CGACGCGCCTGCGTGCGCGCTAGGTATAAATAGGTCCCAGGAGGCAGCCACTGGGCAGAACTGG
GCTACGGGCGCCGCGGGCCATGGCGGGCGAGAACCACCAGTGGCAGGGCAGCATCCTCTACAAC
ATGCTTATGAGCGGAAGCAAACGCGCGGGCTCCTGAGGCTCCAGAGACGCGGCTGGTGGATC
AGTGCTGGGGCTGTTTCGTGCGGCGATGAGCCCGGGTTGGGCAGAGAGGGGCTGCTGGGCGGGCG
GAACGTGGCGCTCCTGTACCGCTGCTGCTTTTTCGGTAAAGACCACCCACGGCAGGGCAGCATC
CTCTACAGCATGCTGACGAGCGCAAAGCAAACGTACGCGGCACCGAAGGCGCCGAGGCGACGC
TGGGTCCGTGCTGGGGCTGTTTCGTGCGGCTCTGATCCCGGGTTGGGCAGAGCGGGGCTTCCGGG
TGGGCGGCCCGTGGCACTCCTGTACCGCTGCTGCTTTTGTGGTGAAGACCACCCGCGGCAGGGC
AGCATCCTCTACAGCTTGCTCACTAGCTCAAAGCAAACGCACGTGGCTCCGGCAGCGCCCGAGG
CACGGCCAGGGGGCGCGTGGTGGGACCGCTCCTACTTCGCGCAGAGGCCAGGGGGTAAAGAGGC
GCTACCAGGCGGGCGGGCCACGGCGCTTCTGTACCGCTGCTGCTTTTTCGGTGAAGACCACCG
CAGCAGGGCAGCACCCCTCTACTGCGTGCCACGAGCACAAATCAAGCGCAGGCGGCTCCGGAGG
AGCGGCCGAGGGCCCCCTGGTGGGACACCTCCTCTGGTGCCTGCGGCCGGTGGCGCTCAAGAG
TCCACAGGTGGTCTGCGAGGCAGCCTCAGCGGGCCTGTTGAAGACGCTGCGCTTCGTCAAGTAC
TTGCCCTGCTTCCAGGTGCTGCCCTGGACCAGCAGCTGGTGTGGTGCGCAACTGCTGGGCGT
CCCTGCTCATGCTTGAGCTGGCCAGGACCGCTTGACAGTTCGAGACTGTGGAAGTCTCGGAGCC
CAGCATGCTGCAGAAGATCCTCACCACCAGGCGGCGGGAGACCGGGGGCAACGAGCCACTGCC
GTGCCACGCTGCAGCACCATTTGGCACCCCGGCGGAGGCCAGGAAGGTGCCCTCCGCCCTCC
AGGTCCAAGCCATCAAGTGCCTTCTTTCCAAATGCTGGAGTCTGAACATCAGTACCAAGGAGTA
CGCCTACCTCAAGGGGACCGTGTCTTTTAACCCGGGTAAGGGTACTGGCCTTAGGCGCCGGCCTT
TTCCCAGCTCACAAAAGCATCGGGCAGTGCCTATCTAGGGGCGCGGGCAGTAACGAGTTTTCAG
TGATCAGGAGAGTGTGCGGGCAAAGGTGAAGAAATCGTGACTAACTCAGCAGAGTTGGGGTGGG
GAGCTCCAGGAACCACTTCTGCTGGGTGGGCTGCTATCAGAAACTCAGCCAAGAGGAGGGGAGT
TGTTTGTTTAGGTTTGTACTTGGCTCTCTACACATTTCTTACCATAGAAAAGTTTGTGCCTTCA
TGGGAAATGGTTATTCTTTCTTTAGCTTTCTTTAAGTCCAGAGCATATCTTTTTCTAAAA
AAAGTTTT
```

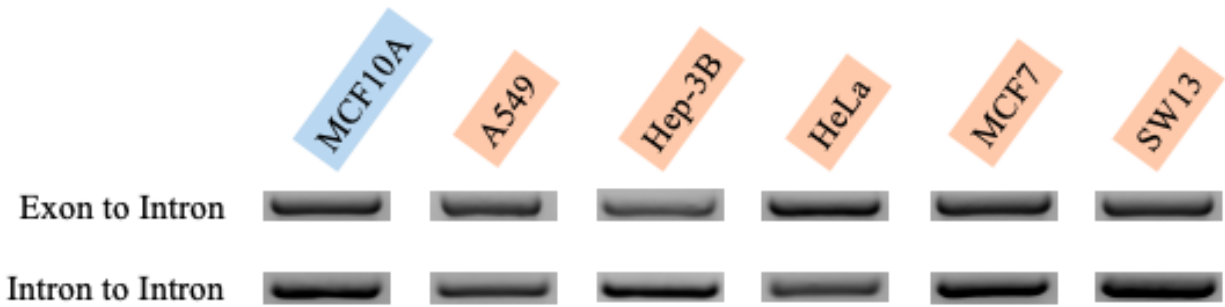
**Figure 2.4** The DNA sequence of *DAX-1* promoter region with MSRE primers. Five different primer sets are shown, each amplifying a different CpG island. Forward and reverse primers are highlighted along with the CpG islands the amplified region encompasses. Primer design Region A is yellow, Region B is blue, Region C is purple and overlaps with Region D in pink, Region E is in green.

All PCR reactions were performed using Promega GoTaq Green Master Mix (catalog # M7121) (**Table A.1; Appendix A**). Endpoint PCR products were separated by electrophoresis through a 2% agarose gel with ethidium bromide and visualized using the BioRad Gel Doc Imager. Only products that had not been digested by the enzyme could be amplified via PCR, resulting in a product visible on the agarose gel. Quantitative values were derived from band intensity via densitometry using the ImageLab software associated with the gel doc (*Image Lab Software | Life Science Research | Bio-Rad, n.d.*).

## ***Results***

### *gDNA DAX-1 Detection*

The initial confirmational assay was crucial to determining that DAX-1 is present within the cancerous and immortalized cell lines. Cancer frequently involves mutagenesis, often resulting in chromosomal aberrations (Chinnaiyan & Palanisamy, 2010). Since the *DAX-1* gene is found on the X chromosome, determining that a potential chromosomal aberration had not disrupted this target gene was critical prior to assessing RNA and protein level expression of DAX-1. To check this, *DAX-1* genomic level detection was assessed with standard PCR and the products were visualized using gel electrophoresis. As shown in **Figure 2.5**, PCR products of the appropriate size in all cell lines assayed, confirm the *DAX-1* gene is intact and mutation in these cell lines has not compromised the target gene. Though not shown in triplicate, these results are consistent with multiple repetitions.

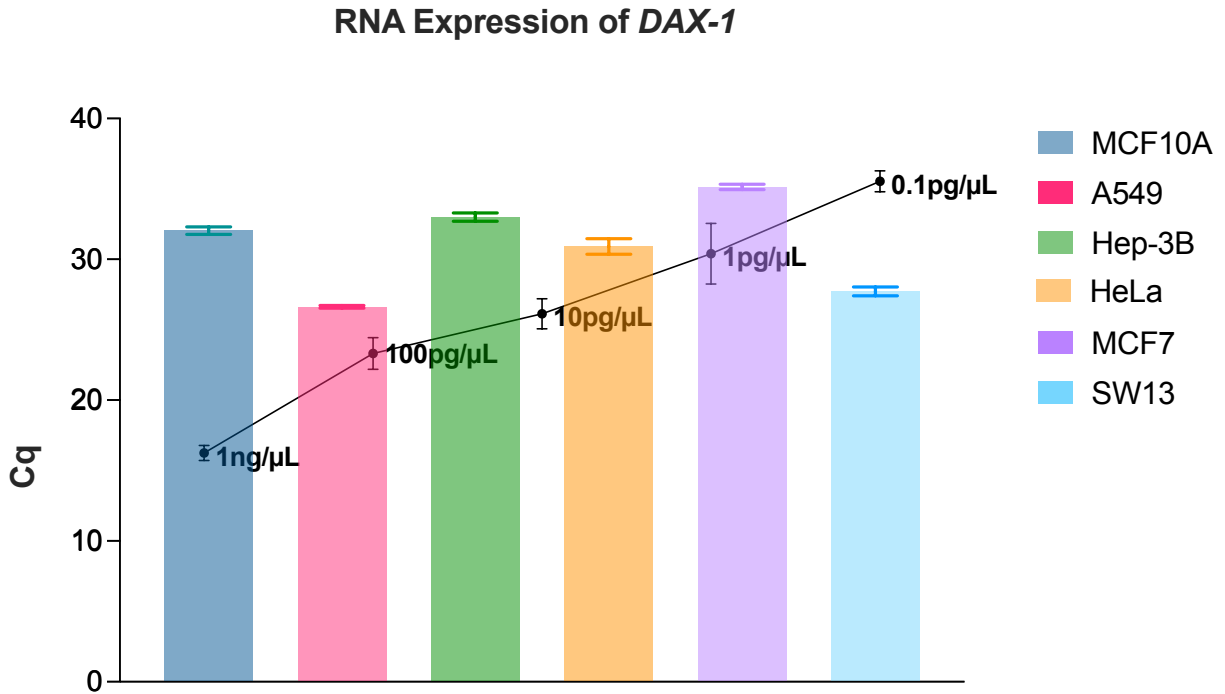


**Figure 2.5 Detection of DAX-1 in the genome.** Amplification of two distinct regions of the genome containing the DAX-1 gene followed by gel electrophoresis is shown. Six different cell lines were analyzed: MCF10A non-cancerous immortalized breast cells, A549 lung carcinoma, HeLa cervical cancer, Hep-3B liver carcinoma, MCF7 breast cancer, and SW13 adrenal cancer. The control cell line is indicated in blue, while the cancerous cell lines are denoted by orange highlighting.

### *DAX-1 RNA Level Expression*

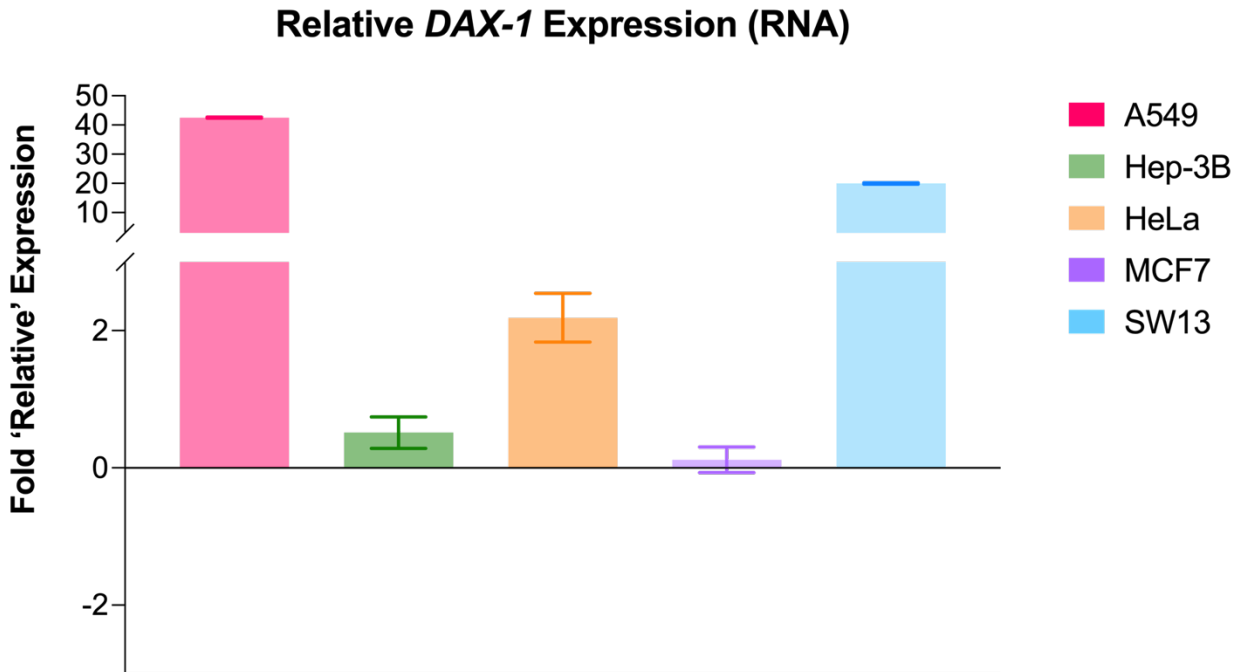
Quantitative PCR (qPCR) was utilized to measure the level of *DAX-1* gene expression in each cell line. For these experiments, two quantification methods were employed. In the first approach, a standard curve was generated using known input amounts generated from PCR amplification using a *DAX-1* expressing plasmid as the DNA template. In the standard curve method, a range of known concentrations of *DAX-1* plasmid were used to derive quantitative comparisons of RNA level expression. Beginning at 1ng/ $\mu$ L and decreasing to a low concentration of 0.1pg/ $\mu$ L, the number of amplification cycles needed to detect *DAX-1* in the plasmid increases as concentration decreases. By comparing the resulting Cq value (the number of amplification cycles) derived from the standard curve to the Cq values of the experimental samples, relative levels of *DAX-1* expression in the cancerous and noncancerous cell lines was determined (**Figure 2.6**). In this quantification method, the higher Cq value indicates an increased amount of qPCR cycles required to detect *DAX-1*. Thus, the larger the Cq, the lower the level of *DAX-1* expression. Based on this method of mRNA expression analysis, the highest level of *DAX-1* expression is observed in the A549 lung carcinoma cell line. This high level of expression is followed closely by the SW13 adrenal carcinoma cancer cell line. In contrast, it took much longer for the qPCR to detect *DAX-1* RNA expression in the MCF7 breast cancer cell lines. Alternatively, *DAX-1* expression in HeLa and Hep-3B (cervical and hepatocellular carcinoma), was between 1pg/ $\mu$ L and 0.1pg/ $\mu$ L, slightly higher than that detected in the MCF7 cell line. The *DAX-1* RNA expression in the MCF10A control cell line was also relatively low. This was to be expected as breast cells are not major producers of *DAX-1* such as adrenal cells that require *DAX-1* to regulate steroid hormone production (Dishington, 2017; Scandurra, 2014).





**Figure 2.6** Quantitative assessment of the *DAX-1* RNA level expression compared to a standard curve developed from the *DAX-1* plasmid at varying concentrations. The standard curve generated from the *DAX-1* plasmid superimposed over the average Cq levels of each tested cell line.

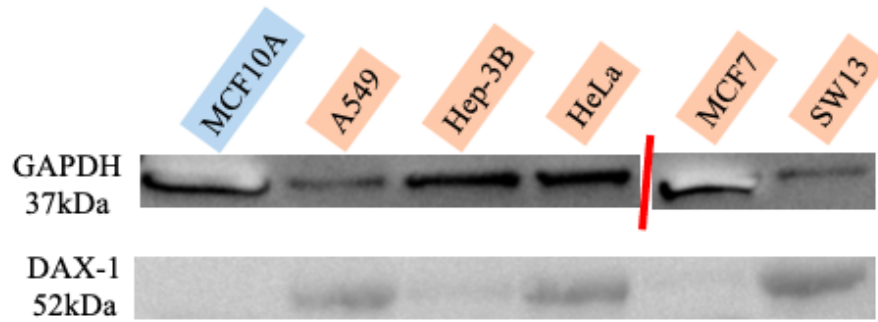
In a more qualitative approach comparing relative *DAX-1* expression levels in the cancerous cell lines to the control, the differences in expression is striking (**Figure 2.7**). When compared to the MCF10A non-cancerous control cell line, it is evident that the A549 lung carcinoma and SW13 adrenal carcinoma have substantially higher levels of DAX-1 expression than the Hep-3B hepatocellular carcinoma, the HeLa cervical carcinoma, or the MCF7 breast cancer cell lines. Notably, the MCF7 breast cancer cells show the lowest RNA level expression of DAX-1.



**Figure 2.7 Fold 'Relative' Expression of *DAX-1*.** Each cancerous cell line was normalized against the control, non-cancerous cell line for relative *DAX-1* RNA level expression. A549 and SW13 cell lines exhibit the highest level of *DAX-1* mRNA expression and MCF7 cells exhibit the lowest.

### *DAX-1 Protein Level Expression*

Western Blot analysis, that was used to determine the qualitative level of *DAX-1* gene expression at the protein level paralleled what was observed at the mRNA level. Protein expression was compared to that of GAPDH, a housekeeping gene that is constitutively expressed in all cells but may vary slightly amongst different cell types. Expression levels were based on the intensity of the product band during chemiluminescent imaging. Similar to the RNA level experiments, the western blot results confirm differential expression of DAX-1 across the cell lines (**Figure 2.8**). In line with what was observed at the RNA level, lung (A549) and adrenal (SW13) carcinomas demonstrated the highest DAX-1 protein expression while the breast cancer cell line (MCF7) had low expression. The hepatocellular carcinoma (Hep-3B) cells gave protein expression results consistent with those obtained from the RNA level analyses, categorizing them as low expressors of DAX-1 in both experiments but having slightly higher expression than that of the MCF7 cell line. However, some variation is observed when analyzing the qualitative results of the western blot compared to what was observed through qPCR. While the MCF10A control cells were average expressors of *DAX-1* mRNA, a protein product is not detected in the western blot. This could indicate a translational mutation in which the *DAX-1* RNA is not fully converted to protein or some other mechanism of translational control that does not align with transcriptional control in this cell line. In contrast, the cervical carcinoma (HeLa) cells are high expressors of DAX-1 at the protein level but not at the mRNA level.



**Figure 2.8 DAX-1 protein expression assessed via western blot.** The control cell line is labeled in blue and cancerous cell lines are shown in orange. Red slash represents a cropped lane on the image analysis.

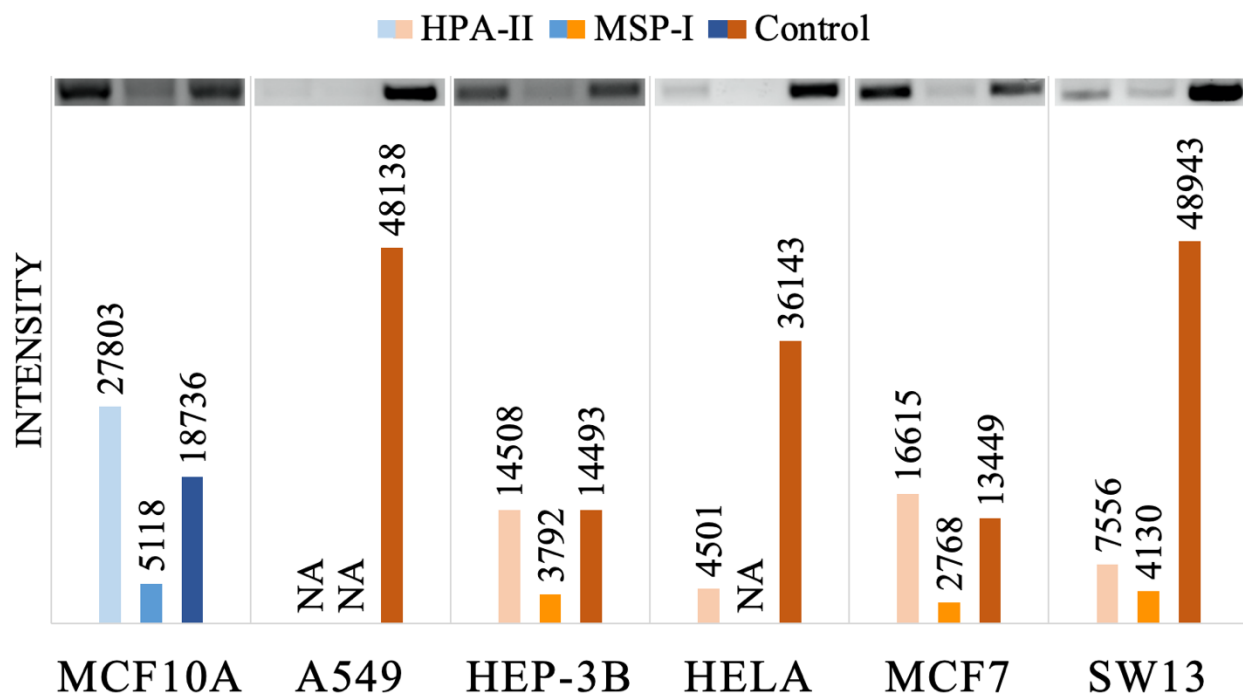
## MSRE

Having observed differential DAX-1 expression at both the RNA and protein levels, methylation specific restriction enzyme analysis provided a means to investigate the potential correlation between methylation and expression. Using the isoschizomer enzyme pair *HpaII* and *MspI*, the methylation status of the nine CCGG CpG islands in the DAX-1 promoter was crudely assessed. A product should always be observed in the control, undigested sample. The gDNA treated with *HpaII* enzyme will cut differentially based on the location and degree of methylation. Finally, while the *MspI* enzyme should cut regardless of methylation status and therefore theoretically never show a band, there are instances in which not all the gDNA was cut or it was cut in a way that the primers could still anneal, resulting in some product amplification.

Beginning with Region A, containing one CCGG CpG island, there was considerable variation in methylation status across the six cell lines (**Figure 2.9**). Based on the gel product shown above the bar graph and the quantitative values indicated by the blue bars, the MCF10A control cells are either methylated or hemi-methylated at this CpG island. In this case, the categorization of either hemi-methylated or methylated results from a greater band intensity following *HpaII* digestion, as well as some product following *MspI* digestion. Furthermore, both digest products are comparable to the results of the control. Denoted in orange, the cancerous cell lines can be assessed both qualitatively with the gel images or quantitatively with band intensity. The *DAX-1* gene in SW13 adrenal gland carcinoma, Hep-3B hepatocellular carcinoma, and MCF7 breast cancer cells are all hemi-methylated or methylated at this CpG island. This was determined based on the relative intensity of bands following PCR amplification. The Hep-3B cells showed some product following both digests, with the band intensity following *HpaII* digestion being comparable to that of the control. Products from both digests are observed in the MCF7 cells as

well, however with the SW13 cells it is more difficult to group this region into hemi-methylation or methylation because of the intensity of the control when compared to either digest product. In clear contrast however, the A549 lung carcinoma cells appear to be almost certainly unmethylated at this region further upstream of the *DAX-1* promoter with negligible results following the restriction digest.

## REGION A

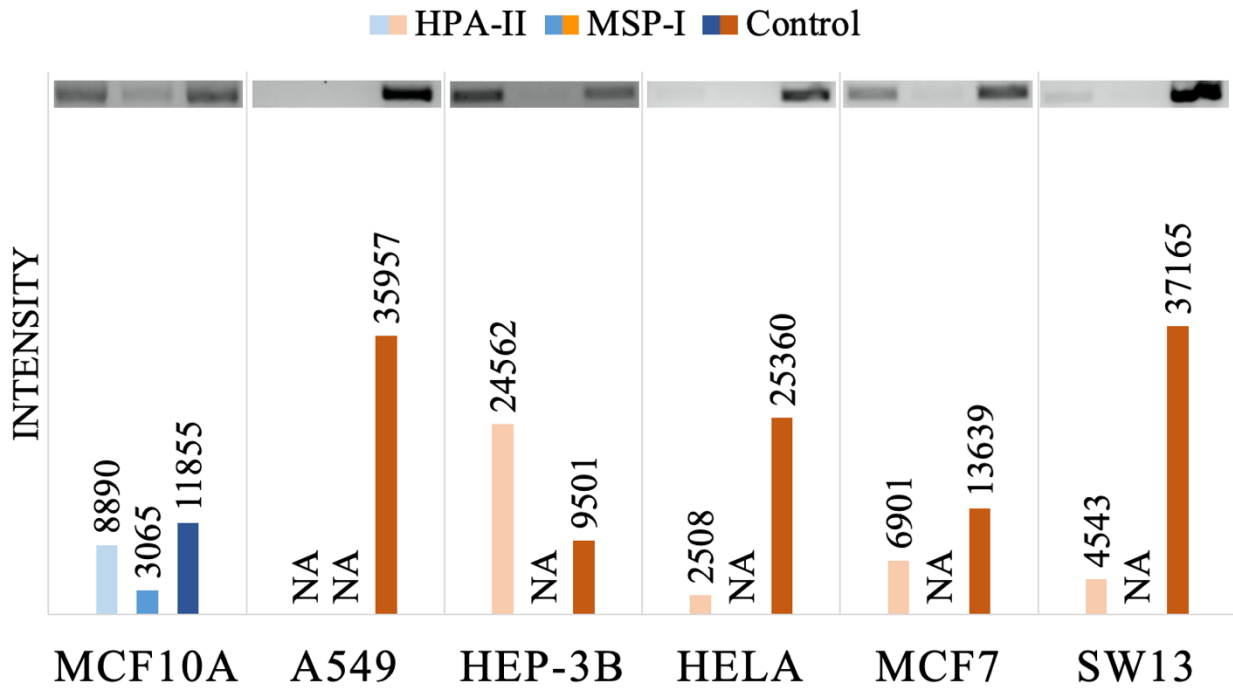


**Figure 2.9 Methylation status of DAX-1 Region A as assayed by MSRE.** Based on the PCR product following *HpaII* and *MspI* digestion, the following crude assessments can be made of this single CCGG CpG island: methylated or hemi-methylated in the control MCF10A cells; unmethylated in the A549 lung carcinoma cells; methylated or hemi-methylated in the Hep-3B hepatocellular carcinoma cells; unmethylated in the HeLa cervical adenocarcinoma cells; methylated or hemi-methylated in the MCF7 breast cancer cells; and methylated or hemi-methylated in the SW13 adrenal gland carcinoma.



The restriction digest results from the SW13 cell line in Region A highlight one of the reasons why MSRE can only be used to crudely assess methylation status. Analysis of Region B provides another example of why this technique is generally useful to begin honing in on areas of interest in the DAX-1 gene, but cannot be used for a precise determination of methylation status. This region, following the transcriptional start site and TATA box, contains three CCGG CpG islands that may all be methylated differently and the MSRE analysis can only indicate an overall methylation status and cannot distinguish each CCGG CpG island independently (**Figure 2.10**). The MCF10A noncancerous cells are either methylated or hemi-methylated in this region, as are the MCF7 breast cancer cells. The Hep-3B hepatocellular cells are likely methylated, and the SW13 adrenal carcinoma, A549 lung carcinoma, and HeLa cervical adenocarcinoma cell lines are unmethylated.

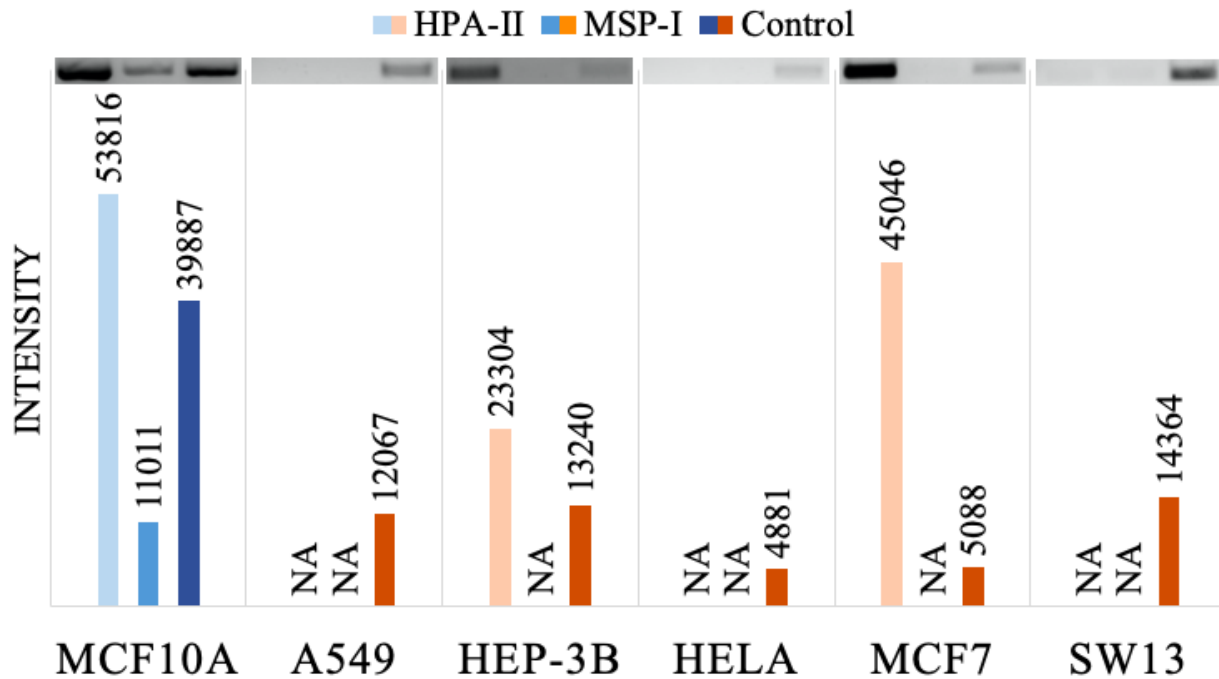
## REGION B



**Figure 2.10 Methylation status of DAX-1 Region B as assayed by MSRE.** Based on the PCR product following *HpaII* and *MspI* digestion, the following crude assessments can be made of this region that encompasses three CCGG CpG islands: methylated or hemi-methylated in the control MCF10A cells; unmethylated in the A549 lung carcinoma cells; methylated in the Hep-3B hepatocellular carcinoma cells; unmethylated in the HeLa cervical adenocarcinoma cells; methylated or hemi-methylated in the MCF7 breast cancer cells; and unmethylated in the SW13 adrenal gland carcinoma.

Moving downstream, Region C contains one unique CCGG CpG island and two that are also amplified in Region D. After analyzing the Region C patterns and comparing them to Regions A and B, a trend amongst the cell lines emerges (**Figure 2.11**). Once again, the MCF10A noncancerous cell line is methylated at this region of the *DAX-1* promoter, as are the Hep-3B hepatocellular carcinoma cells and the MCF7 breast cancer cells. In comparison, the lack of any bands, even faint, in the A549 lung carcinoma, HeLa cervical adenocarcinoma, and SW13 adrenal gland carcinoma indicates these CCGG CpG islands are unmethylated.

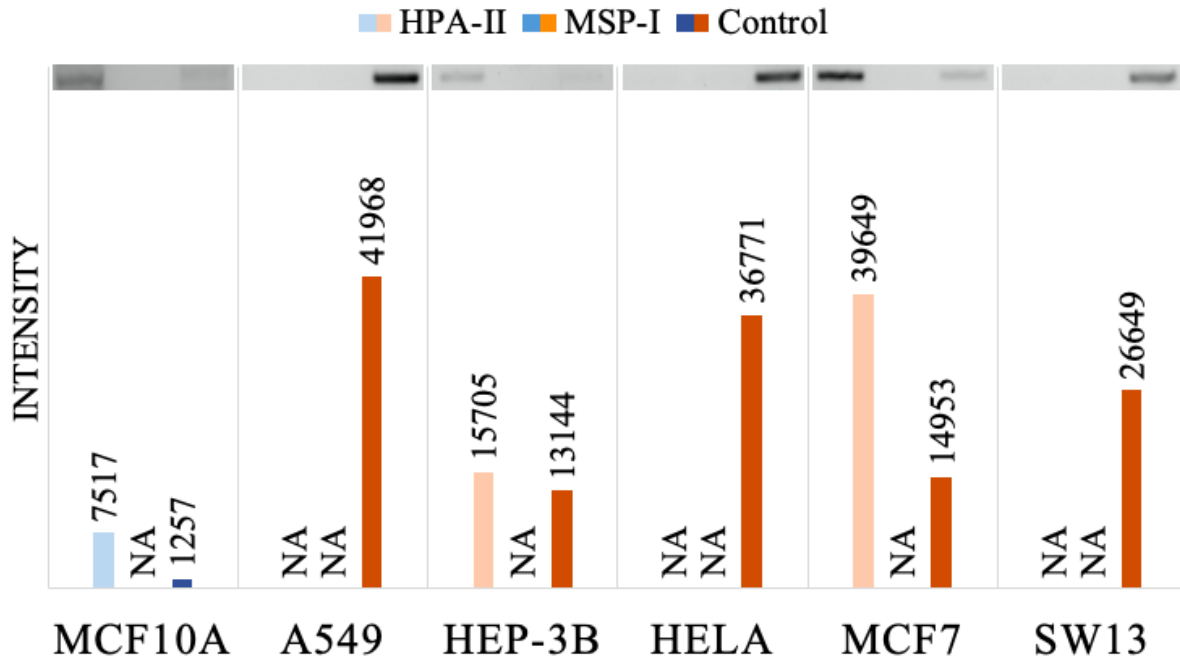
## REGION C



**Figure 2.11 Methylation status of DAX-1 Region C as assayed by MSRE.** Based on the PCR product following *HpaII* and *MspI* digestion, the following crude assessments can be made of this single unique CCGG CpG island: methylated in the control MCF10A cells; unmethylated in the A549 lung carcinoma cells; methylated in the Hep-3B hepatocellular carcinoma cells; unmethylated in the HeLa cervical adenocarcinoma cells; methylated in the MCF7 breast cancer cells; and unmethylated in the SW13 adrenal gland carcinoma.

Methylation status of Region D continues to support the pattern that the six cell lines fall into two categories: differential methylation across the *DAX-1* promoter and little to no methylation in the *DAX-1* promoter. Within Region D, containing one unique CCGG CpG island and two shared with Region C, the noncancerous cells, hepatocellular carcinoma cells, and breast cancer cells are all methylated, while the lung, adrenal, and cervical carcinomas are unmethylated (**Figure 2.12**).

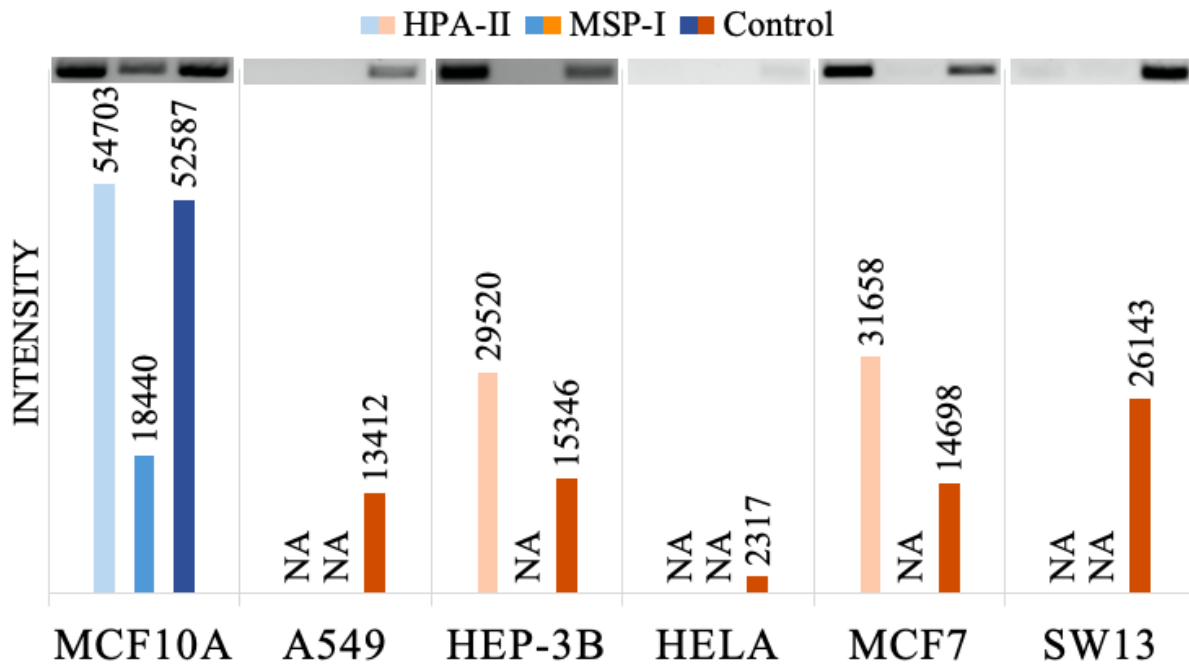
## REGION D



**Figure 2.12 Methylation status of DAX-1 Region D as assayed by MSRE.** Based on the PCR product following *HpaII* and *MspI* digestion, the following crude assessments can be made of this single unique CCGG CpG island: methylated in the control MCF10A cells; unmethylated in the A549 lung carcinoma cells; methylated in the Hep-3B hepatocellular carcinoma cells; unmethylated in the HeLa cervical adenocarcinoma cells; methylated in the MCF7 breast cancer cells; and unmethylated in the SW13 adrenal gland carcinoma.

Finally, when analyzing Region E, which contains one CCGG CpG island, the pattern of differential methylation across the *DAX-1* promoter or little to no methylation in the *DAX-1* promoter amongst the cell lines is further substantiated (**Figure 2.13**). The intense bands from the *HpaII* digest in the MCF10A, Hep-3B, and MCF7 cell lines indicated that all are likely methylated at this CpG island. In contrast, the lack of a product indicates that the *HpaII* and *MspI* enzymes were able to digest the gDNA. Therefore, the CpG island in Region E in the A549, HeLa, and SW13 cell lines was not protected via methylation.

## REGION E



**Figure 2.13 Methylation status of DAX-1 Region E as assayed by MSRE.** Based on the PCR product following *HpaII* and *MspI* digestion, the following crude assessments can be made of this single unique CCGG CpG island: methylated or hemi-methylated in the control MCF10A cells; unmethylated in the A549 lung carcinoma cells; methylated in the Hep-3B hepatocellular carcinoma cells; unmethylated in the HeLa cervical adenocarcinoma cells; methylated in the MCF7 breast cancer cells; and unmethylated in the SW13 adrenal gland carcinoma.



The pattern of hemi-methylated or methylated versus unmethylated throughout the *DAX-1* promoter is increasingly evident following the MSRE analysis (**Table 2.2**). Overall, the A549 lung carcinoma cells, HeLa cervical adenocarcinoma cells, and the SW13 adrenal gland carcinoma cells exhibited the lowest degree of methylation in the *DAX-1* promoter region. The remaining cancerous cell lines, Hep-3B hepatocellular carcinoma and MCF7 breast cancer, were at least hemi-methylated at each amplified region containing a minimum of one CCGG CpG island. Surprisingly, the MCF10A control, noncancerous cell line was also consistently methylated or hemi-methylated in the *DAX-1* promoter region.

**Table 2.2. Summary of MSRE results grouped by cell line and amplified region of the promoter.** The MCF10A cell line is the control, non-cancerous cell line while the remaining cell lines noted in orange are cancerous.

Region and Number of Unique CpG Islands	Cell Line					
	MCF10A	A549	Hep-3B	HeLa	MCF7	SW-13
<b>Region A (1 CpG)</b>	hemi/methylated	unmethylated	hemi/methylated	unmethylated	hemi/methylated	hemi/methylated
<b>Region B (3 CpG)</b>	hemi/methylated	unmethylated	methylated	unmethylated	hemi/methylated	unmethylated
<b>Region C (1 CpG)</b>	methylated	unmethylated	methylated	unmethylated	methylated	unmethylated
<b>Region D (1 CpG)</b>	methylated	unmethylated	methylated	unmethylated	methylated	unmethylated
<b>Region E (1 CpG)</b>	hemi/methylated	unmethylated	methylated	unmethylated	methylated	unmethylated

## ***Conclusion***

The RNA and protein level analyses confirmed *DAX-1* expression varies between the different types of cancer cell lines analyzed. The highest level of *DAX-1* expression at both the RNA and protein levels was found in lung and adrenal carcinomas. Conversely the lowest expression was detected in the metastatic breast cancer cell line. To further test the hypothesis that expression may be decreased due to methylation of CpG islands, methylation specific restriction enzyme analysis was used as a crude quantification of the degree of methylation of CpG islands in the promoter region of the *DAX-1* gene. Comparing these expression based results to the crude assessment of methylation status of CpG islands within the promoter region, methylation is greater in the cell lines that expressed low levels of DAX-1. Notably, the MCF7 breast cancer and Hep-3B hepatocellular carcinomas were hemi-methylated or methylated at each amplified region containing a minimum of 1 CCGG CpG island. Furthermore, amongst the cancerous cell lines the highest expressor of *DAX-1* at both RNA and protein levels was the A549 lung carcinoma and no methylation was observed with MSRE analysis. The SW13 adrenal carcinoma was also a high expressor of DAX-1 based on the qPCR and western blot experiments, but the methylation status of the CpG island furthest upstream could not be determined with confidence with MSRE. The two interesting outliers following the first set of experiments are the MCF10A noncancerous cells and the HeLa cervical adenocarcinoma cells. Although the MCF10A showed average levels of DAX-1 at the RNA level, at the protein level a product was barely visible. Furthermore, the MSRE revealed the *DAX-1* promoter is hemi-methylated or methylated throughout in the MCF10A noncancerous cell line. This may be due to the irregular behavior and the role of DAX-1 occasionally observed mammary cells (Judge, 2011). While the cause of this variability is unknown, it may be linked to cell growth conditions such as cell density. Indeed, it has been well

documented that there is a heterogeneity and variability in the MCF7 cell line, although it continues to be one of the most widely studied human breast cancer cell line (Lee et al., 2015, p. 7). In contrast the HeLa cells expressed low levels of *DAX-1* at the RNA level, but DAX-1 was abundantly expressed at the protein level. This incongruity between DAX-1 expression levels in RNA versus protein may be the result of translational regulation, where translation is not directly related to transcription (Kelen et al., 2009). The RNA and protein data from the HeLa cancer cell line aligned with the MSRE analysis results from the lung and adrenal carcinoma cell lines, revealing a lack of methylation in each amplified region. This could indicate that an alternative means of translational regulation is controlling DAX-1 expression in HeLa cervical adenocarcinoma cells.

Ultimately, the results of these experiments confirmed that DAX-1 is differentially expressed across multiple human cancer cell lines and that methylation patterns correlate with some of this variation. These results also narrowed down which cell lines are likely exhibiting regulation of DAX-1 expression via methylation as well as where the critical methylation site is located in the promoter region. The first CpG island located nearest to the 5' end of the promoter region, and upstream from the transcriptional start site TATA box, was determined to be the most critical island for further investigation. This evaluation was based on the results of the MSRE analysis which demonstrated significant variation in methylation status across all six cell lines at this CpG island, and was further supported by literature highlighting the importance of CpG islands at the 5' end of the promoter (Cross & Bird, 1995; Janitz & Janitz, 2011; Sleutels & Barlow, 2002). Bisulfite sequencing was determined to be the best means to elucidate whether this CpG island is protected via methylation in three cell lines: A549 lung carcinoma – the highest expressor of the DAX-1 at both RNA and protein levels with the least amount of methylation, MCF7 – the lowest

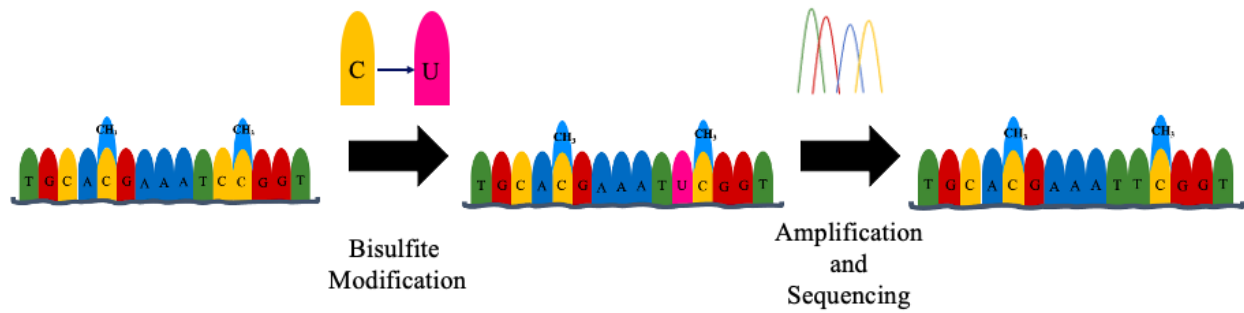
expressor of DAX-1 that was methylated in the promoter, and MCF10A – the noncancerous cell line. These results are presented and discussed in Chapter 3.

## Chapter 3: Identification of methylated CpG islands in the DAX-1 promoter

### *Introduction*

The second aim of this project was to identify the CpG islands that are methylated in the *DAX-1* promoter. Specific focus was targeted on CCGG sequences surrounding the transcriptional start site and TATA box. This aim was accomplished via bisulfite sequencing, where bisulfite conversion and sequence analysis were carried out on the lung carcinoma cell line (A549), the breast carcinoma cell line (MCF7), and the control (MCF10A), immortalized mammary gland cell line. These three cell lines were selected based on the results of the DAX-1 expression and MSRE analyses. The A549 cell line exhibited the highest RNA and protein level expression of DAX-1 and had the least amount of methylation in all five CpG rich regions in the promoter. Alternatively, the MCF7 cell line consistently showed the lowest level *DAX-1* expression and had one of the highest degrees of methylation in all five regions of the promoter. The MCF10A cell line was included as a control and counterpart to the breast cancer cells.

Bisulfite sequencing is the gold standard for determining the methylation status of gDNA (L. C. Li & Dahiya, 2002; Wreczycka et al., 2017; *Zymo Bisulfite Converted DNA Amplification Guide*, 2015). After gDNA is isolated, it is treated with sodium bisulfite, which deaminates unmethylated cytosines to uracil. The converted UG regions are isolated using amplification and directly sequenced with Sanger Sequencing (**Figure 3.1**). Bisulfite treatment does not deaminate methylated cytosines, which are protected by methylation and remain as cytosines during DNA sequencing. Therefore, the location of methylated cytosines is determined by comparing DNA sequence analysis of bisulfite treated and untreated samples. By introducing site specific changes, bisulfite treatment illuminates the methylation status of individual cytosine residues.



**Figure 3.1 Methodology of bisulfite conversion.** Bisulfite sequencing allows for the precise determination of methylation status in the genome. During bisulfite modification, unmethylated cytosines are deaminated and converted to uracils. Therefore, after amplification and sequencing the unmethylated cytosines will be denoted as thymine.

In conjunction with results from bisulfite sequencing, chromatin immunoprecipitation (ChIP) was utilized in order to build a model of methyl binding protein occupancy in the two mammary cells lines. This approach was central to the identification of the methylating proteins occupying the *DAX-1* promoter region and to which CpG islands they are binding. There are two primary families of proteins that directly interact with methylated DNA: DNA Methyltransferases (DNMTs) and Methyl-CpG-Binding Proteins (MBPs) (L. Li et al., 2015).

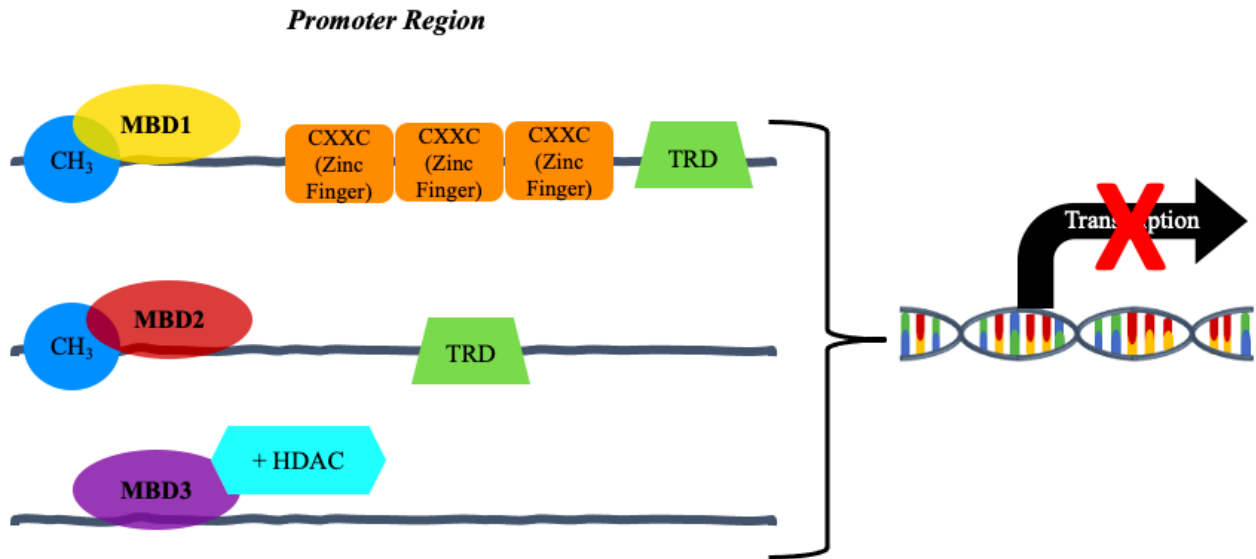
DNMTs catalyze the transfer of a methyl group to 5' cytosines. However, DNMTs are essential to cell division and growth and therefore are a challenging target to use in narrowing down methylation location via methylation modifying proteins. The second family, MBPs, are composed of three sub-groups of proteins: Set and Ring Associated (SRA) domain proteins, Kaiso and Kaiso-like proteins, and Methyl-CpG-Binding Domain proteins (MBD) (Sasai et al., 2010).

SRA domain proteins bind to methylated CpG islands and are observed in plants and animals. However, they perform a diverse range of functions beyond methylation and have been shown to bind methylated cytosines that are not part of CpG island in plants (Fournier et al., 2012). Due to their diverse role and ability to bind any cytosine, this family of proteins is not as pertinent to the investigation of specific CCGG CpG methylation.

The Kaiso and Kaiso-like family of proteins are an active field of research. First identified as DNA-binding factors, these proteins can serve as transcriptional repressors when bound to methylated CpG islands. Kaiso proteins are unique in their ability to also bind specific target sequences (Fournier et al., 2012). However, Kaiso and Kaiso-like proteins can also bind to regions not containing CpG islands, as well as regions containing a CpG island that cannot be methylated. Due to their diverse occupancy, these are not a viable set of proteins for the aim of this project.



Finally, Methyl-CpG binding proteins (MBP) or methyl-CpG binding domain proteins (MBD proteins) are key regulators of repressed gene expression and recruit other epigenetic regulators (Fournier et al., 2012; *MBD1 Antibody (Clone 100B272.1)*, n.d., p. 1). Though this protein family is large, consisting of eleven different proteins categorized further into three sub-groups, the MBD sub-group of proteins have non-overlapping functions and bind to symmetrically methylated CpG islands (Roloff et al., 2003). Furthermore, this protein family is known for their role in epigenetic regulation and binding DNA with symmetrically methylated CpG islands (Fournier et al., 2012; Hendrich & Tweedie, 2003; Roloff et al., 2003). Surveying various members of the family illuminates their unique roles. MBD1 and MBD2 bind to methylated DNA, while MBD3 does not (Fournier et al., 2012). Interestingly, while MBD1 occupies both methylated and non-methylated regions and therefore should bind indiscriminately, it has an affinity for unmethylated DNA (L. Li et al., 2015). MBD1 can also recruit other methylating proteins and form a complex that methylates the DNA and represses transcription (L. Li et al., 2015). MBD2 is a transcriptional repressor and along with HDAC, will package gDNA into inactive chromatin. Therefore, areas in which MBD2 binds are likely regions in which *DAX-1* is being repressed. Finally, MBD3 forms a complex with HDAC in regions containing 5-hydroxymethyl cytosine methylation. In addition to interacting with HDAC and colocalized DNMTs, when MBD2 and MBD3 form dimerized complexes, they have an increased affinity to hemi-methylated DNA regions (Tatematsu et al., 2000). The diverse roles each of these methylating proteins play in epigenetic regulation and DNA binding can be utilized to clarify specific methylation status in the promoter region of the *DAX-1* gene (**Figure 3.2**).



**Figure 3.2 Summary of MBD proteins mechanism for repressing transcription.** Adapted from L. Li et al., 2015 and Liyanage et al., 2014, MBD1 and MBD2 bind to methylated promoters and repress transcription. (TRD: transcription repression domain found with MBD1 and MBD2 repressed regions). MBD3 cannot bind to methylated regions, however, it can recruit other epigenetic regulatory proteins, including HDAC and MBD2, to repress transcription.

## ***Materials and Methods***

### *Bisulfite treatment*

Thermo Scientific EpiJet Bisulfite Conversion Kit (REF: K1461) was used after literature review revealed this kit is one of the premier bisulfite treatments available, preserving the integrity of the gDNA more so than other commercially available kits (Brouwer, 2013; Darst et al., 2010; L. C. Li & Dahiya, 2002; Schock & Traeger, 2011; Tierling et al., 2018; Worm Ørntoft et al., 2017; Wreczycka et al., 2017; *Zymo Bisulfite Converted DNA Amplification Guide*, 2015). Optimized results were achieved through Protocol A, the ‘long protocol’, as it had a higher DNA conversion frequency (>99% versus >95%) and a lower degradation frequency. Modifying reagents were added to purified and quantified gDNA. Following bisulfite conversion, the modified gDNA was cleaned and desulphonated before amplification with PCR (**Table A.1; Appendix A**).

Primers were designed with the recommended EpiDesigner bisulfite modified primer software and were initially optimized using a temperature gradient for PCR, as well as minor adjustments to the PCR protocol (*EpiDesigner*, 2017). The primers for bisulfite sequencing amplified the region encompassing the first CCGG CpG island upstream from the TATA box (**Table A.2; Appendix A**). A slightly larger region was amplified than previously seen in the MSRE since sequencing often results in degraded base pairs at the beginning and end of the sequence (**Figure 3.3**).

### Human orphan nuclear receptor (DAX1) gene

1306 - 3106 shown

**TATA Box:** 1521-1525

Exon 1: 1580-2747

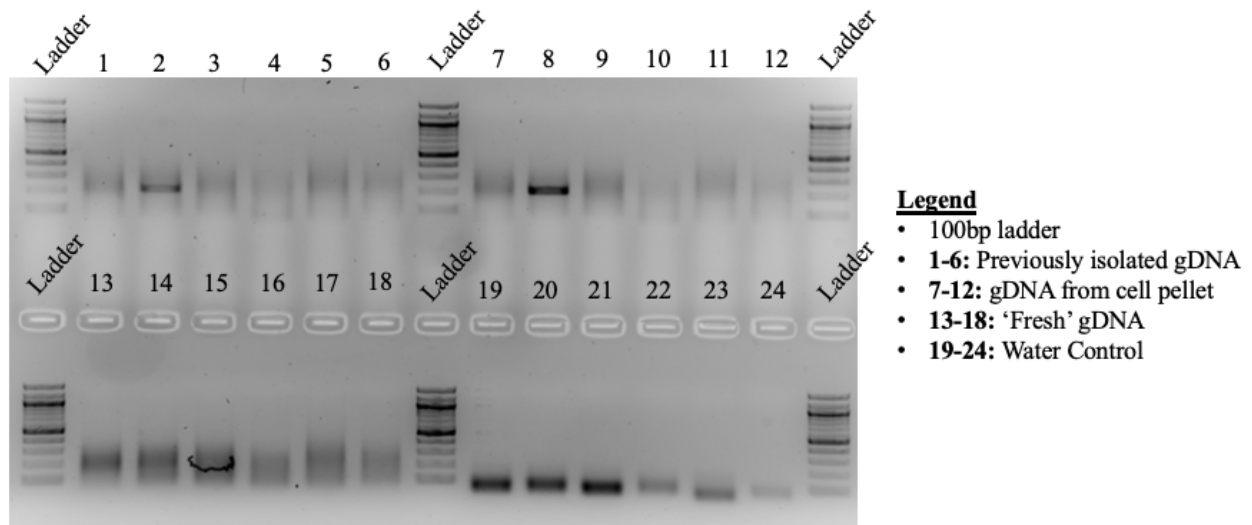
Intron: 2748-6132

Exon 2: 6133-6377

```
CAGGGAAAGGGGTAATGAGAGGAAGGAGGAAAAGTGTCCAGGAGCTCCACGCTGCTGTTCTTCC
ATTTCCAGCTTTTAAAGAGCACCCGCCCTTCGAACCACCGAGGTCATGGGCGAACACACCGA
GCGCAGCACCGCGCCCCCGCACACCCGCCCGCCTCCGCGCCCTTGCCCAGACCGAGGCGGC
CGACGCGCCTGCGTGCGCGCTAGGTATAAAATAGGTCCCAGGAGGCAGCCACTGGGCAGAACTGG
GCTACGGGCGCCGCGGGCCATGGCGGGCGAGAACCACCAGTGGCAGGGCAGCATTCCTCTACAAC
ATGCTTATGAGCGCGAAGCAAACGCGCGGGCTCCTGAGGCTCCAGAGACGCGGCTGGTGGATC
AGTGTGGGGCTGTTTCGTGCGGCGATGAGCCCGGGGTGGGCAGAGAGGGGCTGCTGGGCGGGCG
GAACGTGGCGCTCCTGTACCGCTGCTGCTTTTTCGGTAAAGACCACCCACGGCAGGGCAGCATC
CTCTACAGCATGCTGACGAGCGCAAAGCAAACGTACGCGGCACCGAAGGCGCCGAGGCGACGC
TGGGTCCGTGCTGGGGCTGTTCGTGCGGCTCTGATCCCGGGGTGGGCAGAGCGGGGCTTCCGGG
TGGGCGGCCCGTGGCACTCCTGTACCGCTGCTGCTTTTGTGGTGAAGACCACCCGCGGCAGGGC
AGCATCCTCTACAGCTTGCTCACTAGCTCAAAGCAAACGCACGTGGCTCCGGCAGCGCCCGAGG
CACGGCCAGGGGGCGCGTGGTGGGACCGCTCCTACTTCGCGCAGAGGCCAGGGGGTAAAGAGGC
GCTACCAGGCGGGCGGGCCACGGCGCTTCTGTACCGCTGCTGCTTTTTCGGTGAAGACCACCCG
CAGCAGGGCAGCACCCCTCTACTGCGTGCCCACGAGCACAAATCAAGCGCAGGCGGCTCCGGAGG
AGCGGCCGAGGGCCCCCTGGTGGGACACCTCCTCTGGTTCGCTGCGGCCGGTGGCGCTCAAGAG
TCCACAGGTGGTCTGCGAGGCAGCCTCAGCGGGCCTGTTGAAGACGCTGCGCTTCGTCAAGTAC
TTGCCCTGCTTCCAGGTGCTGCCCTGGACCAGCAGCTGGTGGTGGTGGCAACTGCTGGGCGT
CCCTGCTCATGCTTGGAGCTGGCCAGGACCGCTTGCAGTTCGAGACTGTGGAAGTCTCGGAGCC
CAGCATGCTGCAGAAGATCCTCACCACCAGGCGGCGGGAGACCAGGGGGCAACGAGCCACTGCC
GTGCCACGCTGCAGCACCATTTGGCACCGCCGGCGGAGGCCAGGAAGGTGCCCTCCGCCTCC
AGGTCCAAGCCATCAAGTGCCTTTCTTTCAAATGCTGGAGTCTGAACATCAGTACCAAGGAGTA
CGCCTACCTCAAGGGGACCGTGCTCTTTAACC CGGTAAAGGGTACTGGCCTTAGGCGCCGGCTT
TTCCAGCTCACAAAAGCATCGGGCAGTGCCTATCTAGGGGCGCGGGCAGTAACGAGTTTTTCAG
TGATCAGGAGAGTGTTCGGGGCAAAGGTGAAGAAATCGTACTAACTCAGCAGAGTTGGGGTGGG
GAGCTCCAGGAACCACTTCTGCTGGGTGGGCTGCTATCAGAAACTCAGCCAAGAGGAGGGGAGT
TGTTTGTTTAGGTTTGTACTTGGCTCTCTACACATTTCTTACCATAGAAAAGTTTGTGCCTTCA
TGGGAAATGGTTATTCTTTCTTTAGCTTTCTTTAAGTCCAGAGCATATCTTTTTCTAAAA
AAAGTTTT
```

**Figure 3.3** The DNA sequence of *DAX-1* promoter region with bisulfite primers. The primers amplify the region nearest the transcriptional start site, specifically targeting the CpG island prior to the TATA box.

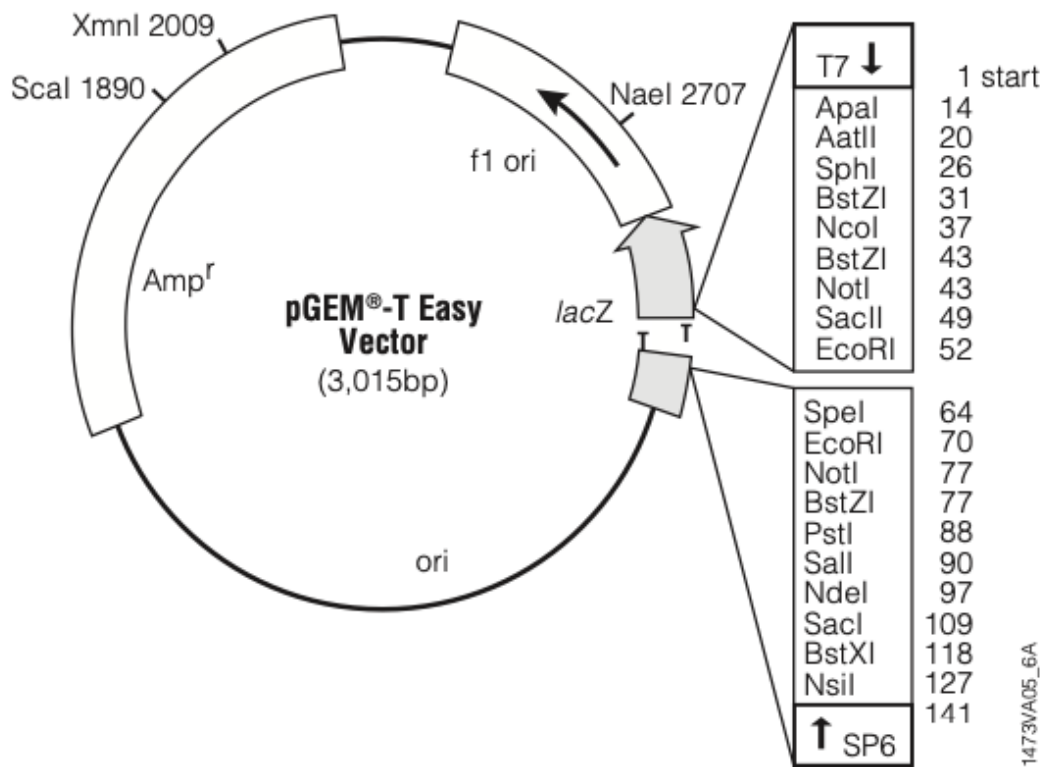
Bisulfite primers were first tested on a survey of gDNA to ensure optimized amplification by PCR regardless of the timeframe in which the gDNA was isolated. Assessing the result of bisulfite modification on previously isolated gDNA, gDNA taken from a preserved cell pellet, and gDNA purified from recently lifted cells have similar relative levels of amplification (**Figure 3.4**). However, the gDNA from the cell pellet gave the most robust amplification and therefore this method of gDNA isolation was used as input for bisulfite modification.



**Figure 3.4 Comparison of source of gDNA used for bisulfite modification.** Multiple bisulfite primers were tested in A549 bisulfite converted gDNA to compare quality of PCR product depending on different isolation sources. Shown in each set of six lanes are different primer sets isolating various regions of the *DAX-1* promoter that correspond with regions segmented for the methylation specific restriction enzyme analyses. Water control samples (lanes 19-24) resulted in a non-specific, primer-dimer product.

Amplification via PCR was repeated for a total of three times, where the input for the second and third rounds was 4 $\mu$ L of PCR product from the previous cycle. Following the third and final PCR, 18 $\mu$ L of product was electrophoresed through a 2% agarose gel. The appropriately sized PCR product was isolated from the gel, melted, and purified with the Wizard® SV Gel and PCR Clean-Up System (REF: A9281, Promega). The resulting purified PCR product was cloned directly into the pGEM T Easy plasmid (Promega) using the pGEM®-T Easy Vector System 1. Following a 2 hour ligation at room temperature, the ligated product was transformed into competent DH5a cells (One Shot®OmniMAX™, Invitrogen) and transformants were selected by plating on LB agar plates containing ampicillin (100  $\mu$ g/mL final concentration). After an overnight incubation at 37°C, 10 well isolated colonies were selected and transferred to LB ampicillin liquid cultures to grow overnight at 37°C with shaking at 250rpm. The following day, plasmid DNA was purified from the bacterial cultures using the PureYield™ Plasmid Miniprep System (Promega, REF A1222).

To confirm the correct product had been isolated and successfully cloned into pGEM-T Easy, 5 $\mu$ L of the 25 $\mu$ L miniprep yield was used as input into a restriction digest reaction. Enzyme volumes were between 0.3 $\mu$ L and 0.5 $\mu$ L per 10 $\mu$ L sample, with 1 $\mu$ L of corresponding NEB buffer, and nuclease free water. Enzymes were chosen based on the pGEM-T Easy vector map (**Figure 3.5**). Restriction digest reactions were incubated overnight at 37°C and analyzed the following day by adding 2  $\mu$ L Gel Loading Dye Purple (6x) (New England Biolabs #B7024S) prior to electrophoresis of digested products on a 2% agarose gel.



**Figure 3.5 pGEM®-T Easy Vector map.** Acquired from Promega pGEM®-T Easy Protocol (Promega, 2018). Corresponding enzymes used for the restriction digest were selected from this vector map to release the double stranded bisulfite modified DNA.



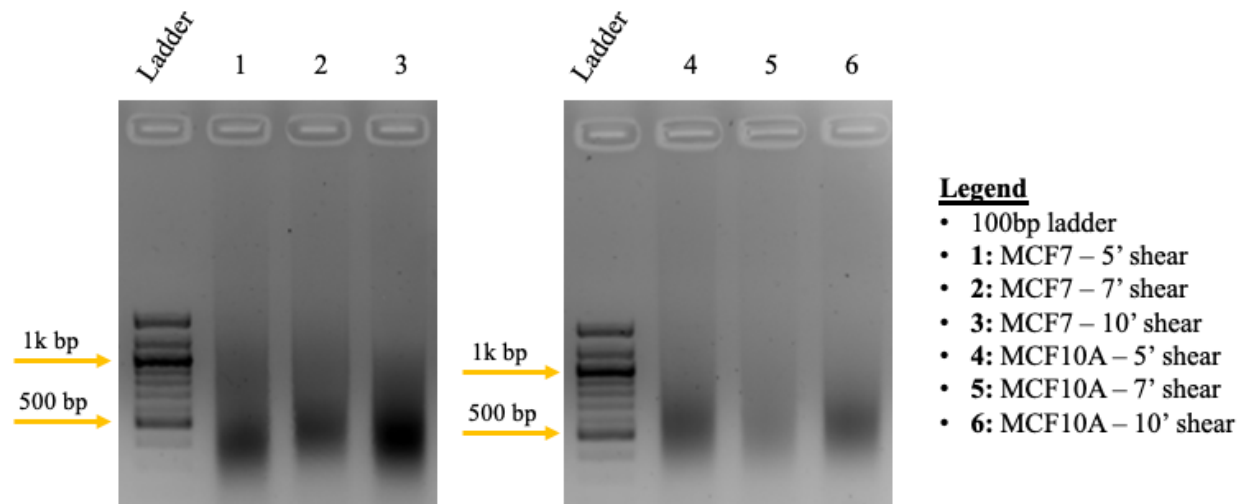
Enzymes and corresponding buffers were utilized in the following restriction digest reactions: ApaI with NdeI and NotI with BstXI (New England Biolabs, Inc). Only plasmids that released a band corresponding to the PCR product size were submitted for DNA sequence analysis (Molecular Cloning Laboratories) using M13 forward and reverse primers (**Figure A.1**). Control sequences of non-bisulfite modified gDNA from each of the cell lines were sequenced using the same amplification and isolation protocol to confirm DNA sequences match to known wildtype *DAX-1* sequences from NCBI.

Sequence products were analyzed manually and confirmed by Clustal Omega alignments with SnapGene software (*SnapGene | Software for Everyday Molecular Biology*, n.d.).

### *ChIP assays*

Following the determination of differential methylation status of CpG islands in the *DAX-1* promoter, it was important to understand the mechanism of this epigenetic regulation. Specifically, determining the identity of the methylating proteins that were likely mediating changes in the methylation status of the *DAX-1* gene was essential in order to elucidate the mechanism. To address this, chromatin immunoprecipitation (ChIP) assays were carried out using the MCF7 (breast cancer) and MCF10A (mammary gland immortalized) cell lines. ChIP assays provide a means to isolate proteins that are physically bound to the CpG island sites in the *DAX-1* promoter and exon 1, indicating their direct association with the *DAX-1* epigenetic regulatory region. Antibodies directed against known methylating proteins were used in the ChIP assays allowing determination of whether a particular epigenetic regulatory protein is associated with the *DAX-1* promoter and/or exon 1 region. Subsequent PCR analysis allows for the correlation of protein binding to a specific DNA region. ChIP can be used to specifically target methylating proteins associated with the silencing of gene expression (Fuks et al., 2003; Viré et al., 2006). The same primer sets utilized in Chapter 2 for the methylation specific restriction enzyme analysis were also used in the ChIP assays.

ChIP assays were carried out using the ab500-ChIP kit (Abcam). Sonication of cross-linked chromatin was performed by water bath sonication using a Misonix S-4000 sonicator in order to fragment the chromatin into smaller pieces. The optimal size of sonicated chromatin should be between 200 and 1000 base pairs. Sonication time was optimized by analyzing genomic DNA fragment size after 5 minutes, 7 minutes, and 10 minutes of 30 second intervals. The resulting DNA products were electrophoresed through a 2% agarose gel (**Figure 3.6**). Through these experiments, it was determined that 7 minutes was the optimal sonication time.



**Figure 3.6 Comparison of different chromatin sonication times in the cancerous MCF7 and control MCF10A cell lines.** Alternating 30 seconds shear and 30 seconds off, optimized chromatin product size was produced after 7 minutes of sonication. Ideal fragment size is between 200bp and 1000bp.

Control ChIP reactions included non-crosslinked sheared chromatin samples that underwent all other experimental conditions. Positive ChIP reactions included immunoprecipitations using the HDAC antibody. Sheared chromatin that did not undergo further experimental conditions was included as an “input” control. After sonication, sheared chromatin was diluted in buffer and 3 $\mu$ g of the following antibodies were added for crosslinking:

- anti-MBD1 (methyl-CpG binding domain protein 1), rabbit polyclonal,  
abCam (catalog # ab2846-100)
- anti-MBD2a (methyl-CpG binding domain protein 2), rabbit polyclonal,  
abCam (catalog # ab3754-100)
- anti-MBD3 (methyl-CpG binding domain protein 3), rabbit polyclonal,  
abCam (catalog # ab3755-100)
- anti-HDAC3 (histone deacetylase), rabbit polyclonal,  
abCam (catalog # ab47237)

Reactions were incubated at 4°C with rotation overnight prior to clean-up. A 50% slurry of Protein A agarose beads was used to purify the antibody/chromatin product along with the recommended number of wash steps. Maximum input of the final cross-linked and purified product was used as a template for PCR amplification. Finally, reaction products were electrophoresed through a 2% agarose gel stained with ethidium bromide. Based on the presence or absence of a product following PCR amplification, a model of protein occupancy throughout the promoter region was assessed.

## ***Results***

### *Bisulfite Sequencing*

Sequence analysis of control, non-bisulfite modified sequences aligned with NCBI *NR0BI* gene sequence in the non-cancerous MCF10A breast cell line and lung carcinoma A549 cell line (**Figure 3.7**). Although the MCF7 amplicon is consistent with the primers designed to segment the region surrounding the TATA box and first CpG island, the results were not included alongside the MCF10A and A549 initial alignment shown in **Figure 3.7**. Unfortunately, while the MCF7 breast cancer non-bisulfite modified product was still within the *DAX-1* gene, the amplicon showed a different sequence. Across multiple biological replicates with ten clones each, all resulted in successful primer alignment and had the same amplicon region (**Figure A.2; Appendix A**). This difference in MCF7 sequence results could be due to the previously discussed heterogeneity and variability well documented by other researchers (Lee et al., 2015). Furthermore, when entered into BLAST (*NCBI BLAST*, n.d.) these sequences matched the *NR0BI* gene, confirming that we were analyzing the *DAX-1* gene in MCF7 cells and could continue with bisulfite analyses.

DAX-1 Control	AGGGCAGCATCCTCTACAACATGCTTATGAGCGCGAAGCAAACGCGCGCGGGCTCCTGAGG	60
MCF10A Control	AGGGCAGCATCCTCTACAACATGCTATGAGCGCGAAGCAAACGCGCGCGGGCTCCTGAGG	60
A549 Control	AGGGCAGCATCCTCTACAACATGCTTATGAGCGCGAAGCAAACGCGCGCGGGCTCCTGAGG	60
DAX-1 Control	CTCCAGAGACGCGGGCTGGTGGATCAGTGCTGGGGCTGTTTCGTGCGGGCGATGAGCCCCGGGG	120
MCF10A Control	CTCCAGAGACGCGGGCTGGTGGATCAGTGCTGGGGCTGTTTCGTGCGGGCGATGAGCCCCGGGG	120
A549 Control	CTCCAGAGACGCGGGCTGGTGGATCAGTGCTGGGGCTGTTTCGTGCGGGCGATGAGCCCCGGGG	120
DAX-1 Control	TGGGCAGAGAGGGGGCTGCTGGGCGGGCGGAACGTGGCGCTCCTGTACCGCTGCTGCTTTT	180
MCF10A Control	TGGGCAGAGAGGGGGCTGCTGGGCGGGCGGAACGTGGCGCTCCTGTACCGCTGCTGCTTTT	180
A549 Control	TGGGCAGAGAGGGGGCTGCTGGGCGGGCGGAACGTGGCGCTCCTGTACCGCTGCTGCTTTT	180
DAX-1 Control	GCGGTAAGACCACCCACGGCAGGGCAGCATCCTCTACAGCATGCTGACGAGCGCAAAGC	240
MCF10A Control	GCGGTAAGACCACCCACGGCAGGGCAGCATCCTCTACAGCATGCTGACGAGCGCAAAGC	240
A549 Control	GCGGTAAGACCACCCACGGCAGGGCAGCATCCTCTACAGCATGCTGACGAGCGCAAAGC	240
DAX-1 Control	AAACGTACGCGGCACCGAAGGGCGCCGAGGGCAGCGCTGGGTCCGTGCTGGGGCTGTTTCGT	300
MCF10A Control	AAACGTACGCGGCACCGAAGGGCGCCGAGGGCAGCGCTGGGTCCGTGCTGGGGCTGTTTCGT	300
A549 Control	AAACGTACGCGGCACCGAAGGGCGCCGAGGGCAGCGCTGGGTCCGTGCTGGGGCTGTTTCGT	300
DAX-1 Control	GCGGCTCTGATCCCGGGGTGGGCAGAGCGGGGCTTCCGGGTGGGCGGCCCGTGGCACTCC	360
MCF10A Control	GCGGCTCTGATCCCGGGGTGGGCAGAGCGGGGCTTCCGGGTGGGCGGCCCGTGGCACTCC	360
A549 Control	GCGGCTCTGATCCCGGGGTGGGCAGAGCGGGGCTTCCGGGTGGGCGGCCCGTGGCACTCC	360
DAX-1 Control	TGTACCGCTGCTGCTTTTGTGGTGAAGA	388
MCF10A Control	TGTACCGCTGCTGCTTTTGTGGTGAAGA	388
A549 Control	TGTACCGCTGCTGCTTTTGTGGTGAAGA	388

**Figure 3.7 Sequence alignment of *DAX-1* promoter region.** Sequence alignment comparison of the control, non-bisulfite converted MCF10A and A549 cell lines to the NCBI sequence. The clonal sequences tested had a high rate of similarity (**Figures A.2, A.3, and A.4; Appendix A**). MCF7 data is not shown on this alignment due to slightly different amplicon falling between these primers. The clonal alignments are shown in **Figure A.2; Appendix A**.

In comparison, the bisulfite treated data was heavily degraded and was more challenging to align. A crude alignment did show successful conversion of most cytosines to uracil (**Figure 3.8**). Within this region, each cytosine not protected by a methyl group was converted to a uracil, reading as a thymine in the final DNA sequence analysis. This selected area demonstrates the power of bisulfite conversion in unmethylated sequences. Furthermore, as this region is early in the sequence, this data confirms each of the three cell lines were successfully bisulfite modified and that the region being amplified is on target.

### Human orphan nuclear receptor (DAX1) gene

1306 - 3106 shown

**TATA Box:** 1521-1525

Exon 1: 1580-2747

Intron: 2748-6132

Exon 2: 6133-6377

CAGGGAAAGGGTAA  AAGGAGGAAAGTGTCCAGGAGCTCCACGCTGCTGTTCTTCC  
ATTTCCAGCTTTTAAAGAGCACCCGCCCTTCGAACCACCGAGGTCATGGGCGAACACA **CCGGA**  
GCGCAGCACCGCGCCCCCGCACACCCGCCCGCCTCCGCGCCCTTGCCCAGACCGAGGCGGC  
CGACGCGCCTGCGTGCGCGCTAGG **TATA** AATAGGTCCCAGGAGGCAGCCACTGGGCAGAACTGG  
GCTACGGGCGCCGCGGGCCATGGCGGGCGAGAACCACAGTGGCAGGGCAGCATCCTCTACAAC  
ATGCTTATGAGCGCGAAGCAAACGCGCGGGCTCCTGAGGCTCCAGAGACGCGGCTGGTGGATC  
AGTGCTGGGGCTGTTTCGTGCGGCGATGAGC **CCGG**GGTGGGCAGAGAGGGGCTGCTGGGCGGGCG  
GAACGTGGCGCTCCTGTACCGCTGCTGCTTTTGCGGTAAAGACCACCACGGCAGGGCAGCATC

5' 3'

DAX-1 (NCBI)	AAGGAGGAAAGTGTCCAGGAGCTC
DAX-1 (MCF10A B.S.)	AAGGAGGAAAGTGT <b>TT</b> AGGAG <b>TTT</b>
DAX-1 (MCF7 B.S.)	AAGGAGGAAAGTGT <b>TT</b> AGGAG <b>TTT</b>
DAX-1 (A549 B.S.)	AAGGAGGAAAGTGT <b>TT</b> AGGAG <b>TTT</b>

Figure 3.8 Sequence alignment of deaminated cytosines in *DAX-1* promoter region of bisulfite modified DNA. Highlighting the successful alignment and conversion of unmethylated cytosine into uracil, which translates to thymine during sequencing.



Highlighting a second region in the bisulfite modified sequence that follows the CCGG CpG island and TATA box demonstrates the protection of certain cytosines (**Figure 3.9**). Cytosine methylation can occur at non CCGG CpG islands as well as independent cytosine residues. These protected cytosines are not deaminated during bisulfite modification.

### Human orphan nuclear receptor (DAX1) gene

1306 - 3106 shown

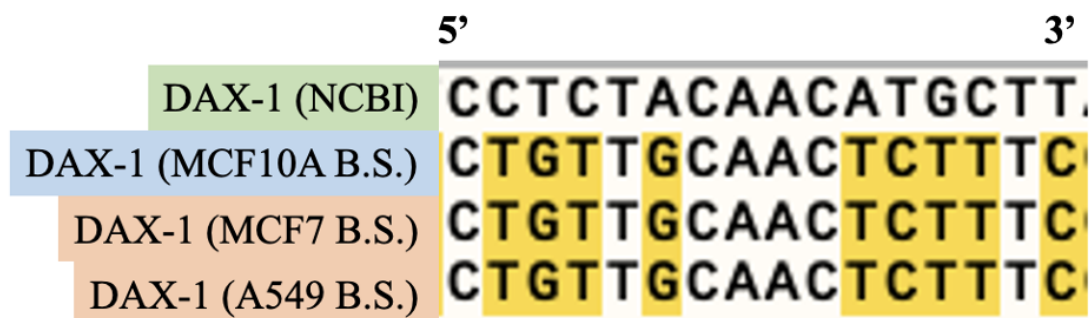
**TATA Box:** 1521-1525

Exon 1: 1580-2747

Intron: 2748-6132

Exon 2: 6133-6377

```
CAGGGAAAGGGGTAATGAGAGGAAGGAGGAAAGTGTCCAGGAGCTCCCACGCTGCTGTTCTTCC
ATTTCCAGCTTTTAAAGAGCACCCGCCCTTCGAACCACCGAGGTCATGGGCGAACACACCGGA
GCGCAGCACCCGCGCCCCCGCACACCCGCCCGCCTCCGCGCCCTTGCCCAGACCGAGGCGGC
CGACGCGCCTGCGTGCGCGCTAGGTATAAATAGGTCCCAGGAGGCAGCCACTGGGCAGAACTGG
GCTACGGGCGCCGCGGGCCATGGCGGGCGAGAACCACCAGTGGCAGG CCTCTACAAC
ATGCTTATGAGCGCGAAGCAAACGCGCGGGCTCCTGAGGCTCCAGAGACGCGGGCTGGTGGATC
AGTGCTGGGGCTGTTTCGTGCGGCGATGAGCCCGGGGTGGGCAGAGAGGGGGCTGCTGGGCGGGCG
GAACGTGGCGCTCCTGTACCGCTGCTGCTTTTGCGGTAAAGACCACCACGGCAGGGCAGCATC
```



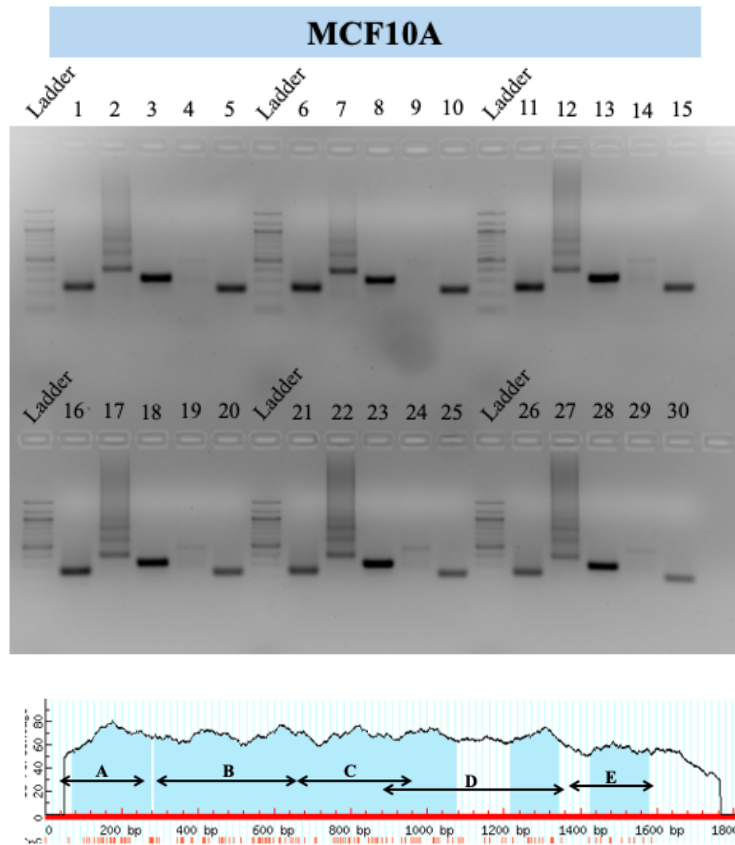
**Figure 3.9** Sequence alignment of protected cytosines in *DAX-1* promoter region of bisulfite modified DNA. Not all cytosine residues are deaminated within the gDNA. Those that are not deaminated by bisulfite modification are likely protected via methylation.

Refining the focus to the specific CCGG CpG island of interest, differential conversion is observed (**Figure 3.10**). Although the bisulfite modification severely damages the sequence in certain places, an alignment can be identified based on specific base pairs. Overall, the least degraded sequence came from the MCF10A noncancerous control cell line. Aligning this sequence as best as possible against the NCBI wild type allowed for a clear alignment of the two cancerous cell lines. Systematically looking at the CCGG sequence, this CpG island in the MCF10A cell line is likely, this CpG island is hemi-methylated and therefore only partially protected via methylation. The MCF7 breast cancer cells produced the most degraded sequence, in line with expectation from previous research on the irregularities observed in breast cancer and DAX-1 expression. When taking into account the preservation of both guanines and the successful conversion of one cytosine to thymine, this island is likely hemi-methylated and mostly protected. Finally, this CpG island in the A549 lung carcinoma cell line is thoroughly degraded, implying no protection by a methyl group.



## *ChIP*

Taking into consideration the size of the target region being amplified, a band of correct molecular weight indicates the presence of the methyl-CpG binding domain protein at the CpG islands located within the amplified regions. Honing in on protein occupancy in Region B located shortly after the transcriptional start site, none of the MBD proteins were found to occupy the three CpG islands located in this area of the DAX-1 promoter in the control MCF10A cell line (**Figure 3.11**). Conversely, all three MBD proteins were found in Region A and E, each containing 1 CpG island, and Region C, which encompasses three CpG islands.



**Top Row:**

Lanes 1-5: MBD 1    Lanes 6-10: MBD 2    Lanes 11-15: MBD 3

- 1: Region A      • 6: Region A      • 11: Region A
- 2: Region B      • 7: Region B      • 12: Region B
- 3: Region C      • 8: Region C      • 13: Region C
- 4: Region D      • 9: Region D      • 14: Region D
- 5: Region E      • 10: Region E     • 15: Region E

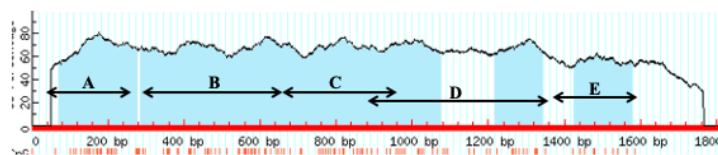
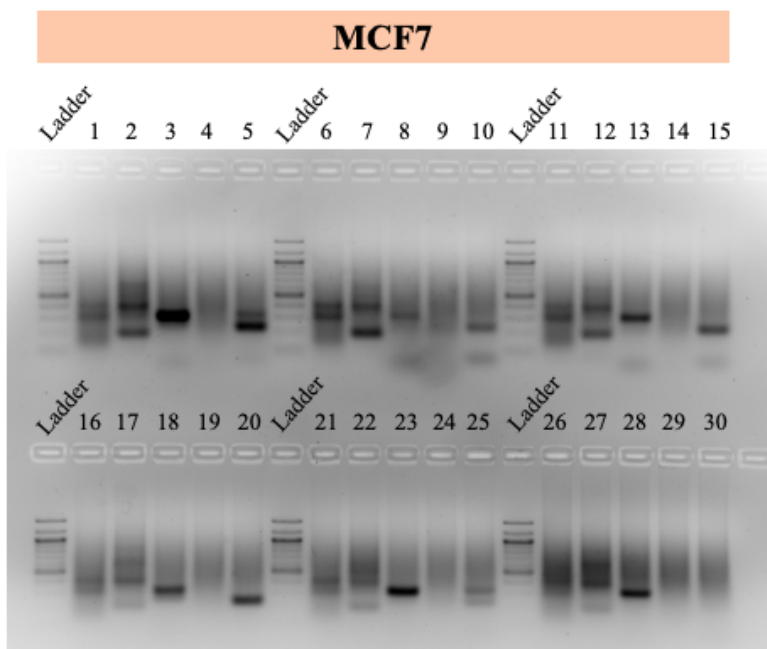
**Bottom Row:**

Lanes 16-20: HDAC    Lanes 21-25: Control    Lanes 26-30: Input

- 16: Region A      • 21: Region A      • 26: Region A
- 17: Region B      • 22: Region B      • 27: Region B
- 18: Region C      • 23: Region C      • 28: Region C
- 19: Region D      • 24: Region D      • 29: Region D
- 20: Region E      • 25: Region E      • 30: Region E

**Figure 3.11 PCR amplification product following ChIP in MCF10A non-cancerous mammary gland control cells.** The top row indicates results for MBD1, 2, and 3 binding. Within these results, clear, on-target products are detected in PCR amplified regions A, C, and E.

In comparison to the MCF10A ChIP products, the MCF7 products provide much more intense bands in some regions, notably in Region B. MCF7 cells demonstrated occupancy by all three MBD proteins and HDAC in all amplified promoter segments, excluding Region D (**Figure 3.12**).



**Top Row:**

Lanes 1-5: MBD 1    Lanes 6-10: MBD 2    Lanes 11-15: MBD 3

- 1: Region A    • 6: Region A    • 11: Region A
- 2: Region B    • 7: Region B    • 12: Region B
- 3: Region C    • 8: Region C    • 13: Region C
- 4: Region D    • 9: Region D    • 14: Region D
- 5: Region E    • 10: Region E    • 15: Region E

**Bottom Row:**

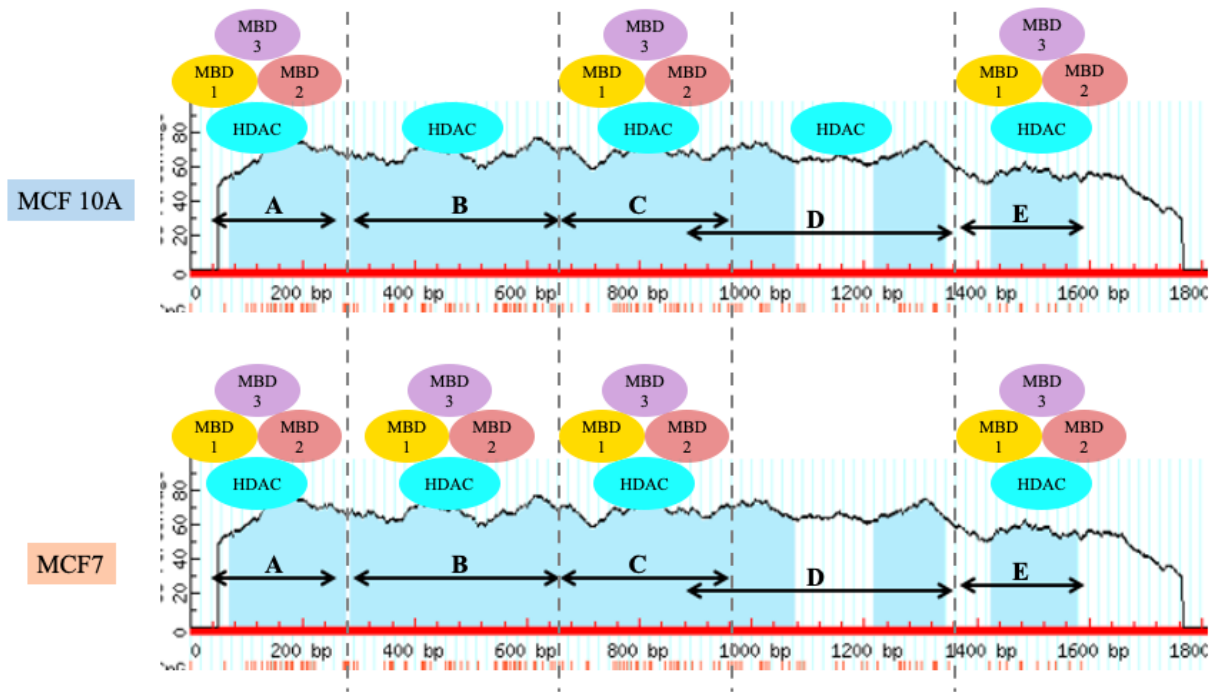
Lanes 16-20: HDAC    Lanes 21-25: Control    Lanes 26-30: Input

- 16: Region A    • 21: Region A    • 26: Region A
- 17: Region B    • 22: Region B    • 27: Region B
- 18: Region C    • 23: Region C    • 28: Region C
- 19: Region D    • 24: Region D    • 29: Region D
- 20: Region E    • 25: Region E    • 30: Region E

**Figure 3.12 PCR amplification product following ChIP in MCF7 breast cancer cells.** The top row indicates results for MBD1, 2, and 3 binding. PCR products are detected in regions A, B, C, and E. Region D only gives faint bands in the control settings indicating that it is not a target of the MBD binding family of proteins.



Following analysis of amplified ChIP products, a schematic of MBD protein occupancy highlights the difference between control and cancerous breast cell lines (**Figure 3.13**). Most striking is the occupancy of all the MBD proteins in Region B in the cancerous cell line but not the control. This region contains three CCGG CpG islands and is located directly after the TATA box. The presence of all three MBD proteins and HDAC indicates that this region is being repressed via methylation in this cancer cell line (e.g. MCF7 cells, shown in the lower half of the figure) but not in the control line (e.g. MCF10A, shown in the upper half of the figure).



**Figure 3.13 Model of methyl-CpG binding protein occupancy on the *DAX-1* gene in MCF10A control and MCF7 breast cancer cell lines.** In both cell lines, there is a great deal of occupancy by these proteins, however, there is a clear difference when focusing on amplified Region B. Located near the TATA box, this region is repressed by MBD1, MBD2, and MBD3 in the breast cancer cell line (MCF7) but is unoccupied in the control mammary gland cell line (MCF10A).

## ***Conclusion***

Through bisulfite sequence analysis and chromatin immunoprecipitation, a model of the difference between methylation status of CpG islands in the *DAX-1* promoter region was developed. The A549 cells were heavily modified at the CpG island of interest, concluding that this region was not protected via methylation. This aligns with results from Chapter 2 that identified this lung carcinoma cell line as the highest expressor of DAX-1 at the RNA and proteins levels. Additionally, bisulfite sequencing gave a more precise depiction of what the MSRE analysis revealed: the CpG island, located further upstream in the *DAX-1* promoter, preceding the TATA box, is unmethylated in the A549 lung carcinoma cells. Bisulfite sequencing also revealed that MCF7 breast cancer and MCF10A noncancerous mammary gland cells are likely hemi-methylated at this CpG island, confirming the results of MSRE analysis from Chapter 2. The hemi-methylation in MCF7 cells could be correlated with the decreased expression of DAX-1 at the RNA and protein levels previously observed in the first aim. Additionally, methyl-CpG-binding domain protein occupancy in this region of the MCF10A *DAX-1* promoter determined via ChIP confirmed the hemi-methylation status concluded from bisulfite sequencing. Furthermore, ChIP analyses highlighted a region following the TATA box where MBD occupancy varies between the cancerous and noncancerous breast cells.

## Chapter 4: Discussion

The DAX-1 orphan hormone nuclear receptor has been shown to suppress tumor progression in cancer metastasis. The hypothesis of this thesis was that *DAX-1* gene expression is differentially expressed across a survey of various cancers and that differential expression of *DAX-1* was, at least in part, due to the epigenetic repression via methylation. Methylation is a form of epigenetic modification that can prevent transcription factors from binding to DNA in the promoter region and thereby silencing gene expression. The implementation of qPCR and Western Blotting confirmed that DAX-1 is being differentially expressed in the six human cell lines investigated. Furthermore, methylation specific restriction enzyme analysis and bisulfite sequencing provided evidence of methylation resulting in repressed gene expression. Finally, chromatin immunoprecipitation confirmed a difference in methyl protein binding occupancy in cancerous versus noncancerous cell types. Interestingly, methylation was also observed in the control cell line. Though somewhat surprising, this is not altogether unexpected. The mammary glands are composed of a frequently changing cellular landscape and the presence of DAX-1 fluctuates (Judge, 2011). Additionally, the control cell line utilized was not ‘normal’ as it was isolated from a diseased, but not tumorigenic, tissue.

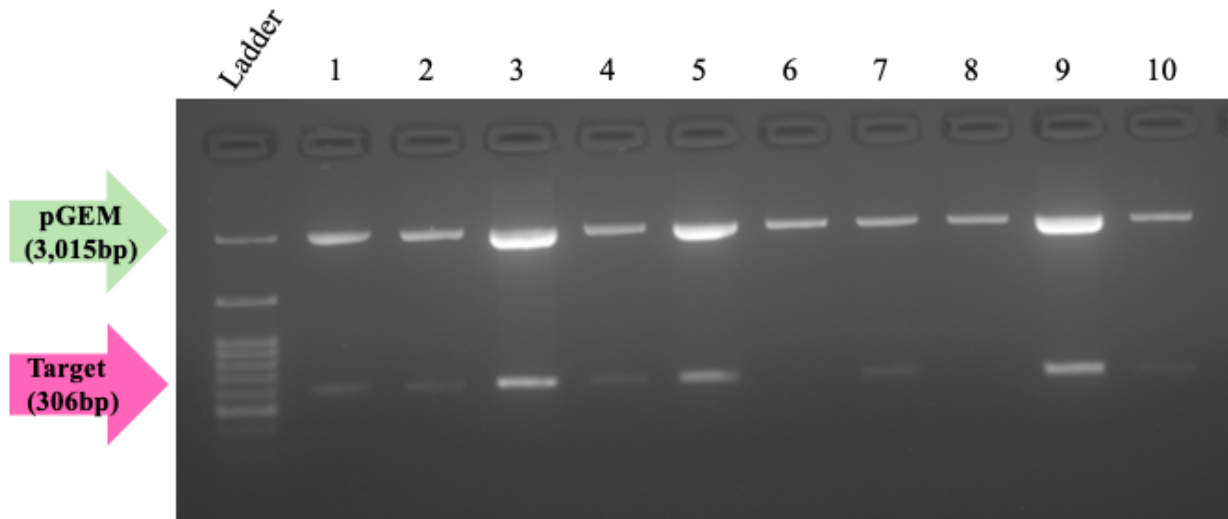
Given the role of DAX-1 in mediating sexual determination in humans and regulating differentiation of embryonic stem cells, it is not surprising it is epigenetically regulated. Studies have shown that proper DNA methylation plays a key role in cell growth and differentiation, as well as embryonic development (Iyer & McCabe, 2004; Lalli, 2014; Lalli et al., 1997; McCabe, 2007). Proper timing of DAX-1 expression is likely, at least in part, epigenetically controlled. Previous studies in the Tzagarakis-Foster lab have demonstrated that the reintroduction of DAX-1 at a physiological level slows the cell proliferation of MCF7 breast cancer cells and tumor

formations in mouse xenograft models (Tzagarakis-Foster, manuscript in preparation). Extrapolating the results shown in this project suggests that releasing the epigenetic control in a cell line may, in turn, slow proliferation in tumor growth.

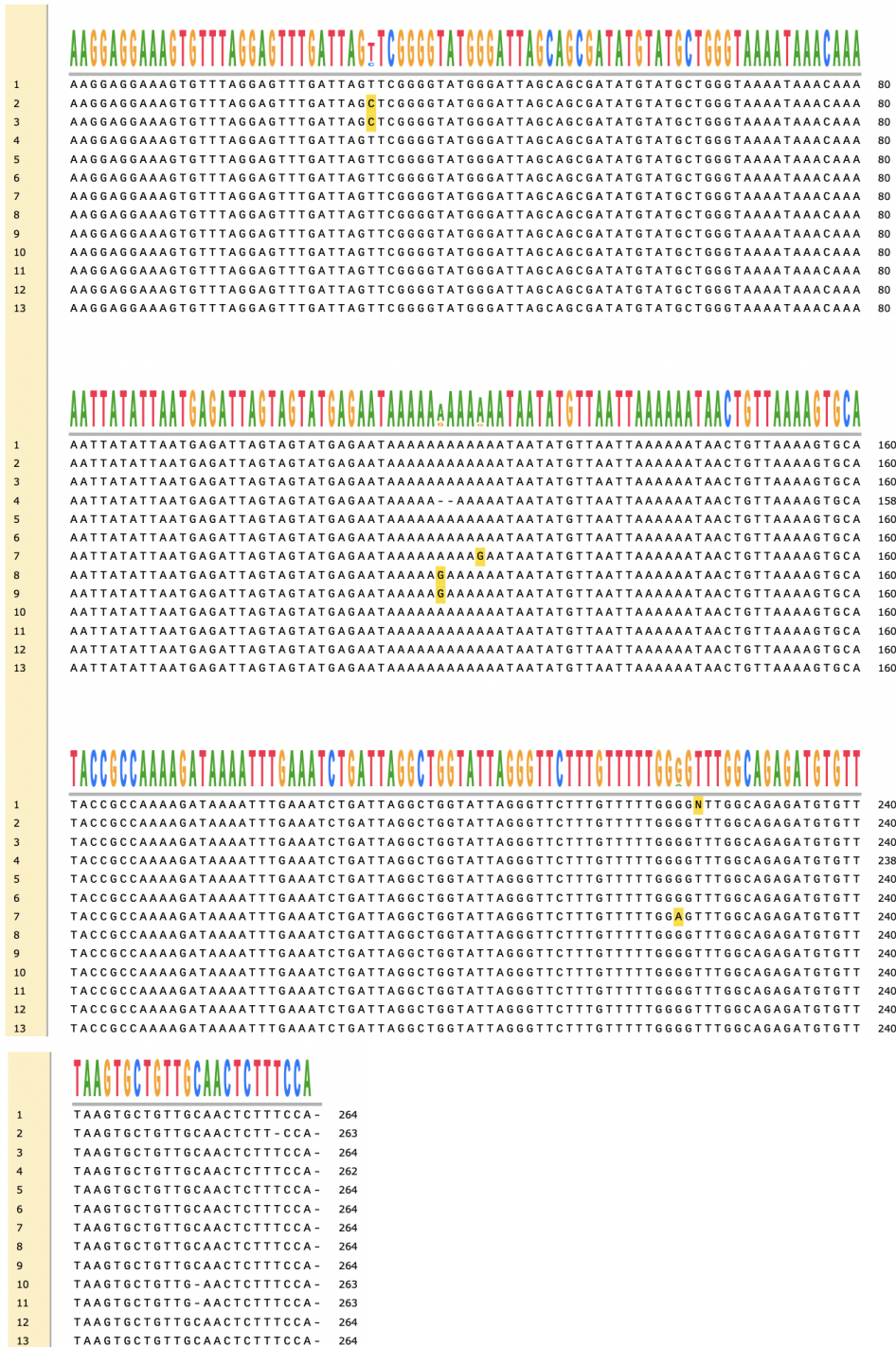
Cancer epigenetics is currently a cutting-edge field of research. Specifically, epigenetic regulation of nuclear hormone receptors in tumorigenesis, has been the target of investigation for new cancer therapies. The role of NHRs in cancer is complex and diverse. However, by targeting methyl binding proteins to either release or induce epigenetic regulation of NHR gene expression, alternative therapeutic targets may be developed in the future. Additionally, evaluating the degree of methylation in tissue samples could be a viable biomarker for cancer screening.

As a nuclear hormone receptor, DAX-1 may potentially serve as a biomarker for the increased likelihood of tumor development and cancer progression. Clinically, DAX-1 has been extensively reviewed for its role in Adrenal Hypoplasia Congenita (AHC) and Dosage Sensitive Sex reversal (DSS). Combined with its interdisciplinary connections to disease, as well as the rise of nuclear hormone receptors, specifically in the orphan family, and methylation status as oncogenic biomarkers, further investigation of the role of DAX-1 in hormone regulated cancers could lead to future clinical applications. Future research integrating a more in depth bioinformatic approach studying the *DAX-1* epigenome and patient tissue samples could elucidate the importance of DAX-1 in cancer tumor suppression, particularly in breast tissues. Accessing methylation specific cancer databases and alignments from patient data against the wild type *DAX-1* gene would further determine the importance of methylation in the promoter region. Additionally, understanding to what extent methylation represses gene expression could give rise to applications that would release epigenetic control. In conclusion, the study of methylation status and NHRs may uncover novel biomedical and therapeutic approaches to detecting and treating cancer.

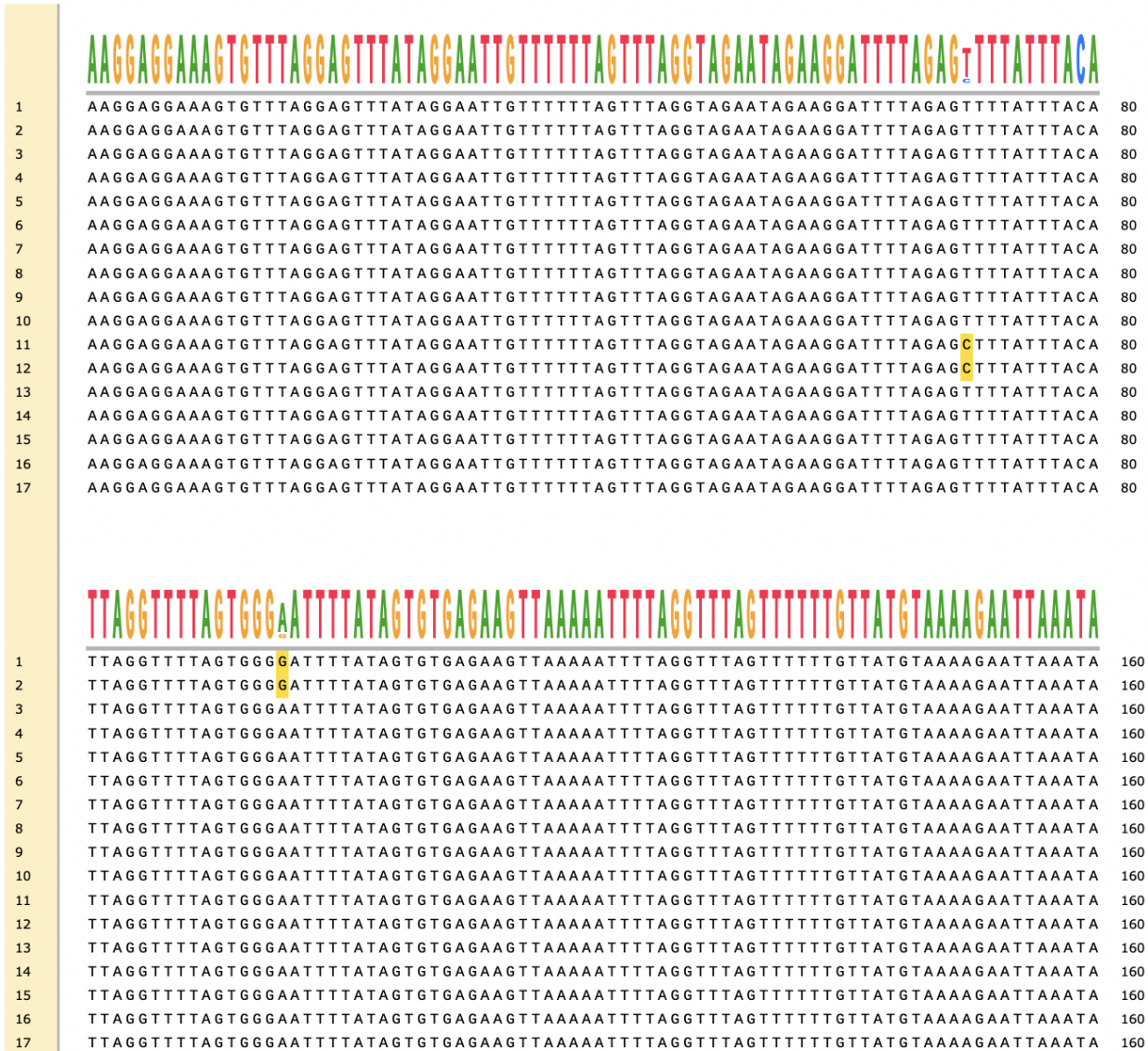
## Appendix A: Supplementary Figures and Tables



**Figure A.1 Restriction digest analysis of pGEM-T Easy and converted or control DNA constructs.** Following restriction digestion, constructs releasing a 300bp insert were submitted for sequencing.

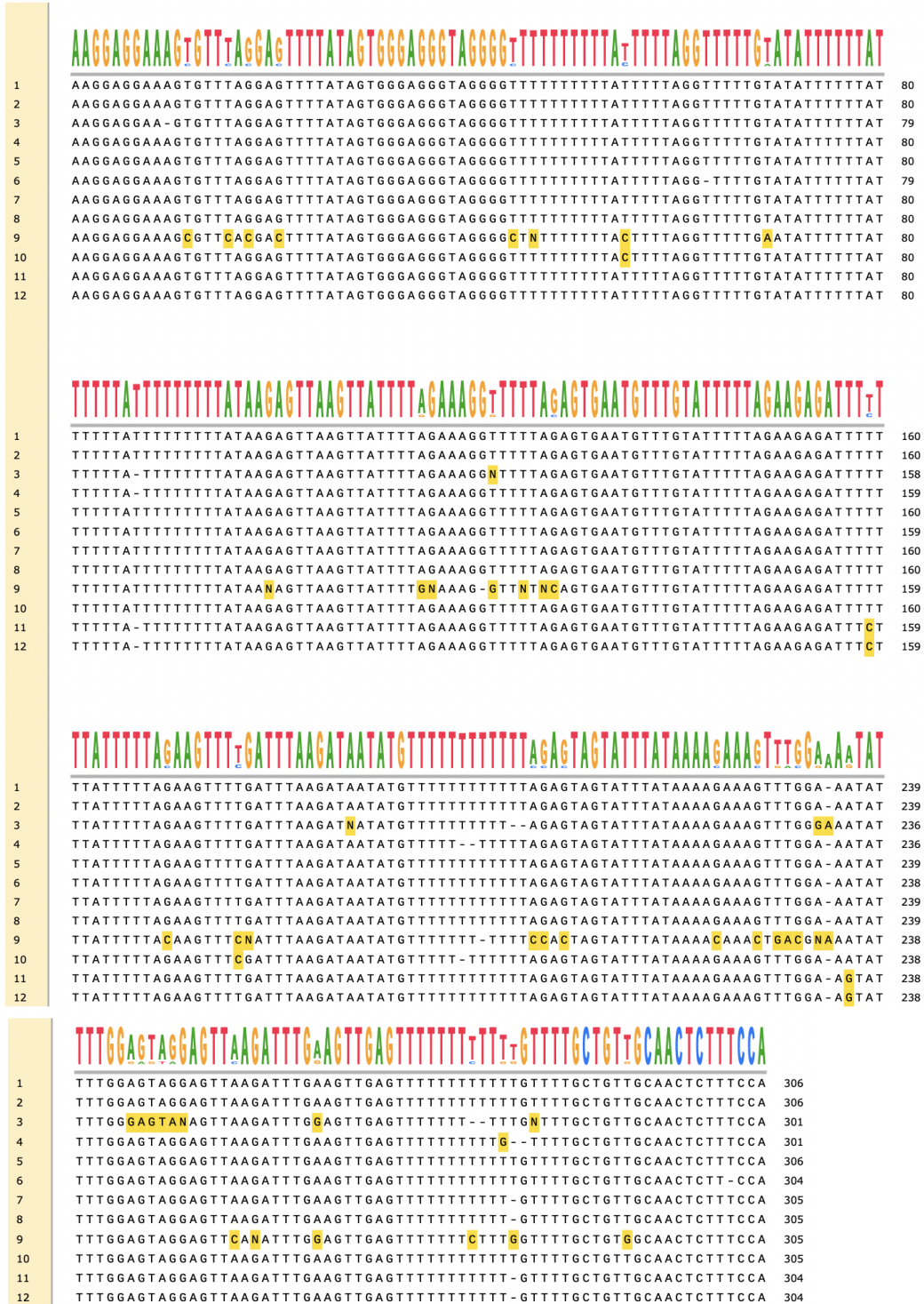


**Figure A.2 Sequence alignment of A549 bisulfite modified gDNA.** Obtained from multiple clones, there are few discrepancies (highlighted in yellow) between the multiple bisulfite modified DNA samples.



**Figure A.3** Sequence alignment of MCF7 bisulfite modified gDNA. There are only minor discrepancies (highlighted in yellow) between the multiple bisulfite modified DNA samples obtained from plasmid clones.





**Figure A.4** Sequence alignment of MCF10A bisulfite modified gDNA. Obtained from multiple clones, there are some discrepancies (highlighted in yellow) between the multiple bisulfite modified DNA samples.

**Table A.1 Summary table of PCR running protocol parameters**

<b>Protocol</b>	<b>Cycling Parameters</b>	
DAX-1 gDNA Detection via PCR	95°C x 3 minutes	1 Repeat
	95°C x 30 seconds 55°C x 30 seconds 72°C x 1 minute	Repeat 35 times
	72°C x 5 minutes	1 Repeat
	4°C x infinite hold	1 Repeat
DAX-1 mRNA Expression via qPCR	95°C x 10 seconds	1 cycle
	95°C x 15 seconds 60°C x 15 seconds	40 cycles
Methylation Specific Restriction Digest PCR	95°C x 3 minutes	1 Repeat
	95°C x 20 seconds 61°C x 30 seconds 72°C x 1 minute	Repeat 32-40 times
	72°C x 5 minutes	1 Repeat
	4°C x infinite hold	1 Repeat
PCR Amplification of Bisulfite Converted gDNA	95°C x 3 minutes	1 Repeat
	95°C x 20 seconds 52.3°C x 30 seconds 72°C x 60 seconds	Repeat 35 - 45 times
	72°C x 5 minutes	1 Repeat
	4°C x infinite hold	1 Repeat
PCR Amplification on Isolated ChIP Products	95°C x 3 minutes	1 Repeat
	95°C x 20 seconds 61°C x 30 seconds 72°C x 60 seconds	Repeat 50 times
	72°C x 5 minutes	1 Repeat
	4°C x infinite hold	1 Repeat

**Table A.2 Summary table of the primers used in PCR and qPCR**

<b>Target</b>	<b>Forward Primer</b>	<b>Reverse Primer</b>
Primers to detect genomic DAX-1 spanning Exon 1 (676) to Intron (1251) in gDNA:	5' - CCC ACG ACA AAT CAA GC - 3'	5' - CTG CCC GAT GCT TTT GTG AG - 3'
Primers to detect genomic DAX-1 spanning Intron (1232) to Intron (2399) in gDNA:	5' - CTC ACA AAA GCA TCG GGC AG - 3'	5' - GGG GTG AGC TGA GGT CTC TAG - 3'
Primers to detect <i>DAX-1</i> gene expression in qPCR	5' - GAC TCC AGT GGG GAA CTC AG - 3'	5' - ATG ATG GGC CTG AAG AAC AG - 3'
Primers to detect <i>GAPDH</i> gene expression (positive control):	5' - CCA TCA CCA TCT TCC AGG AGC G - 3'	5' - AGA GAT GAT GAC CCT TTT GGC - 3'
Primer CpG Rich Region A (Used for MSRE and ChIP)	5' - GAA GGA GGA AAG TGT CCA GGA GCT C -3'	5' - AGC CCA GTT CTG CCC AGT GGC TGC C -3'
Primer CpG Rich Region B (Used for MSRE and ChIP)	5' - AGG GCA GCA TCC TCT AGA AC - 3'	5' - TCT TCA CCA CAA AAG CAG CA - 3'
Primer CpG Rich Region C (Used for MSRE and ChIP)	5' - CTC AAA GCA AAC GCA CGT G - 3'	5' - CAC CTG TGG ACT CTT GAG CG - 3'
Primer CpG Rich Region D (Used for MSRE and ChIP)	5' - GAA GAC CAC CCG CAG CAG - 3'	5' - CAC TTG ATG GCT TGG ACC TG - 3'
Primer CpG Rich Region E (Used for MSRE and ChIP)	5' - AAT GCT GGA GTC TGA ACA TCA GTA CCA AGG - 3'	5' - CCA CCC CAA CTC TGC TGA GTT AGT C - 3'
Amplification of Bisulfite Modified gDNA Region Containing TATA Box and First CpG Island	5' - AAG GAG GAA AGT GTT TAG GAG TTT - 3'	5' - TGG AAA GAG TTG CAA CAG CA - 3'

## References

- Abi Khalil, C. (2014). The emerging role of epigenetics in cardiovascular disease. *Therapeutic Advances in Chronic Disease*, 5(4), 178–187. <https://doi.org/10.1177/2040622314529325>
- Anglim, P. P., Galler, J. S., Koss, M. N., Hagen, J. A., Turla, S., Campan, M., Weisenberger, D. J., Laird, P. W., Siegmund, K. D., & Laird-Offringa, I. A. (2008). Identification of a panel of sensitive and specific DNA methylation markers for squamous cell lung cancer. *Molecular Cancer*, 7:62(1), 1–13. <https://doi.org/10.1186/1476-4598-7-62>
- ATCC Cell Lines. (n.d.). American Type Culture Collection. Retrieved April 29, 2021, from [https://www.atcc.org/en/Products/Cells\\_and\\_Microorganisms/Cell\\_Lines.aspx](https://www.atcc.org/en/Products/Cells_and_Microorganisms/Cell_Lines.aspx)
- Ball, M. P., Li, J. B., Gao, Y., Lee, J.-H., LeProust, E. M., Park, I.-H., Xie, B., Daley, G. Q., & Church, G. M. (2009). Targeted and genome-scale strategies reveal gene-body methylation signatures in human cells. *Nature Biotechnology*, 27(4), 361–368. <https://doi.org/10.1038/nbt.1533>
- Bell, J. T., & Spector, T. D. (2011). A twin approach to unraveling epigenetics. *Trends in Genetics*, 27(3), 116–125. <https://doi.org/10.1016/j.tig.2010.12.005>
- Bhat, M. K., Yu, C., Yap, N., Zhan, Q., Hayashi, Y., Seth, P., & Cheng, S. (1997). Tumor Suppressor p53 Is a Negative Regulator in Thyroid Hormone Receptor Signaling Pathways. *Journal of Biological Chemistry*, 272(46), 28989–28993. <https://doi.org/10.1074/jbc.272.46.28989>
- Bird, A. (2002). DNA methylation patterns and epigenetic memory. *Genes & Development*, 16(1), 6–21. <https://doi.org/10.1101/gad.947102>
- Bird, A. (2007). Perceptions of epigenetics. *Nature*, 447(7143), 396–398. <https://doi.org/10.1038/nature05913>

- Boitano, M. T. (2009). *Epigenetic regulation of the human DAX-1 promoter* (Theses, Dissertations, Capstones and Projects: Master's Theses) [The University of San Francisco]. University of San Francisco Scholarship Repository.  
<https://repository.usfca.edu/cgi/viewcontent.cgi?article=1685&context=theses>
- Breton, C. V., Byun, H.-M., Wenten, M., Pan, F., Yang, A., & Gilliland, F. D. (2009). Prenatal Tobacco Smoke Exposure Affects Global and Gene-specific DNA Methylation. *American Journal of Respiratory and Critical Care Medicine*, *180*(5), 462–467.  
<https://doi.org/10.1164/rccm.200901-0135OC>
- Brouwer, J. R. (2013, January 18). 10 Ways to Improve Your Bisulfite Sequencing Results. *Bitesize Bio*. <https://bitesizebio.com/9957/10-ways-to-improve-your-bisulfite-sequencing-results/>
- Brown, S. E., Weaver, I. C. G., Meaney, M. J., & Szyf, M. (2008). Regional-specific global cytosine methylation and DNA methyltransferase expression in the adult rat hippocampus. *Neuroscience Letters*, *440*(1), 49–53.  
<https://doi.org/10.1016/j.neulet.2008.05.028>
- Call, S. G., Duren, R. P., Panigrahi, A. K., Nguyen, L., Freire, P. R., Grimm, S. L., Coarfa, C., & Conneely, O. M. (2020). Targeting Oncogenic Super Enhancers in MYC-Dependent AML Using a Small Molecule Activator of NR4A Nuclear Receptors. *Scientific Reports*, *10*: 2851(1), 1–15. <https://doi.org/10.1038/s41598-020-59469-3>
- Cancer epigenetics—Latest research and news | Nature*. (n.d.). Nature Portfolio. Retrieved April 29, 2021, from <https://www.nature.com/subjects/cancer-epigenetics>

- Cancer Statistics—National Cancer Institute* (nciglobal,ncienterprise). (2015, April 2). [CgvArticle]. National Cancer Institute (NIH). <https://www.cancer.gov/about-cancer/understanding/statistics>
- Cardiovascular diseases*. (n.d.). World Health Organization (WHO). Retrieved April 29, 2021, from <https://www.who.int/westernpacific/health-topics/cardiovascular-diseases>
- Cedar, H., & Bergman, Y. (2011). Epigenetics of haematopoietic cell development. *Nature Reviews Immunology*, *11*(7), 478–488. <https://doi.org/10.1038/nri2991>
- Cheng, Y. Y., Yu, J., Wong, Y. P., Man, E. P. S., To, K. F., Jin, V. X., Li, J., Tao, Q., Sung, J. J. Y., Chan, F. K. L., & Leung, W. K. (2007). Frequent epigenetic inactivation of secreted frizzled-related protein 2 (SFRP2) by promoter methylation in human gastric cancer. *British Journal of Cancer*, *97*(7), 895–901. <https://doi.org/10.1038/sj.bjc.6603968>
- Chinnaiyan, A. M., & Palanisamy, N. (2010). Chapter 4—Chromosomal Aberrations in Solid Tumors. In R. W. Ruddon (Ed.), *Progress in Molecular Biology and Translational Science* (Vol. 95, pp. 55–94). Academic Press. <https://doi.org/10.1016/B978-0-12-385071-3.00004-6>
- Comparison of means calculator* (20.009). (2021). [Computer software]. MedCalc Software Ltd. [https://www.medcalc.org/calc/comparison\\_of\\_means.php](https://www.medcalc.org/calc/comparison_of_means.php)
- Conde, I., Alfaro, J. M., Fraile, B., Ruíz, A., Paniagua, R., & Arenas, M. I. (2004). DAX-1 expression in human breast cancer: Comparison with estrogen receptors ER- $\alpha$ , ER- $\beta$  and androgen receptor status. *Breast Cancer Research*, *6*(3), R140–R148. <https://doi.org/10.1186/bcr766>
- Cross, S. H., & Bird, A. P. (1995). CpG islands and genes. *Current Opinion in Genetics & Development*, *5*(3), 309–314. [https://doi.org/10.1016/0959-437X\(95\)80044-1](https://doi.org/10.1016/0959-437X(95)80044-1)

- Darst, R. P., Pardo, C. E., Ai, L., Brown, K. D., & Kladde, M. P. (2010). Bisulfite Sequencing of DNA. *Current Protocols in Molecular Biology / Edited by Frederick M. Ausubel ... [et Al.]*, 91(1), 7–9. <https://doi.org/10.1002/0471142727.mb0709s91>
- Dishington, E. (2017). *The role of orphan nuclear receptor DAX-1 (NR0B1) in human breast cancer cells: Expression, proliferation and metastasis* (Theses, Dissertations, Capstones and Projects: Master's Theses) [The University of San Francisco]. <https://repository.usfca.edu/cgi/viewcontent.cgi?article=1348&context=thes>
- Eckhardt, F., Lewin, J., Cortese, R., Rakyan, V. K., Attwood, J., Burger, M., Burton, J., Cox, T. V., Davies, R., Down, T. A., Haefliger, C., Horton, R., Howe, K., Jackson, D. K., Kunde, J., Koenig, C., Liddle, J., Niblett, D., Otto, T., ... Beck, S. (2006). DNA methylation profiling of human chromosomes 6, 20 and 22. *Nature Genetics*, 38(12), 1378–1385. <https://doi.org/10.1038/ng1909>
- Egger, G., Liang, G., Aparicio, A., & Jones, P. A. (2004). Epigenetics in human disease and prospects for epigenetic therapy. *Nature*, 429(6990), 457–463. <https://doi.org/10.1038/nature02625>
- EpiDesigner*. (2017). Agena Bioscience, Inc. <http://www.epidesigner.com/>
- Feng Han, Q., Zhao, W., Bentel, J., Shearwood, A.-M., Zeps, N., Joseph, D., Iacopetta, B., & Dharmarajan, A. (2006). Expression of sFRP-4 and  $\beta$ -catenin in human colorectal carcinoma. *Cancer Letters*, 231(1), 129–137. <https://doi.org/10.1016/j.canlet.2005.01.026>
- Fournier, A., Sasai, N., Nakao, M., & Defossez, P.-A. (2012). The role of methyl-binding proteins in chromatin organization and epigenome maintenance. *Briefings in Functional Genomics*, 11(3), 251–264. <https://doi.org/10.1093/bfpg/elr040>

- Fruchart, J.-C., Santos, R. D., Aguilar-Salinas, C., Aikawa, M., Al Rasadi, K., Amarenco, P., Barter, P. J., Ceska, R., Corsini, A., Després, J.-P., Duriez, P., Eckel, R. H., Ezhov, M. V., Farnier, M., Ginsberg, H. N., Hermans, M. P., Ishibashi, S., Karpe, F., Kodama, T., ... Libby, P. (2019). The selective peroxisome proliferator-activated receptor alpha modulator (SPPARM $\alpha$ ) paradigm: Conceptual framework and therapeutic potential: A consensus statement from the International Atherosclerosis Society (IAS) and the Residual Risk Reduction Initiative (R3i) Foundation. *Cardiovascular Diabetology*, *18*:71(1), 1–20. <https://doi.org/10.1186/s12933-019-0864-7>
- Fu, C., Li, L., Wu, W., Li, M., Yu, X., & Yu, L. (2012). Assessment of genetic and epigenetic variation during long-term *Taxus* cell culture. *Plant Cell Reports*, *31*(7), 1321–1331. <https://doi.org/10.1007/s00299-012-1251-y>
- Fuks, F., Hurd, P. J., Wolf, D., Nan, X., Bird, A. P., & Kouzarides, T. (2003). The Methyl-CpG-binding Protein MeCP2 Links DNA Methylation to Histone Methylation. *Journal of Biological Chemistry*, *278*(6), 4035–4040. <https://doi.org/10.1074/jbc.M210256200>
- Guo, L.-H., & Ren, X.-M. (2013). *Molecular toxicology of polybrominated diphenyl ethers: Nuclear hormone receptor mediated pathways*. *15*(4), 702–708.
- Halušková, J. (2009). *Review Article Epigenetic Studies in Human Diseases*. *56*(3), 83–96.
- Hansen, K. D., Timp, W., Bravo, H. C., Sabunciyan, S., Langmead, B., McDonald, O. G., Wen, B., Wu, H., Liu, Y., Diep, D., Briem, E., Zhang, K., Irizarry, R. A., & Feinberg, A. P. (2011). Increased methylation variation in epigenetic domains across cancer types. *Nature Genetics*, *43*(8), 768–775. <https://doi.org/10.1038/ng.865>
- He, N., Park, K., Zhang, Y., Huang, J., Lu, S., & Wang, L. (2008). Epigenetic Inhibition of Nuclear Receptor Small Heterodimer Partner Is Associated With and Regulates



- Hepatocellular Carcinoma Growth. *Gastroenterology*, 134(3), 793–802.  
<https://doi.org/10.1053/j.gastro.2008.01.006>
- Heard, E., Clerc, P., & Avner, P. (1997). X-Chromosome Inactivation in Mammals. *Annual Review of Genetics*, 31(1), 571–610. <https://doi.org/10.1146/annurev.genet.31.1.571>
- Hendrich, B., & Tweedie, S. (2003). The methyl-CpG binding domain and the evolving role of DNA methylation in animals. *Trends in Genetics*, 19(5), 269–277.  
[https://doi.org/10.1016/S0168-9525\(03\)00080-5](https://doi.org/10.1016/S0168-9525(03)00080-5)
- Heskett, M. B. (2014). *Epigenetic Regulation of Nuclear Hormone Receptor DAX-1* (Theses, Dissertations, Capstones and Projects: Master's Theses) [The University of San Francisco]. University of San Francisco Scholarship Repository.  
<https://repository.usfca.edu/cgi/viewcontent.cgi?article=1132&context=theses>
- Image Lab Software* | *Life Science Research* | *Bio-Rad* (6.1). (n.d.). [Computer software]. Life Science Research. Retrieved May 27, 2021, from <https://www.bio-rad.com/en-us/product/image-lab-software?ID=KRE6P5E8Z>
- Iyer, A. K., & McCabe, E. R. B. (2004). Molecular mechanisms of DAX1 action. *Molecular Genetics and Metabolism*, 83(1–2), 60–73. <https://doi.org/10.1016/j.ymgme.2004.07.018>
- Janitz, K., & Janitz, M. (2011). Chapter 12—Assessing Epigenetic Information. In T. Tollefsbol (Ed.), *Handbook of Epigenetics—The New Molecular and Medical Genetics* (pp. 173–181). Academic Press. <https://doi.org/10.1016/B978-0-12-375709-8.00012-5>
- Jiang, H.-L., Xu, D., Yu, H., Ma, X., Lin, G.-F., Ma, D.-Y., & Jin, J.-Z. (2014). DAX-1 Inhibits Hepatocellular Carcinoma Proliferation by Inhibiting  $\beta$ -Catenin Transcriptional Activity. *Cellular Physiology and Biochemistry*, 34(3), 734–742.  
<https://doi.org/10.1159/000363038>

- Jintaridith, P., & Mutirangura, A. (2010). Distinctive patterns of age-dependent hypomethylation in interspersed repetitive sequences. *Physiological Genomics*, *41*(2), 194–200. <https://doi.org/10.1152/physiolgenomics.00146.2009>
- Jones, P. A., & Takai, D. (2001). The Role of DNA Methylation in Mammalian Epigenetics. *Science*, *293*(5532), 1068–1070. <https://doi.org/10.1126/science.1063852>
- Judge, S. J. O. (2011). *Epigenetic regulation by methylation status of the DAX-1 gene in normal and cancerous breast cell lines* (Theses, Dissertations, Capstones and Projects: Master's Theses) [The University of San Francisco]. University of San Francisco Scholarship Repository. <https://repository.usfca.edu/cgi/viewcontent.cgi?article=1688&context=theses>
- Kawano, Y., & Kypta, R. (2003). Secreted antagonists of the Wnt signalling pathway. *Journal of Cell Science*, *116*(13), 2627–2634. <https://doi.org/10.1242/jcs.00623>
- Ke, N., Claassen, G., Yu, D.-H., Albers, A., Fan, W., Tan, P., Grifman, M., Hu, X., DeFife, K., Nguy, V., Meyhack, B., Brachat, A., Wong-Staal, F., & Li, Q.-X. (2004). Nuclear Hormone Receptor NR4A2 Is Involved in Cell Transformation and Apoptosis. *Cancer Research*, *64*(22), 8208–8212. <https://doi.org/10.1158/0008-5472.CAN-04-2134>
- Kelen, K. V. D., Beyaert, R., Inzé, D., & Veylder, L. D. (2009). Translational control of eukaryotic gene expression. *Critical Reviews in Biochemistry and Molecular Biology*, *44*(4), 143–168. <https://doi.org/10.1080/10409230902882090>
- Kerachian, M. A., Javadmanesh, A., Azghandi, M., Mojtabanezhad Shariatpanahi, A., Yassi, M., Shams Davodly, E., Talebi, A., Khadangi, F., Soltani, G., Hayatbakhsh, A., & Ghaffarzagdegan, K. (2020). Crosstalk between DNA methylation and gene expression in colorectal cancer, a potential plasma biomarker for tracing this tumor. *Scientific Reports*, *10*(1), 2813. <https://doi.org/10.1038/s41598-020-59690-0>

- Klinge, C. (1997). Binding of type II nuclear receptors and estrogen receptor to full and half-site estrogen response elements in vitro. *Nucleic Acids Research*, 25(10), 1903–1912.  
<https://doi.org/10.1093/nar/25.10.1903>
- Kõressaar, T., Lepamets, M., Kaplinski, L., Raime, K., Andreson, R., & Remm, M. (2018). Primer3\_masker: Integrating masking of template sequence with primer design software. *Bioinformatics (Oxford, England)*, 34(11), 1937–1938.  
<https://doi.org/10.1093/bioinformatics/bty036>
- Koressaar, T., & Remm, M. (2007). Enhancements and modifications of primer design program Primer3. *Bioinformatics (Oxford, England)*, 23(10), 1289–1291.  
<https://doi.org/10.1093/bioinformatics/btm091>
- Kudryavtseva, A. V., Nyushko, K. M., Zaretsky, A. R., Shagin, D. A., Sadritdinova, A. F., Fedorova, M. S., Savvateeva, M. V., Guvatova, Z. G., Pudova, E. A., Alekseev, B. Y., Dmitriev, A. A., & Snezhkina, A. V. (2018). Suppression of NR0B2 gene in Clear Cell Renal Cell Carcinoma Is Associated with Hypermethylation of Its Promoter. *Molecular Biology*, 52(3), 414–418. <https://doi.org/10.1134/S0026893318030081>
- Kumata, H., Murakami, K., Ishida, K., Miyagi, S., Arakawa, A., Inayama, Y., Kinowaki, K., Ochiai, A., Kojima, M., Higashi, M., Moritani, S., Kuwahara, K., Nakatani, Y., Kajiura, D., Tamura, G., Kijima, H., Yamakawa, M., Shiraishi, T., Inadome, Y., ... Sasano, H. (2018). Steroidogenesis in ovarian-like mesenchymal stroma of hepatic and pancreatic mucinous cystic neoplasms: Steroidogenesis in hepatic MCN. *Hepatology Research*, 48(12), 989–999. <https://doi.org/10.1111/hepr.13201>
- Kwabi-Addo, B., Chung, W., Shen, L., Ittmann, M., Wheeler, T., Jelinek, J., & Issa, J.-P. J. (2007). Age-Related DNA Methylation Changes in Normal Human Prostate Tissues.

- Clinical Cancer Research*, 13(13), 3796–3802. <https://doi.org/10.1158/1078-0432.CCR-07-0085>
- Lalli, E. (2014). Role of Orphan Nuclear Receptor DAX-1/NR0B1 in Development, Physiology, and Disease. *Advances in Biology*, 2014, 1–19. <https://doi.org/10.1155/2014/582749>
- Lalli, E., Bardoni, B., Zazopoulos, E., Wurtz, J.-M., Strom, T. M., Moras, D., & Sassone-Corsi, P. (1997). A Transcriptional Silencing Domain in DAX-1 Whose Mutation Causes Adrenal Hypoplasia Congenita. *Molecular Endocrinology*, 11(13), 1950–1960. <https://doi.org/10.1210/mend.11.13.0038>
- Lee, A. V., Oesterreich, S., & Davidson, N. E. (2015). MCF-7 Cells—Changing the Course of Breast Cancer Research and Care for 45 Years. *JNCI Journal of the National Cancer Institute*, 107(7), djv073–djv073. <https://doi.org/10.1093/jnci/djv073>
- Li, E., Beard, C., & Jaenisch, R. (1993). Role for DNA methylation in genomic imprinting. *Nature*, 366(6453), 362–365. <https://doi.org/10.1038/366362a0>
- Li, E., Bestor, T. H., & Jaenisch, R. (1992). Targeted mutation of the DNA methyltransferase gene results in embryonic lethality. *Cell*, 69(6), 915–926. [https://doi.org/10.1016/0092-8674\(92\)90611-F](https://doi.org/10.1016/0092-8674(92)90611-F)
- Li, L. C., & Dahiya, R. (2002). MethPrimer: Designing primers for methylation PCRs. *Bioinformatics*, 18(11), 1427–1431. <https://doi.org/10.1093/bioinformatics/18.11.1427>
- Li, L., Chen, B.-F., & Chan, W.-Y. (2015). An Epigenetic Regulator: Methyl-CpG-Binding Domain Protein 1 (MBD1). *International Journal of Molecular Sciences*, 16(3), 5125–5140. <https://doi.org/10.3390/ijms16035125>

- Liu, X.-F., Li, X.-Y., Zheng, P.-S., & Yang, W.-T. (2018). DAX1 promotes cervical cancer cell growth and tumorigenicity through activation of Wnt/ $\beta$ -catenin pathway via GSK3 $\beta$ . *Cell Death & Disease*, 9(3), 339. <https://doi.org/10.1038/s41419-018-0359-6>
- Liyanage, V., Jarmasz, J., Murugesan, N., Del Bigio, M., Rastegar, M., & Davie, J. (2014). DNA Modifications: Function and Applications in Normal and Disease States. *Biology*, 3, 670–723. <https://doi.org/10.3390/biology3040670>
- Malekzadeh, K., Sobti, R. C., Nikbakht, M., Shekari, M., Hosseini, S. A., Tamandani, D. K., & Singh, S. K. (2009). Methylation Patterns of Rb1 and Casp-8 Promoters and Their Impact on Their Expression in Bladder Cancer. *Cancer Investigation*, 27(1), 70–80. <https://doi.org/10.1080/07357900802172085>
- Manel, E. (2008). Epigenetics in Cancer. *N Engl J Med*, 358(11), 1148–1159.
- Mangelsdorf, D. J., Thummel, C., Beato, M., Herrlich, P., Schütz, G., Umesono, K., Blumberg, B., Kastner, P., Mark, M., Chambon, P., & Evans, R. M. (1995). The nuclear receptor superfamily: The second decade. *Cell*, 83(6), 835–839. [https://doi.org/10.1016/0092-8674\(95\)90199-X](https://doi.org/10.1016/0092-8674(95)90199-X)
- Manoochchri, M., Borhani, N., Karbasi, A., Koochaki, A., & Kazemi, B. (2016). Promoter hypermethylation and downregulation of the FAS gene may be involved in colorectal carcinogenesis. *Oncology Letters*, 12(1), 285–290. <https://doi.org/10.3892/ol.2016.4578>
- Martin, D. I. K., Copley, J. E., & Suter, C. M. (2011). Epigenetics in disease: Leader or follower? *Epigenetics*, 6(7), 843–848. <https://doi.org/10.4161/epi.6.7.16498>
- MBD1 antibody (Clone 100B272.1)*. (n.d.). Active Motif. Retrieved April 29, 2021, from <https://www.activemotif.com/catalog/details/39215/mbd1-antibody-mab>

- McCabe, E. R. B. (2007). DAX1: Increasing complexity in the roles of this novel nuclear receptor. *Molecular and Cellular Endocrinology*, 265–266, 179–182.  
<https://doi.org/10.1016/j.mce.2006.12.017>
- Melnikov, A. A. (2005). MSRE-PCR for analysis of gene-specific DNA methylation. *Nucleic Acids Research*, 33(10), e93–e93. <https://doi.org/10.1093/nar/gni092>
- Microsoft. (n.d.). *STDEV function* [Office Support]. Microsoft. Retrieved July 21, 2021, from <https://support.microsoft.com/en-us/office/stdev-function-51fecaaa-231e-4bbb-9230-33650a72c9b0>
- Moore, L. D., Le, T., & Fan, G. (2013). DNA Methylation and Its Basic Function. *Neuropsychopharmacology*, 38(1), 23–38. <https://doi.org/10.1038/npp.2012.112>
- Murgatroyd, C., & Spengler, D. (2011). Epigenetics of Early Child Development. *Frontiers in Psychiatry*, 2. <https://doi.org/10.3389/fpsyt.2011.00016>
- Nucleotide BLAST: Search nucleotide databases using a nucleotide query.* (n.d.). [Basic Local Alignment Search Tool]. U.S. National Library of Medicine, National Center for Biotechnology Information (NIH:NCBI). Retrieved May 3, 2021, from <https://blast.ncbi.nlm.nih.gov/Blast.cgi>
- Ordovás, J. M., & Smith, C. E. (2010). Epigenetics and cardiovascular disease. *Nature Reviews Cardiology*, 7(9), 510–519. <https://doi.org/10.1038/nrcardio.2010.104>
- Promega. (2018, December). *PGEM®-T Easy Vector Systems*. Promega.  
<https://www.promega.com/products/pcr/pcr-cloning/pgem-t-easy-vector-systems/>
- Qiagen. (n.d.). *What is the standard curve method for qPCR assay data analysis? How is the standard curve method for qPCR assay data analysis performed? - QIAGEN*. Frequently Asked Questions. Retrieved July 21, 2021, from

<https://www.qiagen.com/us/resources/faq?id=411524f1-fe07-41bc-bbd2-32e1ce16b497&lang=en>

- Rakyan, V. K., Hildmann, T., Novik, K. L., Lewin, J., Tost, J., Cox, A. V., Andrews, T. D., Howe, K. L., Otto, T., Olek, A., Fischer, J., Gut, I. G., Berlin, K., & Beck, S. (2004). DNA Methylation Profiling of the Human Major Histocompatibility Complex: A Pilot Study for the Human Epigenome Project. *PLoS Biology*, 2(12), e405. <https://doi.org/10.1371/journal.pbio.0020405>
- Robertson, K. D. (2005). DNA methylation and human disease. *Nature Reviews Genetics*, 6(8), 597–610. <https://doi.org/10.1038/nrg1655>
- Rodenhiser, D., & Mann, M. (2006). Epigenetics and human disease: Translating basic biology into clinical applications. *Canadian Medical Association Journal*, 174(3), 341–348. <https://doi.org/10.1503/cmaj.050774>
- Roloff, T. C., Ropers, H. H., & Nuber, U. A. (2003). Comparative study of methyl-CpG-binding domain proteins. *BMC Genomics*, 4(1), 1–9. <https://doi.org/10.1186/1471-2164-4-1>
- Russo, V. E. A. (Vincenzo E. A. ), Martienssen, R. A., & Riggs, A. D. (1996). *Epigenetic mechanisms of gene regulation*. Cold Spring Harbor Laboratory Press. <https://agris.fao.org/agris-search/search.do?recordID=US201300304567>
- Salmon, A., Clotault, J., Jenczewski, E., Chable, V., & Manzanares-Dauleux, M. J. (2008). Brassica oleracea displays a high level of DNA methylation polymorphism. *Plant Science*, 174(1), 61–70. <https://doi.org/10.1016/j.plantsci.2007.09.012>
- Sasai, N., Nakao, M., & Defossez, P.-A. (2010). Sequence-specific recognition of methylated DNA by human zinc-finger proteins. *Nucleic Acids Research*, 38(15), 5015–5022. <https://doi.org/10.1093/nar/gkq280>

- Scandurra, A. E. (2014). *Examining the Role of DAX-1 in Regulation of Cell Proliferation in Human Breast Cells* (Theses, Dissertations, Capstones and Projects: Master's Theses) [University of San Francisco]. University of San Francisco Scholarship Repository. [https://repository.usfca.edu/cgi/viewcontent.cgi?article=1128&=&context=thes&=&sei-redir=1&referer=https%253A%252F%252Fscholar.google.com%252Fscholar%253Fq%253DMCF10A%252BDAX1%252Bexpression%2526hl%253Den%2526as\\_sdt%253D0%2526as\\_vis%253D1%2526oi%253Dscholar#search=%22MCF10A%20DAX1%20expression%22](https://repository.usfca.edu/cgi/viewcontent.cgi?article=1128&=&context=thes&=&sei-redir=1&referer=https%253A%252F%252Fscholar.google.com%252Fscholar%253Fq%253DMCF10A%252BDAX1%252Bexpression%2526hl%253Den%2526as_sdt%253D0%2526as_vis%253D1%2526oi%253Dscholar#search=%22MCF10A%20DAX1%20expression%22)
- Schock, G., & Traeger, T. (2011). *Techniques to overcome bottlenecks in epigenetics research*. Qiagen. <https://www.qiagen.com/us/resources/resourcedetail?id=230b8d92-8c30-4062-b48d-b30affb0caa3&lang=en>
- Shih, Y.-L., Hsieh, C.-B., Lai, H.-C., Yan, M.-D., Hsieh, T.-Y., Chao, Y.-C., & Lin, Y.-W. (2007). SFRP1 suppressed hepatoma cells growth through Wnt canonical signaling pathway. *International Journal of Cancer*, *121*(5), 1028–1035. <https://doi.org/10.1002/ijc.22750>
- Sleutels, F., & Barlow, D. (2002). 5—The origins of genomic imprinting in mammals. In J. Dunlap & C. -ting Wu (Eds.), *Homology Effects* (Vol. 46, pp. 119–163). [https://doi.org/10.1016/S0065-2660\(02\)46006-3](https://doi.org/10.1016/S0065-2660(02)46006-3)
- SnapGene | Software for everyday molecular biology*. (n.d.). Insightful Science. Retrieved May 3, 2021, from <https://www.snapgene.com/>
- Su, H.-Y., Lai, H.-C., Lin, Y.-W., Chou, Y.-C., Liu, C.-Y., & Yu, M.-H. (2009). An epigenetic marker panel for screening and prognostic prediction of ovarian cancer. *International Journal of Cancer*, *124*(2), 387–393. <https://doi.org/10.1002/ijc.23957>



- Suzuki, M. M., & Bird, A. (2008). DNA methylation landscapes: Provocative insights from epigenomics. *Nature Reviews Genetics*, *9*(6), 465–476. <https://doi.org/10.1038/nrg2341>
- Tatematsu, K., Yamazaki, T., & Ishikawa, F. (2000). MBD2-MBD3 complex binds to hemimethylated DNA and forms a complex containing DNMT1 at the replication foci in late S phase. *Genes to Cells*, *5*(8), 677–688. <https://doi.org/10.1046/j.1365-2443.2000.00359.x>
- Tierling, S., Schmitt, B., & Walter, J. (2018). Comprehensive Evaluation of Commercial Bisulfite-Based DNA Methylation Kits and Development of an Alternative Protocol With Improved Conversion Performance. *Genetics & Epigenetics*, *10*, 1179237X1876609. <https://doi.org/10.1177/1179237X18766097>
- Turan, N., Katari, S., Coutifaris, C., & Sapienza, C. (2010). Explaining inter-individual variability in phenotype: Is epigenetics up to the challenge? *Epigenetics*, *5*(1), 16–19. <https://doi.org/10.4161/epi.5.1.10557>
- Untergasser, A., Cutcutache, I., Koressaar, T., Ye, J., Faircloth, B. C., Remm, M., & Rozen, S. G. (2012). Primer3—New capabilities and interfaces. *Nucleic Acids Research*, *40*(15), e115, 1–12. <https://doi.org/10.1093/nar/gks596>
- van IJzendoorn, M. H., Bakermans-Kranenburg, M. J., & Ebstein, R. P. (2011). Methylation Matters in Child Development: Toward Developmental Behavioral Epigenetics: Methylation in Child Development. *Child Development Perspectives*, *5*(4), 305–310. <https://doi.org/10.1111/j.1750-8606.2011.00202.x>
- Vanden Heuvel, J. (2015). *Gene Expression: Nuclear Receptors*. INDIGO Biosciences. <https://indigobiosciences.com/gene-expression-nuclear-receptors/>

- Verma, M., & Manne, U. (2006). Genetic and epigenetic biomarkers in cancer diagnosis and identifying high risk populations. *Critical Reviews in Oncology/Hematology*, 60(1), 9–18. <https://doi.org/10.1016/j.critrevonc.2006.04.002>
- Viré, E., Brenner, C., Deplus, R., Blanchon, L., Fraga, M., Didelot, C., Morey, L., Van Eynde, A., Bernard, D., Vanderwinden, J.-M., Bollen, M., Esteller, M., Di Croce, L., de Launoit, Y., & Fuks, F. (2006). The Polycomb group protein EZH2 directly controls DNA methylation. *Nature*, 439(7078), 871–874. <https://doi.org/10.1038/nature04431>
- Waddington, C. H. (2014). *The Strategy of the Genes: A Discussion of Some Aspects of Theoretical Biology*. Routledge.
- Weber, M., Hellmann, I., Stadler, M. B., Ramos, L., Pääbo, S., Rebhan, M., & Schübeler, D. (2007). Distribution, silencing potential and evolutionary impact of promoter DNA methylation in the human genome. *Nature Genetics*, 39(4), 457–466. <https://doi.org/10.1038/ng1990>
- Wong, E. M., Southey, M. C., & Terry, M. B. (2020). Integrating DNA methylation measures to improve clinical risk assessment: Are we there yet? The case of BRCA1 methylation marks to improve clinical risk assessment of breast cancer. *British Journal of Cancer*, 122, 1133–1140. <https://doi.org/10.1038/s41416-019-0720-2>
- Wong, M. L., & Medrano, J. F. (2005). Real-time PCR for mRNA quantitation. *BioTechniques*, 39(1), 75–85. <https://doi.org/10.2144/05391RV01>
- Worm Ørntoft, M.-B., Jensen, S. Ø., Hansen, T. B., Bramsen, J. B., & Andersen, C. L. (2017). Comparative analysis of 12 different kits for bisulfite conversion of circulating cell-free DNA. *Epigenetics*, 12(8), 626–636. <https://doi.org/10.1080/15592294.2017.1334024>

- Wreczycka, K., Gosdschan, A., Yusuf, D., Grüning, B., Assenov, Y., & Akalin, A. (2017). Strategies for analyzing bisulfite sequencing data. *Journal of Biotechnology*, 261, 105–115. <https://doi.org/10.1016/j.jbiotec.2017.08.007>
- Yang, C., Zhang, M., Niu, W., Yang, R., Zhang, Y., Qiu, Z., Sun, B., & Zhao, Z. (2011). Analysis of DNA Methylation in Various Swine Tissues. *PLOS ONE*, 6(1), e16229. <https://doi.org/10.1371/journal.pone.0016229>
- Zanaria, E., Muscatelli, F., Bardoni, B., Strom, T. M., Guioli, S., Guo, W., Lalli, E., Moser, C., Walker, A. P., McCabe, E. R. B., Meitinger, T., Monaco, A. P., Sassone-Corsi, P., & Camerino, G. (1994). An unusual member of the nuclear hormone receptor superfamily responsible for X-linked adrenal hypoplasia congenita. *Nature*, 372(6507), 635–641. <https://doi.org/10.1038/372635a0>
- Zeisel, S. H. (2007). Nutrigenomics and metabolomics will change clinical nutrition and public health practice: Insights from studies on dietary requirements for choline. *The American Journal of Clinical Nutrition*, 86(3), 542–548. <https://doi.org/10.1093/ajcn/86.3.542>
- Zeisel, S. H. (2009). Epigenetic mechanisms for nutrition determinants of later health outcomes. *The American Journal of Clinical Nutrition*, 89(5), 1488S-1493S. <https://doi.org/10.3945/ajcn.2009.27113B>
- Zhang, H., Zhang, S., Cui, J., Zhang, A., Shen, L., & Yu, H. (2008). Expression and promoter methylation status of mismatch repair gene hMLH1 and hMSH2 in epithelial ovarian cancer. *Australian and New Zealand Journal of Obstetrics and Gynaecology*, 48(5), 505–509. <https://doi.org/10.1111/j.1479-828X.2008.00892.x>

Zhu, J., & Yao, X. (2007). Use of DNA Methylation for Cancer Detection and Molecular Classification. *BMB Reports*, 40(2), 135–141.

<https://doi.org/10.5483/BMBRep.2007.40.2.135>

*Zymo Bisulfite Converted DNA Amplification Guide*. (2015, January 12). EpiGenie | Epigenetics, Stem Cell, and Synthetic Biology News. <https://epigenie.com/guide-bisulfite-converted-dna-amplification/>